



TECHNICKÁ UNIVERZITA V LIBERCI
Fakulta textilní



Metoda tvorby stříhové konstrukce oděvů z elastických materiálů

Disertační práce

Studijní program: P3106 – Textile Engineering
Studijní obor: 3106V015 – Textile Technics and Materials Engineering
Autor práce: **Nareerut Jariyapunya, M.Eng.**
Vedoucí práce: Ing. Blažena Musilová, Ph.D.





TECHNICAL UNIVERSITY OF LIBEREC
Faculty of Textile Engineering



Clothing Patternmaking Method for Stretch Fabrics

Dissertation

Study programme: P3106 – Textile Engineering
Study branch: 3106V015 – Textile Technics and Materials Engineering
Author: **Nareerut Jariyapunya, M.Eng.**
Supervisor: Ing. Blažena Musilová, Ph.D.



Declaration

I hereby certify I have been informed that my dissertation is fully governed by Act No. 121/2000 Coll., the Copyright Act, in particular Article 60 – School Work.

I acknowledge that the Technical University of Liberec (TUL) does not infringe my copyrights by using my dissertation for the TUL's internal purposes.

I am aware of my obligation to inform the TUL on having used or granted license to use the results of my dissertation; in such a case the TUL may require reimbursement of the costs incurred for creating the result up to their actual amount.

I have written my dissertation myself using the literature listed below and consulting it with my thesis supervisor and my tutor.

At the same time, I honestly declare that the texts of the printed version of my dissertation and of the electronic version uploaded into the IS STAG are identical.

20. 3. 2019

Nareerut Jariyapunya, M.Eng.

Acknowledgement

In my PhD journey, there are a number of people who played a significant role in helping me reach my destination. I would like to express my thanks to all of them.

Firstly, I would like to express my gratitude to my supervisor, Ing. Blažena Musilová, Ph.D for her patient guidance, kind help, and great support to my research work. Thanks for her continues encouragement, giving me confidence to solve difficulties and conduct scientific research systematically. My sincere thanks to Professor Zdeněk Kůs, in-charge Head Department of Clothing Technology, Faculty of Textile Engineering and doc. Antonín Havelka for altruistic guidance and professional suggestions during my PhD journey.

I am especially indebted to Professor Bohuslav Neckář for sharing his immense expertise and knowledge of pressure theory for the cylindrical model. I also thank doc. Maroš Tunák for his supporting in image processing and analysis. My hearty thanks to Professor Jiří Militký and Assoc. prof. Rajesh Mishra who were supportive of my scientific work and provided me extensive professional guidance to complete this work. My special thanks to the Dean of Faculty of Textile Engineering Ing. Jana Drašarová and Vice Dean Dr. Gabriela Krupincová for continuous support through SGS projects for providing funding and arranging special devices for my research work. Thanks to Vice Dean Dr. Pavla Těšinová for always helping and arrangement of internship mobility. I also deeply thank the nice ladies Hana Musilová and Bohumila Keilová for their seamless coordination along my journey. Besides, I appreciate the opportunity of studying and proud to graduate from this esteemed institution of Technical University of Liberec.

I express my deep gratitude to Professor Jelka Geršak at University of Maribor, in Slovenia for the kind support and thank you for teaching me many lessons during internship, that I will carry into my professional researcher. I am thankful to LISCA d.d. company in Slovenia, LIPOELASTIC company in Czech Republic and Pacific Knitting Factory Co., Ltd. in Thailand for supporting me with their materials.

In particular, I am grateful to Assoc. Prof. Prasert Pinprathomrat, the President of Rajamangala University of Technology Thanyaburi (RMUTT), Thailand who has brought me an opportunity to fulfil my highest education in order to bring the knowledge back for teaching the students and improve scientific research in my home country. My grateful appreciation to the lab in-charges who were kind enough to provide access to laboratory facilities. This thesis may not have been possible without the contribution, support, help and coordination of the faculty and staff of Department of Clothing Technology, Faculty of Textile Engineering.

Thanks for my dear friends who stood by me and with whom I have so many happy and great memories together at the Technical University of Liberec.

Finally, I send my most heartfelt thanks to my parents and sister who always encourage me and also owe so much to my dearest Mr. Phongthep Kumarin who has given me his love and motivation and always stayed with me until the completion of Ph.D journey.

Synopsis

In garment industry, stretch fabrics are obtained from the elastomeric fibres that have widely been accepted for its properties especially for the production of tight silhouette and compression garment (CG). The peculiarity of mechanical characteristics of stretch fabric exerted on the part of the body is the pressure of clothing which it is originated from size differences between body dimensions and pattern construction abscissa. The advantage of realizing the importance of the pressure can be implemented and helped produce different types of garment including sportswear, body shaping, lingerie, medical treatment etc. Therefore, the methodology of scientific knowledge for calculating the size of patternmaking in order to obtain the specific pressure from the human body is considered to be one of the very most significant factors for pressure garment production.

Thus, the purpose of this research is to develop the clothing pattern construction abscissa according to human body physical dimensions and mechanical property of stretch fabric. The definition of the mechanical property of stretch fabric achieves from the force-elongation behaviour by tensile testing. The reason is because when fabric is being elongated by force, the amount of the pressure on the surface of the human body will occur. This certain fabric mechanical property will help improve the patternmaking method by determining the value of elastic coefficient which will have a significant influence on the pattern construction abscissa and on the pressure distributing of the stretch fabric. With these reasons, the clarification of both theoretical and practical research were required in order to orient towards the development of computational method that is applied in the process of pattern construction abscissa.

The aim of this work is to develop method of clothing patternmaking for stretch fabric and to define size of pattern construction abscissa by predicting mathematical modelling to achieve the exact shape and size of pattern construction net depending on the specific pressure required.

The experimental investigation is divided into two steps:

1. To define the method for determining the dimension of a particular structural segment of the pattern construction net that is capable of calculating the size of that pattern construction segment according to the dimension of human body thereof.
2. To define the method for calculating the extensibility of fabric from elastic coefficients of clothing that expresses the capability of its specific pressure required for correction of the dimension of a particular structural segment of the pattern construction net.

At the first step, determination of particular structural segment of the pattern construction net had been done by applying the regression method while, the dimension of pattern structural segment (dependent variable) can be calculated depending on the body dimension (independent variable). This research emphasizes on examining the two-dimensional (2D)

of patternmaking on the upper part of female body where the body part is similar to the cylindrical shape.

During, the second step of the process, development of methodology was pursued by applying the elastic coefficient by the relevant part of the body and size of patternmaking. The variables are the elastic coefficient of fabric (dependent variables) by changing the value of pressure (independently variable).

Subsequently, a 2D pattern construction abscissa has been investigated and the elastic coefficients were applied in width and length dimensions.

The Elastic Coefficient in Width dimension (ECW) was obtained from the result of stress-strain curve while Elastic Coefficient in Length dimension (ECL) was detected by observing the deformation of fabric stretched behaviour by uniaxial loading and evaluated by digital image analysis using the MATLAB and NIS-Element software.

The prediction of the strain value from the mathematical modelling was related to the geometric model of the cylindrical shape as well as the human body shape and the Laplace's law theory was taken into account. This modelling confirmed the correctness of the strain results by mathematical modelling to calculate the elastic coefficient from the stress-strain curve.

The formulas of patternmaking were derived from elastic coefficient which were applied to the human body under a certain pressure that is necessary to ensure the amount of pressure required for CG applications. A default algorithm has been developed in order to calculate the size of pattern construction net only in particular part as a cylindrical shape of body including fuselage, arms, thighs etc.

This algorithm has successfully been tested to create an automated the block pattern by the PDS Tailor XQ with CAD system which allows the structural segment lines to be modified by inputting the parameter of elasticity coefficients in both ECW and ECL.

The goal of this thesis was successfully realized as well as the problematic area of patternmaking design of clothing for stretch fabrics. At the same time, calculation of the size of pattern construction abscissa investigated the clothing pressure capability was solved by the pilot project.

Keywords: patternmaking; construction abscissa; compression garments; stretch fabric; elastic coefficient; pressure

Anotace

Elastické plošné textilie se ve velké míře využívají pro výrobu oděvů přiléhavé siluety. V některých případech se jedná o kompresní oděvy (dále jen KO). Jejich charakteristickou zvláštností je tlak, kterým působí na tu část těla, na kterou jsou navlečeny, za předpokladu že existuje rozdíl mezi rozměry těla a rozměry výrobku. Mohou to být sportovní oděvy, tvarovací prádlo, oděvy určené pro tlakovou léčbu, apod. Pro jejich navrhování je důležitá znalost metody výpočtu rozměrové deformace při určitém tlaku, jímž výrobek působí na povrch lidského těla. Snahou výrobců KO je tedy vytvořit takový tvar stříhové konstrukce, který odpovídá nejen tělesným rozměrům předpokládaného nositele, ale také tvaru těla a v neposlední řadě mít schopnost vhodně definovat závislost mezi fyzikálně mechanickými charakteristikami (silovými) plošné textilie, z které bude elastický oděv vyrobený, a tlakem kterým výrobek působí na povrch lidského těla. To však vyžaduje teoretický a praktický výzkum, který je orientovaný na vývoj výpočtových metod uplatňovaných v procesu navrhování elastických výrobků.

V této práci je experimentálně měřena roztažnost vybraných elastických pletenin na trhačím zařízení, která je charakterizována poměrným protažením při stanoveném zatížení. Důvodem je to, že když se elastický oděv menších rozměrů než je tělo natáhne silou na jeho povrch, vyvolá se jeho rozměrová deformace. Tato vlastnost plošné textilie, která je vyjádřena koeficientem pružnosti, nám pomůže zlepšit metodu tvorby stříhové konstrukce. Bude mít významný vliv na stanovení přesných hodnot konstrukčních úseček v závislosti na požadovaném tlaku vybrané textilie. Z tohoto důvodu, cílem této práce je vývoj metody pro definici stříhových konstrukčních parametrů KO výpočtovou metodou tak, aby bylo dosaženo přesného tvaru a velikosti stříhových dílů v závislosti na potřebném specifickém tlaku.

Postup experimentálního zkoumání je rozdělen do dvou kroků:

1. definice metody pro stanovení rozměru určité konstrukční úsečky v konstrukční síti tak, aby bylo možné vypočítat změnu velikosti této úsečky na základě změny odpovídajícího rozměru lidského těla nebo jeho části.
2. definice metody pro výpočet koeficientu pružnosti elastické plošné textilie, uplatněné na výrobku tak, aby vyjadřoval jeho žádanou svěrnou schopnost a bylo tak možné provádět odpovídající rozměrové korekce konstrukčních úseček.

V první etapě práce se řeší problém popisu geometrie konstrukční sítě. Byla vybrána výpočtová metoda, s uplatněním typu regresní rovnice, pomocí které lze vypočítat rozměr konstrukční úsečky (závisle proměnné veličiny) na základě změny tělesného rozměru (nezávisle proměnné veličiny). Byl zkoumán 2D model stříhu dámského elastického výrobku, a to trupová část válcového tvaru.

V druhé etapě práce se řeší problém tlaku, jímž má výrobek působit na příslušnou část těla, a otázka jak ovlivní rozměr stříhové konstrukce. Použití vhodné metody pro stanovení koeficientu pružnosti plošné textilie (závisle proměnné veličiny) na základě změny tlaku

(nezávisle proměnné). Následně jsou hodnoceny vybrané druhy elastických pletenin s cílem zjistit hodnotu koeficientu pružnosti, který bude uplatněn při modifikaci délkových a šířkových konstrukčních úseček. Koeficient pružnosti pro šířky je zjištěn z výsledků hodnocení křivky napětí-deformace, zatímco koeficient pro délky byl zjištěn pozorováním deformace napnuté pleteniny jednosměrným zatížením a vyhodnocen analýzou digitálního obrazu pomocí SW MATLAB a SW NIS-Element. Predikce hodnoty deformace z matematického modelování se týkala geometrického modelu válce, válcové části lidského těla a teorie Laplaceova zákona. Toto modelování potvrdilo správnost výsledků zjištěné deformace pleteniny prostřednictvím matematického modelování a definici koeficientu pružnosti z křivky napětí-deformace.

Pomocí vzorců, které byly odvozeny pro výpočet koeficientu pružnosti elastické plošné textilie, která působí na lidské tělo pod určitým tlakem a které jsou nutné pro zajištění požadované hodnoty svěrné síly výrobku, byl vypracován výchozí algoritmus pro výpočty optimálních parametrů stříhové konstrukce. Zejména částí, které pokrývají trup, paže, stehna a lze je geometricky definovat jako válec.

Tento konstrukční algoritmus byl úspěšně ověřen při tvorbě automatizované stříhové konstrukce dámského tílka v prostředí CAD systému PDS Tailor XQ, který umožňuje korekce konstrukčních úseček prostřednictvím koeficientu elasticity materiálu jak ve směru šířky, tak délky. Cíl práce byl úspěšně realizován. Byla pilotně vyřešena problematika související s navrhováním elastických oděvů a výpočtem konstrukčních parametrů v souvislosti se zkoumáním svěrné schopnosti oděvu.

Klíčová slova: Stříhová konstrukce, konstrukční úsečka, kompresní oděv, elastická plošná textilie, koeficient pružnosti, tlak.

คำนำ

ผ้ายัดได้รับความนิยมกันอย่างแพร่หลายในการผลิตเสื้อผ้า โดยเฉพาะอย่างยิ่งเสื้อผ้าที่ทำให้เกิดความคัน ประสิทธิภาพของเสื้อผ้าความคันเกิดจากค่าความคันที่เหมาะสมเพื่อให้ตรงกับวัตถุประสงค์การใช้ประโยชน์ ในขณะที่อุตสาหกรรมการผลิตเสื้อผ้านั้นใช้ประสบการณ์ในการทำงานของตัวเองการสร้างแบบตัด และมีหนังสือน้อยเล่มที่ดีพิมพ์วิธีการทำแบบตัดผ้ายัดโดยประมาณการลดขนาดแบบตัดจากความสามารถในการยืดของผ้า ซึ่งการลดขนาดแบบตัดดังกล่าวนี้ไม่มีประสิทธิภาพเพียงพอที่จะได้รับค่าความคันที่ตรงต่อความต้องการ เนื่องด้วยคุณสมบัติเชิงกลของผ้าที่แตกต่างกันและระดับของการบีบรัดเสื้อผ้านั้นเกิดจากขนาดของแบบตัด

จุดมุ่งหมายของวิทยานิพนธ์ฉบับนี้เพื่อกำหนดวิธีการทำแบบตัดของผ้ายัด เพื่อที่จะได้ขนาดของแบบตัดที่ถูกต้องตามความคันที่ต้องการ การออกแบบการทดลองได้กำหนดตัวแปรหลักสองตัวคือค่าสัมประสิทธิ์ยืดหยุ่นด้านความกว้าง และค่าสัมประสิทธิ์ความยืดหยุ่นด้านความยาว กล่าวถึงค่าของสัมประสิทธิ์ยืดหยุ่นด้านความกว้างนั้นได้จากผลของค่าของความเค้น-ความเครียด และทฤษฎีความดันของลาปลาซ จากนั้นได้ทำประยุกต์เป็นสูตรคณิตศาสตร์สำหรับการคาดการณ์ค่าของความเครียดที่ขึ้นอยู่กับค่าความคันที่ต้องการ ในขณะที่ค่าสัมประสิทธิ์ความยืดหยุ่นด้านความยาวได้มาจากการประมวลภาพเพื่อที่จะหาการเสียรูปทรงของผ้า โดยใช้ซอฟต์แวร์ของ MATLAB และ NIS-Element มาประยุกต์ใช้เพื่อหาค่าของการเสียรูปทรงของผ้า

นอกจากนี้การประยุกต์ใช้สูตรคณิตศาสตร์ได้ถูกตรวจสอบและเปรียบเทียบค่าความคันกับเครื่องวัดความคันโดยใช้โมเดลทรงกลมในการทดลองที่มีปัจจัยที่แตกต่างกัน การประยุกต์ใช้สูตรคณิตศาสตร์นี้ประสบความสำเร็จในการคาดการณ์ค่าความเครียดที่ได้ผลแม่นยำ

วิทยานิพนธ์ฉบับนี้ได้ค้นพบการศึกษาความรู้ทางวิศวกรรมแบบตัดเสื้อผ้าและเทคโนโลยีเพื่อให้บรรลุวัตถุประสงค์ในการทำแบบตัดของผ้ายัดอย่างเป็นระบบ ข้าพเจ้าหวังว่าวิทยานิพนธ์ฉบับนี้จะเป็นประโยชน์ต่อโรงงานอุตสาหกรรมเสื้อผ้าที่ผลิตเสื้อผ้าความคัน โดยใช้วิธีทางวิทยาศาสตร์ในการหาค่าของขนาดแบบตัด

Table of Contents

Table of Contents.....	i
Chapter 1 Introduction	1
1.1 Introduction.....	1
1.2 Objectives	5
1.2.1 Study of fundamental block pattern garment to define mathematical formulas for pattern abscissa.....	5
1.2.2 Study of mechanical properties of stretch fabrics and their performance evaluation.....	6
1.2.3 Defining the relationship between stress- strain behaviour and pressure theory to apply on patternmaking.....	6
1.2.4 Development of patternmaking method for specific pressure clothing by using elastic coefficient.....	6
1.3 Research approach and outline	7
Chapter 2 State of the Art in Literature.....	8
2.1 Stretch fabric	8
2.2 Patternmaking	8
2.2.1 Patternmaking for clothing	9
2.2.2 Patternmaking for compression garment	10
2.3 Compression garments.....	12
2.3.1 The application of compression garment	12
2.3.1.1 Medical application.....	12
2.3.1.2 Athletic application.....	12
2.3.1.3 Body shaping application	12
2.3.2 Pressure range of compression garment and applications.....	13
2.4 Application of pressure theory on fabric garment	15
2.4.1 Laplace's law theory.....	15
2.4.2 Stress in thin-walled pressure vessels	17
2.4.3 Related literature reviews on compression garment.....	18
2.5 Interface Pressure Measurement System	19
2.5.1 The effect of the sensor thickness	21
2.6 Elastic properties for CG	22
2.6.1 Elongation.....	23
2.6.2 Structure of Knitted fabrics.....	23
2.6.3 Weight.....	25
2.6.4 Thickness.....	26
2.6.5 Deformation of elastic fabric	26
2.6.5.1 Poisson's ratio.....	27
2.6.5.2 Longitudinal deformation.....	27
2.6.5.3 Transverse deformation.....	28
2.6.6 Engineering strain.....	28

2.6.7 Engineering stress.....	28
2.6.8 Tensile strength.....	28
2.6.9 Young's modulus and stiffness	29
2.6.10 Elasticity recovery.....	30
2.6.11 Stress relaxation.....	31
2.6.12 Dynamic work recovery	32
Chapter 3 Experimental Materials and Methods.....	33
3.1 Materials	33
3.2 Methods.....	33
3.3 Patternmaking development method for pressure garments	35
3.3.1 Determination of body measurement	35
3.3.2 Analysis of patternmaking for pressure garments.....	37
3.3.2.1 Determination of the patternmaking modification	38
3.3.2.2 Determination of elastic coefficient.....	40
3.3.2.3 Applying the elastic coefficient coordinate with standard sizing system	42
3.3.2.4 Applying the patternmaking method by CAD software	43
3.4 Fabrics performance for pressure garments	43
3.4.1 Mechanical properties of stretch fabrics	43
3.4.1.1 Determination of weight per unit area	43
3.4.1.2 Determination of thickness	44
3.4.1.3 Determination of wale and course per unit length	44
3.4.1.4 Determination of strength and elongation properties	44
3.4.1.5 Determination of stress-strain behaviour.....	44
3.4.1.6 Determination of the elasticity	45
3.4.1.7 Determination of the stress relaxation	46
3.4.2 Fabric deformation measurement by image analysis	48
3.4.2.1 Determination of fabric deformation measurement using MATLAB.....	48
3.4.2.2 Concept of gradient deformation tensor.....	49
3.5 Applying the Laplace's law for CG and evaluating the pressure	50
3.5.1 Applying Laplace's law theory to practice on pressure garment	50
3.5.2 Prediction of strain value using the mathematical modelling.....	52
3.5.3 Designing experiments to investigate the mathematical modelling with the compression tester.....	53
3.5.3.1 Determination of measuring the pressure in vitro model.....	53
3.5.3.2 Effect of sensor thickness for measuring the pressure	54
3.5.3.3 Determination of measuring the pressure in vivo model.....	56
3.5.4 Designing experiment to predict the strain of pressure garments	56
3.5.4.1 Determination of predicted strain by applying compression tester	56
3.6. Development and application of a novel tensile measurement device	57
3.6.1 Designing the novel tensile device	57
3.6.2 Determination of the elasticity	58
3.6.3 Determination of fabric deformation measurement using NIS-Element.....	59
Chapter 4 Results and Discussion	60

4.1 Mechanical properties of elastic fabrics suitable for CGs	60
4.1.1 Preliminary testing of elastic fabrics to obtain preliminary data of fabrics.....	60
4.1.2 Physical testing for performance and serviceability of fabrics.....	60
4.1.2.1 Force and elongation characteristics.....	60
4.1.2.2 Stress and strain behaviour	62
4.1.2.3 Elasticity.....	64
4.1.2.4 Stress relaxation.....	66
4.1.2.5 Dynamic work recovery.....	68
4.2 Characterization of stretch fabric tensile deformation by image analysis	69
4.2.1 Validation of results with simulated images	69
4.2.2 Fabric deformation image was extended by tensile testing machine.....	70
4.2.3 Comparison of fabric deformation with Engineering stress and True stress	73
4.2.4 Prediction of elastic coefficient of ECL from fabric deformation.....	73
4.3 Application of Laplace's law pressure theory on pressure for garments.....	74
4.3.1 Applying the mathematic modelling for prediction of the strain value	75
4.3.2 Evaluation of mathematical modelling of pressure garments.....	77
4.3.2.1 Measurement of pressure garments in vitro model	77
4.3.2.2 The effect of the sensor thickness in vitro model	79
4.3.2.3 Measurement of pressure garments with different circumferences.....	82
4.3.2.4 Measurement of pressure garments in vivo model	84
4.3.3 Evaluation of mathematical modelling for prediction of the strain value	86
4.4 Performance of novel tensile measurement device.....	88
4.4.1 Measurement of fabric properties by novel tensile measurement device.....	88
4.4.2 Fabric deformation image by manual tensile testing.....	91
4.5 Defining patternmaking development procedure for stretch fabrics	93
4.5.1 Body measurement	93
4.5.2 Investigation of elastic fabric performance	94
4.5.3 Patternmaking development method for stretch fabrics	96
4.5.4 Application of patternmaking reduction with standard sizing system	98
4.5.5 Application of patternmaking by using PDS tailor XQ software	99
Chapter 5 Summary and Conclusions	102
5.1 Summary	102
5.2 Conclusions from the research.....	102
5.3 Recommendation from research	105
References.....	107
Research Outputs	117
Curriculum Vitae.....	120
Appendix.....	121

List of f Figures

Figure 2.1	The basic plain method for patternmaking.....	9
Figure 2.2	The basic block patternmaking for compression garment	10
Figure 2.3	Fabric grain lines where the pattern was used the direction for cutting.....	15
Figure 2.4	A small rectangle directions and the surface contact acting with the curvature	16
Figure 2.5	The cylindrical vessels free-body diagram of thin-walled pressure vessels	17
Figure 2.6	The PicoPress® devise of the interface pressure measurement system.....	19
Figure 2.7	Schematic representation of the interface perturbation effect of a sensor placed beneath an extensible bandage over a curved surface	21
Figure 2.8	Typical stress-strain diagram indicating the various stages of deformation.	26
Figure 2.9	Deformation of longitudinal and transversal under tensile loading	27
Figure 2.10	Typical load-extension characteristic curve for a weft-knitted fabric.....	29
Figure 2.11	Typical cycling graph.....	30
Figure 2.12	Graph of force and elongation in hysteresis loops	31
Figure 2.13	Stress response to the stress relaxation test.....	32
Figure 2.14	Dynamic work recovery	32
Figure 3.1	A schematic flowchart of the procedure patternmaking development for stretch fabrics	34
Figure 3.2	The women body measurement chart.....	36
Table 3.2	Women body measurements of the mannequin.....	36
Figure 3.3	The 3D images with point marks using sense TM 2 3D scanner.....	37
Figure 3.4	The 3D images of body cross sections	37
Figure 3.5	Conventional block pattern relationship to the body measurement	38
Figure 3.6	Analysis patternmaking for pressure garment based on pressure area.....	39
Figure 3.7	Deformation changed of stretch fabric of circumferential and lateral strain	41
Figure 3.8	Schematic diagram of patternmaking development relate to a circle shape	41
Figure 3.9	Construction abscissa of 2D pattern net and 3D garment	42
Figure 3.10	Schematic diagram the tensile testing machine.....	45
Figure 3.11	The setting method for testing stress relaxation.....	46
Figure 3.12	Comparative the DWR with different cycle of loading-unloading	47
Figure 3.13	Experimental for setup for image analysis	48
Figure 3.14	Concept of gradient deformation tensor.....	49
Figure 3.15	Image processing steps.....	50
Figure 3.16	Fabric stretch showing the force directions on the cylindrical model.....	51
Figure 3.17	Fabric tension acting on cylindrical model	52
Figure 3.18	The sensor area of compression tester.....	54
Figure 3.19	The sensor of compression tester acting under fabric stretched on the cylindrical model	55
Figure 3.20	The Schematic design of the tensile measurement device	57
Figure 3.21	The experimental design and testing of manual tensile testing device	58

Figure 3.22 The experimental design for capturing the images from manual tensile testing device.....	59
Figure 4.1 Graphs of force-elongation characteristics in different directions	61
Figure 4.2 Graphs Stress-strain different directions of 8 samples.....	63
Figure 4.3 The hysteresis loops 5 th cycle of S7 in course direction	64
Figure 4.4 Graphs comparative the influence of elastane composition on force decay and elastic recovery	65
Figure 4.5 Comparative the stress relaxation over the time	67
Figure 4.6 Graphs of Dynamic Work Recovery at the fifth cycle of eight samples.....	68
Figure 4.7 Simulated images from MATLAB image processing toolbox.....	70
Figure 4.8 Gradient deformation tensor for course direction by tensile testing machine...	71
Figure 4.9 Deformation behaviour of stretch fabric of the sample S6	72
Figure 4.10 The comparative the stress values between TS and ES	73
Figure 4.11 The prediction of elastic coefficient of the sample S6	74
Figure 4.12 The actual mechanical characteristic from stress-strain curves	75
Figure 4.13 The stretch fabric effect of pressure and diameter on the strain	77
Figure 4.14 Comparison of pressure values between predicted pressure and measured pressure.....	79
Figure 4.15 Effect of sensor thickness under fabric stretched on rigid cylindrical model .	79
Figure 4.16 Effect of sensor thickness between correction factor and C_{pp}	80
Figure 4.17 Comparison of the pressure values methods with circumference at 0.79 m. .	82
Figure 4.18 Comparison of the pressure values methods with circumference at 0.505m. .	84
Figure 4.19 Measurement of pressure values between vitro model and vivo model	84
Figure 4.20 Comparison of S6 pressure values with different models between vitro and vivo	85
Figure 4.21 The correlation of predicted strain VS experimental strain of sample S3, S4, S5 and S6	87
Figure 4.22 Comparison of fabric property results of sample S6 between manual test and standard test.....	89
Figure 4.23 Comparison of fabric property results of sample S7 between manual test and standard test.....	90
Figure 4.24 The fabric deformation of the sample S7	92
Figure 4.25 The prediction of the elastic coefficient (ECL) of sample S6, S7 and S8.....	92
Figure 4.26 The graphs of cross sections and circumferences with different parts of the body	93
Figure 4.27 The block patternmaking chart.....	97
Figure 4.28 The reduction of patternmaking method based on fabric tensile property of sample S7.....	98
Figure 4.29 The patternmaking by applying PDS Tailor XQ software	100

List of Tables

Table 2.1 The acceptance of the pressure value range of CG by literatures.....	14
Table 2.2 The classification of elastic fibre	23
Table 2.3 Comparison of appearance and properties of knitted structures [93]	25
Table 3.1. Elastic knitted fabrics characteristics.....	33
Table 3.2 Women body measurements of the mannequin.....	36
Table 4.1 Elastic knitted fabric characteristics	60
Table 4.3 The properties of UTS, strain and Young's modulus with difference directions	64
Table 4.4 The elasticity properties of knitted fabrics in course direction.....	65
Table 4.5 The One-way ANOVA analysis of influence effect of the elastane on force decay and elasticity	66
Table 4.6 The stress relaxation and stress performance between initial and final holding strain at 0.5	67
Table 4.7 The results of fabric energy between loading-unloading and DWR%	69
Table 4.8 Results of gradient tensor deformation in vertical direction.....	72
Table 4.9 Prediction of extension deformation behaviour of knitted fabrics using different fabrics directions.....	72
Table 4.10 Fabric deformation of later strain and elastic coefficient	74
Table 4.11 Prediction of elastic coefficient ECL.....	74
Table 4.12 The coefficients of the 3 rd order polynomial fitting-lines.....	76
Table 4.13 Comparison of S3 pressure values between predicted pressure and measured pressure	78
Table 4.14 Comparison of S4 pressure values between predicted pressure and measured pressure	78
Table 4.15 Comparison of S5 pressure values between predicted pressure and measured pressure	78
Table 4.16 Comparison of S6 pressure values between predicted pressure and measured pressure	78
Table 4.17 Comparison of S3 pressure values in three different methods at 0.79 m circumference	80
Table 4.18 Comparison of S4 pressure values in three different methods at 0.79 m circumference	81
Table 4.19 Comparison of S5 pressure values in three different methods at 0.79 m circumference	81
Table 4.20 Comparison of S6 pressure values in three different methods at 0.79 m circumference	81
Table 4.21 Comparison of S3 pressure values in three different methods at 0.505 m circumference	83
Table 4.22 Comparison of S4 pressure values in three different methods at 0.505 m circumference	83

Table 4.23 Comparison of S5 pressure values in three different methods at 0.505 m circumference	83
Table 4.24 Comparison of S6 pressure values in three different methods at 0.505 m circumference	83
Table 4.25 Comparison of pressure values with different models between vitro and vivo of sample S6.....	85
Table 4.26 Comparison of S3 strain values between experimental strain and predicted strain	86
Table 4.27 Comparison of S4 strain values between experimental strain and predicted strain	86
Table 4.28 Comparison of S5 strain values between experimental strain and predicted strain	86
Table 4.29 Comparison of S6 strain values between experimental strain and predicted strain	87
Table 4.30 The correlation of predicted strain VS experimental strain of sample S3, S4, S5 and S6	88
Table 4.31 The fabric extension values of sample S6 with different weights and cycle loading	88
Table 4.32 The correlation of the strain prediction of the sample S6 with different testing devices	89
Table 4.33 The fabric extension values of sample S7 with different weight and cycle loading	90
Table 4.34 The correlation of the strain prediction of the sample S7 with different testing devices	90
Table 4.35 The results of fabric deformation in strain, width and elastic coefficient	91
Table 4.36 Prediction of elastic coefficient by linear regression of samples S6, S7 and S8	93
Table 4.37 The predictive modelling of strain value of eight samples	94
Table 4.38 The results of predicted strain values with different parts of female body at 1.15 kPa pressure.	94
Table 4.39 The results of predicted strain values with different parts of the female body at pressure 2.4 kPa.....	95
Table 4.40 The size of patternmaking with different parts of the body under the pressure at 2.4 kPa	96
Table 4.41 The elastic coefficient for 2.4 kPa pressure in width and length dimensions in different body parts.....	96
Table 4.42 Fundamental of block patternmaking formulas	97
Table 4.43 Modification standard sizing system of body measurement by applying elastic coefficient	99
Table 4.44 Modification of the pattern construction abscissa PDS Tailor XQ software..	100

List of symbols

Symbol	Unit	Description
a	[m ²]	Area cross-sectional of the fabric
A	[m ²]	Surface contact area of the fabric
B_i	[m]	Body dimension
C	[m]	Circumference of the cylindrical model or the body
C_0	[m]	initial circumference of fabric
ΔC	[m]	fabric changed in circumference length
C_{PP}	-	Coefficient of pressure perturbation
C_{TP}	-	Coefficient of pressure perturbation due to local stretch
D	[m]	Diameter of the cylindrical model or the body
D_s	[m]	Sensor diameter
E_i	-	Elastic coefficient
ECL	-	Elastic coefficient in length dimension
ECW	-	Elastic coefficient in width dimension
F	[N]	Force on the surface contact / Force applied
h	[m]	Fabric thickness
h_s	[m]	Sensor thickness
k	[N.m ⁻¹]	Stiffness
K_i	-	Regression coefficient
l	[m]	Fabric stretched length
l_0	[m]	Initial fabric length
Δl	[m]	Fabric change in length
P	[Pa]	Pressure
q_i	-	Absolute term
R	[m]	Radius of cylindrical model
T	[N.m ⁻¹]	Tension of fabric stretched
U_i	[m]	Construction abscissa
w	[m]	Fabric width
w_0	[m]	Initial fabric width

Symbol	Unit	Description
Δw	[m]	Fabric change in width
δ	[m]	displacement produced by force
ε	-	Engineering strain
$\varepsilon_{Circumferential}$	-	Circumferential strain
$\varepsilon_{Lateral}$	-	Lateral strain
ε_{long}	-	Longitudinal deformation
ε_{trans}	-	Transversal deformation
σ	[Pa]	Fabric stress
σ_c	[Pa]	Circumferential stress
σ_l	[Pa]	Longitudinal stress
φ	[°]	Angle of surface area of fabric stretched

List of Abbreviations

Abbreviations	Description
2D	Two-dimensional
3D	Three-dimensional
ASTM	American Society for Testing and Materials
CAD	Computer Aided Design
CG	Compression Garment
CRE	Constant-rate-extension
DWR	Dynamic Work Recovery
EA	Elastane
ECW	Elastic Coefficient in Width dimension
ECL	Elastic Coefficient in Length dimension
ES	Engineering stress
FEA	Finite Element Analysis
GSM	Gram per Square Meter
mmHg	Millimetres of Mercury
PA	Polyamide
PMM	Pattern Metric Method
PVC	Polyvinyl Chloride
TS	True stress
UTS	Ultimate tensile strength

Chapter 1 Introduction

This chapter consists of an introduction and objective of this research work described in the thesis. The first part describes the motivation to perform the experimental and analytical work included to approach of the study. In the next section, explanations of objective and step for the implementation process of developing the patternmaking method for stretch fabric will be discussed. In the last part, summary of thesis content will be illustrated followed by a chapter that discusses the potential contribution of this thesis in field of garment patternmaking.

1.1 Introduction

Compression garments (CG) is a special type of clothing that has widely been researched and utilized in the fields of medical, athletic and body shaping applications [1, 2]. The method to help produce CG is rather challenging to achieve especially its specific pressure that depends on the aforementioned application functions. Due to the types of CG are different proposes, therefore, there is a need for differential pressure value for the right performance based on the types of CG [3, 4]. Currently, CG is mainly made from stretch fabric that consists of elastomeric fibre while its commonly used structure for production is the knitted one. This type of structure could be applied for enhancing the performance of CG for better extensibility and higher recovery rate that corresponds to the pressure from fabric stretched that comforts the wearer's body [5, 6]. In garment engineering, there is some confusion existing with patternmaking process of stretch fabric, especially, when attempting to coordinate the degree of extensibility inherent in stretch fabrics and the amount of modification needed to estimate the reduction size of patternmaking. Due to the mechanical property of each stretch fabric its unique and the stretch behaviour is insufficient and has the stretch capability differing in course and wale directions of the fabric. Systematic information about patternmaking methodology of the relationship between stretch fabrics and CG forms is less evident in the publication. For the abovementioned reasons, the researcher of this thesis has endeavoured in studying patternmaking for stretch materials in order to find out the solution for modifying the methodology of pattern abscissa that has an actual mechanical property of fabric.

The purpose of this thesis is to develop the systematic patternmaking method for stretch fabric according to the pressure required for customized CG and the four processes of the method are as follows:

1. Acquisition of body size measurement to achieve the actual size of the human body will be conducted.
2. Evaluation the performance of the mechanical property and deformation of stretch fabrics.
3. Estimation of patternmaking size will be done by making prediction of strain value based on the relationship between Laplace's Law theory and the result of stress-strain curve.
4. Development of a new method of patternmaking for stretch materials using CAD systems and inputting the parameter of the elastic coefficient will be done in order to automate the pattern construction abscissa under the regression formula of construction abscissa [2, 7].

Throughout this research dissertation, various sections on Clothing Patternmaking Method for Stretch Fabrics will be provided and discussed in order to provide useful information and clarification on the matter as found below.

Performance of stretch fabrics for garment applications

The extensibility, they can be classified into low elastic fibre with an elongation range from 20%-150%, medium elastic fibre with an elongation range from 150% to 390% which the elastic requirements low or medium of elastomeric fibre could meet for sportswear or body shaping garments. While for the medical purpose should be used high elastic fibre with an elongation up to 400% to 800% to obtain the desired pressure [8, 9].

Elastic recovery, Senthilkumar and Anbumani reported that the dynamic elastic recovery value has an effect on force value when extension of clothing is conducted [10]. For the principle ideal dynamic elastic recovery, the value of force-elongation when fabric was applied loading and repeating should be equal; however, in reality, the force-elongation curve during the first loading potentially has the highest value numbers and the number of force value would drop in the later stages of testing. Nevertheless, Khaburi J. A., Dehghani-

Sanij and et al. have selected the results of loading at the forth cycle of force-elongation curves to analyse a good approximation [11] and Kowalski, Mielicka and et al. also used force-elongation curves in the fifth cycle of loading test [12].

Stress relaxation is one of the important effects on the time during wearing the CG, the interface pressure of clothing was loosed by force decay of fabric stretched. Largely, the CG for medical application has to be worn 23 hours per day therefore the fabric stress under extension for a long and continuous time before the pressure was decayed [13]. Under the condition to wear the CG the research should be concerned about the pressure performance over a prolonged period of time in case of CG for medical application.

Application of pressure theory on stretch fabric for CG

Related to numerous research works, many researchers had decided to apply the force of stretched fabric on the body circumference based on the Laplace's Law theory during their experimental studies in order to make calculation on the pressure value for CG [13, 14, 15, 16, 17] and evidences had been found as follows, for example, Kowalski, Mielicka and et al. used the Laplace's Law theory and assumed the body as the cylindrical shape to predict the pressure and design the compression garments [12] and they analysed the characteristics of knitted vascular prostheses to predict the modelling for determination of circumferential longitudinal force depending on the prosthesis pressure and diameter [14]. Zhao, Li and et al. applied Laplace's Law theory to design the compression sleeves [18] while Chattopadhyay and Bera he developed the pressure prediction of elastic fabric tube based on the principle energy of fabric by using the results from loading elongation graph which was found that the measured pressure numbers on the cylindrical model were to be closer to actual measured values [19].

According to the fabric thickness, pressure is considered to be depending on the fabric tension and the radius of the body based on Laplace's Law theory where wall thickness is not take into account and therefore, Khaburi, Dehghani-Sanij and et al. predicted that for the calculation of interface pressure values based from circumferential stress in thin-walled cylinder theory and thick-walled cylinder theory, those pressure values were being calculated and compared. On one hand, they found that the values of pressures estimated by two models were about 1.8% differences with fabric thickness at 1.2 mm and 35 mm of limb

radius. On the other hand, the large cylinder radiuses larger than 55 mm the pressure results were significantly close [11]. Moreover, Macintyre, Baird and et al. also found that the model was able to predict pressure values accurately when cylinders hold longer length of diameters while the pressures were overestimated when cylinders possess with shorter length of diameters [20]. With these reasons, the prediction for pressure garment assumed that the fabric thickness should be negligible when compared with the human body radius.

Pressure measurement

It could evidently be found measurement of pressure for CG consists two types of methods are including static pressure and dynamic pressure and at the same, regarding the characteristics of model for pressure measurement two types of the model including vitro which is related to the artificial model [21] and vivo being used as living organism model for measuring [2] are found.

The pressure measurement device is necessary for sensor thickness to be considered due to the sensor thickness has the effect on the pressure perturbation when measured pressure [6, 11, 22], in this research is used PicoPress® which is one of the most common types of pressure transducers used to measure the interface pressure under compression of clothing pressure. due to the sensor thickness at 3 mm [23] and when the sensor is measured at the fabric area, the radial component of the tension in the fabric increases hence a higher local pressure is described by Vinckx and Boeckx [22]. With the mentioned reason, they reported that it is necessary to solve the correction factor or perturbation coefficient of this issue to find out a real pressure of fabric stretch.

Moreover, the PicoPress® has been widely accepted by many researchers for its efficacy of measurement in field of garment including Partsch and et al. who reported that the pneumatic device has the advantages of their financially accessibility and their thin and flexible features [24]. The PicoPress® was used by Partsch and Mosti to study thigh compression garment [25] while, Mosti and Rossari represented that the linearity and repeatability of this transducer are respectable [26]. Moreover, they have correspondingly reported that the PicoPress® outperformed Kikuhime® and the SIGaT®. Nevertheless, PicoPress® device has also possess some disadvantages as mentioned by Khaburi, Dehghani-Sanij and et al. as

mentioned in their research that the device overestimated the result of pressure value during the measurement of compression clothing.

Patternmaking method

The patternmaking technique to achieve the specific pressure of CG by finds out the elastic coefficient use to determine how amount of patternmaking size was reduced which smaller size than the body circumference. The Authors Musilová and Nemčoková suggested that the patternmaking for CG due to mechanical properties of fabric stretched should be calculated using regression equations that each of them consists of the sum of characteristics that influence a pattern shape and pressure of clothing [27, 28]. Concerning the reduction factor for CG, the author Hatch recommended the range of reduction factor of patternmaking is used between 35% - 50% of their body circumference [29] and the maximum of the reduction factor at 50% for controlling the shape and proportion of clothing. While the deformation of fabric during stretch should be considered as authors Baheti, Jariyapunya and Tunák revealed in their research work concerning the deformation of elastic fabric under different stretch levels and found that the fabric was deformed depending on the extension level where in longitudinal direction of the fabric was stretched and the other side or transversal direction was shrunk [30, 31]. Therefore, for patternmaker, the behaviour of stretch fabrics in mechanical property and deformation during fabric stretching should be studied.

1.2 Objectives

The aim of this research study is to develop a new method of patternmaking for stretch fabric focusing and implementing specifically for the upper part of female body. Additionally, the pressure value of clothing will also be determined by applying Laplace's Law formula into the mathematical model of the strain values of fabric stretched to find out the reduction of elastic coefficient for producing the patternmaking of CG. Thus, the main objectives of this research are four-fold as follows:

1.2.1 Study of fundamental block pattern garment to define mathematical formulas for pattern abscissa

The block pattern for garment is considered the first step before any modification to reach the advance design and thus, main parameters for making the pattern construction abscissa

of body measurements should be defined predominantly in order to elicit mathematical formulas for making pattern construction abscissa. This research will focus on the upper part of female and use a mannequin according to European standard size 38 for investigation before applying with 3D capturing technologies of 3D scanner so as to find out the somatotype of the body in 3D which can further provide more details on the body measurement.

1.2.2 Study of mechanical properties of stretch fabrics and their performance evaluation

The objective of this study is to evaluate the performance of stretch fabrics undergoing stretch and the properties of stretch fabrics were compared with different factors of elastane composition and knitted structures. The fabrics properties will be tested for stress-strain behaviour using Testometric universal testing machine based on standard EN ISO 13934-1 for testing tensile properties, the standard BS EN 14704-1 for testing the elasticity of fabrics as well as the fabric behaviour of stress relaxation, DWR and deformation were analysis in order to evaluate the fabric performance into the right applications for CG.

1.2.3 Defining the relationship between stress- strain behaviour and pressure theory to apply on patternmaking

In this part of the research, development of mathematical modelling will be achieved by applying the relationship between the pressure theory of Laplace's law and the result of stress-strain curve. The focused objective is to predict strain value according to specific pressure required and predicted strain result can then be calculated the ECW.

1.2.4 Development of patternmaking method for specific pressure clothing by using elastic coefficient

The aim of the thesis is to develop the patternmaking method from the pressure required by using the results of fabric property and fabric deformation from the aforementioned experiments to find out two mains elastic coefficients of ECW and ECL. Next, define the main body area to obtain the pressure in clothing and modify the size of the fundamental block pattern by applying the ECW and ECL into the construction abscissa formulas.

Moreover, the patternmaking technology of CAD used in this research is PDS tailor XQ software and a method for calculation of the construction abscissa formula under the

regression equation so called UNIKON+ will be used in this research. Through this special software, an input of elastic coefficient of ECW and ECL into the parameters function will be applied and then an automation of patternmaking from the obtaining parameters determination will be done for last process.

1.3 Research approach and outline

This thesis was organized into five chapters as follows:

Chapter 1 introduction: Begins by discussing general introduction of this research work such as motivation and detailed research objectives of this thesis.

Chapter 2 State of the Art in Literature: This chapter contains theoretical background, published literature and detailed study of previous articles and understanding of studies conducted, limitations and the current state of the problem in past research.

Chapter 3 Experimental Materials and Methods: Describes the methodology of this research, which includes experimental materials, test equipment and data acquisition used for all experiments performed in this study. This chapter also contains elaborate explanation about theory of Laplace's law was applied to fabric stretched and described the mathematic modelling results from tensile testing.

Chapter 4 Results and Discussion: Results and discussion section of the detailed analysis of the results derived from various experiments. The data and calculated results from elastic fabrics properties and all experiments were tabulated, suitable graphical representations made and detailed statistical analysis was performed. Various interpretations were drawn from the analysis.

Chapter 5 Summary and Conclusions: The final chapter summarizes all the results from the experiments have done and present the new findings from research work. Moreover, section discussing future research and recommendation has been included.

Chapter 2 State of the Art in Literature

In this chapter has integrated the related works of literature and theoretical studies used as a basis for the thesis work. The research conducted in this thesis focussed on the scientific method to predict the size of patternmaking for CG being analysed to achieve specific pressure by reducing the size of circumference of clothing.

2.1 Stretch fabric

Recently, the demand of producing stretch fabrics in garment industry has been growing rapidly especially for sportswear and CG applications. Regarding stretch fabric characteristics, in general, they are defined into three types including one-way stretch which is the fabric that can only stretch across one side and the second one so called the two-ways stretch is the fabric that stretches in cross direction as well as up and down ones. For its properties, stretch fabrics is derived from yarn and stitches. While the four-ways stretch, made up of fibre composition of elastane (EA), places itself in cross, up and down direction [32, 33]. Usually, the stretch fabrics used in field of CG is mainly produced from knitted structure that contains 75%-80% of polyamide (PA) and 20% - 25% of EA [34].

The advantage of stretch fabric, how the fabric could recover itself to its original shape even when stretched repeatedly [34, 35] indicates that this characteristic could benefit the production of CG especially when the fabric itself provides fit well and achieves compression pressure to the body from the garment is stretched. Besides, stretch fabrics also has another advantage particular when the fabrics can be easily blended with either other synthetic materials or natural fibres to produce an overall fabric of brilliant quality and functionality [34].

2.2 Patternmaking

The section described the related studies of patternmaking for compression garment namely the basic of patternmaking, methodology to conduct the construction points of a patternmaking, the literatures of pattern for CG and the standard sizing system which is beneficial for garment production.

2.2.1 Patternmaking for clothing

Flat patternmaking is 2D of the basic way to achieve the pieces of clothing assembly process and in the past, they were used for cutting into the fabric in order to create the optimum size and best fit on the human body. At the very beginning, therefore, basic patternmaking so called “Bodice Sloper or Block Pattern” is used for creating natural line of the human body developed from specific size to represent fundamental shapes and sections of the precise body measurements as well as representing the basic dimension of patternmaking for clothing [36, 37]. When designing the clothing with different styles according to costumer or fashion, the block pattern was used for modifying the patternmaking.

The Authors (Musilová et. al, 2004) [38, 39] applied the Pattern Metric Method (PMM) to define the construction points based on the position on the human body surface and according to the number of construction steps. Figure 2.1, each plain position in horizontal plain's column will be represented in letters while, at the vertical plain column, each plain will be represented in a form of numbers and their definitions are described afterwards.

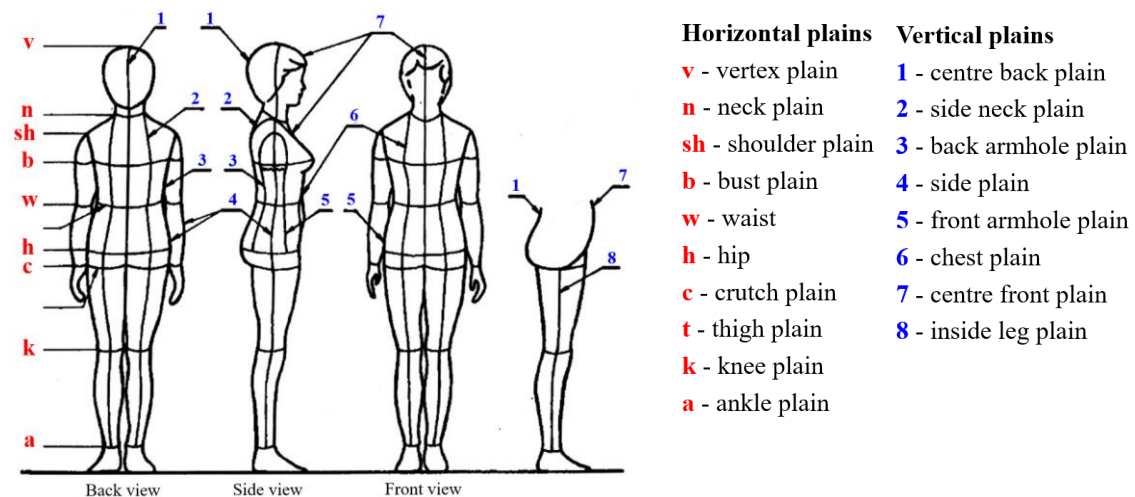


Figure 2.1 The basic plain method for patternmaking [38, 39]

The PMM is one of the possible ways to help understand pattern construction more thoroughly when considering the drafting of block for patternmaking. [5, 18]. The author (Watkins, 2011) designed and developed the block pattern for stretch fabrics without darts called Form Fit block pattern applied for analysing the body suite. He also reported that the optimized contour fitted pattern production for garment should have no wrinkles, minimal stretch distortion and very much conform to the body, rather like a second skin [40].

Therefore, the initial development of block pattern for stretch fabric uses the basis of T-shirt pattern or seamless technology to produce the CG. As shown in Figure 2.2, the illustration of PMM in 2D was used for developing pattern construction and inputting the remark points in vertical and horizontal plains.

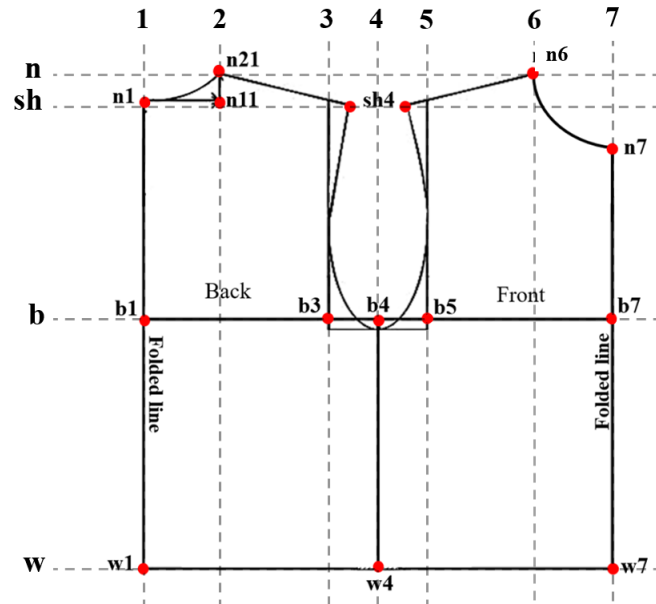


Figure 2.2 The basic block patternmaking for compression garment

2.2.2 Patternmaking for compression garment

Patternmaking has substantially been concerned as one of the most important processes of clothing production. Regarding as a main influential factor of pattern construction that affects production of CG, the interface pressure during wearing on the body [41, 42, 5] is referred to. The CG is generally applied to develop patterns and the dimensions of patterns optimized from the perspective of the stretch ability of elastomeric fabrics [43, 44].

Due to mechanical properties of stretched fabrics, the authors (Musilová and Nemčoková, 2013) reported that the patternmaking for CG should be calculated using regression equations that influence a pattern shape and pressure of clothing [27]. Consequently, the magnitude of pressure value of CG on the body can be reduced based on the size of patternmaking and therefore the mechanical property of elastic stretched fabric provides the appropriate or specific pressure.

Many researchers published the knowledge of pattern of compression garment methods to indicate the suitable fabric for pressure garments which are defined as custom made elastic knitted fabric that exert pressure on the body by virtue of the fact that they are made smaller than the body they are designed to fit [17, 45] and many publications use elastic fabrics for tight-fitting of garments as follows:

The authors (Ng, 1993; Macintyre and Baird, 2006; Macintyre, 2007; Macintyre et. al., 2007) they found that, normally a reduction factor from 5 to 20% of patternmaking size would be applied on different body parts to acquire the presumed pressure [46, 47, 45, 3].

The authors (Doan et. al., 2003) conducted the experiment of the compression garment had a reduction factor of 15% of pattern construction [48].

The authors (Chatard et. al. 2004) studied the experiment was used and found that the pressure garment should obtain the pressure range between 8 - 18 mmHg or 1 – 2.4 kPa [49]. Their results reported that wearing compression garment can also improve sporting performances and the athletes could enhance their performances and alleviate low back pain by wearing compression garments [48, 49].

The authors (Pratt and West, 1995) suggested a mathematical formula of pattern construction for GCs. Basically, all circumferential measurements are reduced by 20% and length measurements are reduced typically by 20%–25% of their total length [50].

The author (Hatch, 1993) found the range of reduction factor for tailored clothing is between 15% - 25%, for sportswear is between 20% - 30%, for active wear is between 35% - 50% and for form fitting garment is between 30% - 40% [29].

However, many researchers reported the reduction factor of pattern construction for CG by suggestion range of reduction factor which it is unprecise to get the specific pressure of clothing. Besides, the CG functions need the optimum range of pressure to get the right performance for garment applications. To create size of patternmaking for CG, therefore, the need of finding the mechanical property of stretch fabric to coordinate with patternmaking is inevitable. Interestingly, the publications and researches about the prediction of patternmaking size according to the specific pressure from the stretch ability of clothing pressure have not been involved to a great extent.

2.3 Compression garments

Compression garments are special clothing have been widely researched and utilized in the fields of medical, athletic and body shaping applications [1]. This part will be introducing main application functions of clothing pressure which is considered to be necessary to be paying attention on the values of constriction or elongation of garment parts depending on the mechanical properties of the elastic fabric, the morphology of the covering body parts, the specific level of required pressure, and the desired effect of shaping. Of these factors, compression pressure is considered a vital one.

2.3.1 The application of compression garment

2.3.1.1 Medical application: The authors (Staley et. al, 1997) reported that compression therapy has been used since 1947s for burn care and has been accepted to help minimize the formation of hypertrophic scars and enhance the maturation process of scars since 1970s [51, 52]. The authors (Partsh et. al, 2015 and Kerckhove et. al 2005) suggested the appropriate pressure is best kept for CG of the medical application should be approximate at 20-30 mmHg or 2.67 - 4.00 kPa [53, 54, 55]. They recommended the CG to be worn for daily 23 hours continually and it should be changed every 2 – 3 months to prevent diminishment in elasticity by (Zurada et. al, 2006 and Sharp et. al, 2016) [56, 57].

2.3.1.2 Athletic application: The CG uses for sport activities with moderate compression was used to enhance the performance of the athletes, decrease the possibility of injury, and accelerate the process of recovery [58, 59, 60, 61, 62, 63]. The Authors (Morooka et. al, 2001) found that the optimal effective and safe compression for swimsuit below 7.5 mmHg or 1 kPa exerted on a trunk was helpful for venous pump action as well as efficiency [64]. The authors (Xu et. al, 2012) reported from the physiological response by pressure developed by female swimsuit that there will be an influence on the pressure comfort during wearing , if the exerted pressure values of chest over 8.6 mmHg or 1.15 kPa, waist exceeded 2.7 mmHg or 0.13 kPa and abdomen exceeded 4.2 mmHg or 0.56 kPa [65].

2.3.1.3 Body shaping application: The benefit of CG can be employed to beautify the body shape and can be used for improving body attractiveness and morphology by compression on specific body parts to the required shapes [66, 67]. To successfully achieve these effects, (Little and Liu, 2012) has introduced the necessity of permissible range of garment pressure,

which has an influence on the physical, physiological, and psychological characteristics of the human body [68]. The author (Fan, 2005) reported the girdle is a typical type of pressure foundation wear worn by female to re-shape at the lower part of the body by uplifting the hips and compressing the abdomen in order to enhance the aesthetic appearance of the wearer and it should not create discomfort nor any detrimental effects on wearer's physiology [69]. Then the authors (Makabe et. al, 1991) studied the pressure of the girdle of the ten different positions and they reported the results that most people can bear relatively higher pressure about 11.5 mmHg or 1.53 kPa and prefer lower pressure about 4.5 mmHg or 0.60 kPa at the hip and the acceptable pressure for the waist part is about 6.5 mmHg or 0.87 kPa and the mean acceptable pressure is about 7.5 mmHg or 1.0 kPa [4].

2.3.2 Pressure range of compression garment and applications

The compression garments have many proposes depending on the functions of the customers need for their activities and the main key to conduct the CG is the specific level of required pressure which is effective and will help improve the performance during wearing.

Many researchers studied the compression garments as the authors (Chan and Fan, 2002) predicted optimal pressure distribution by studying the relationship between the compressive feeling and clothing pressure of tight girdle [67].

According for garment pressure and comfort sensations at the waist, (Makabe et. al, 1993) had observed that in the medium range of garment pressure 11- 18.4 mmHg or 1.47 - 2.45 kPa negligible or only slight discomfort is perceived [70].

The authors (Liu et. Al, 2013) presented results of pressure ranges for best compressive feeling tested at bust position. The results obtained by converting those ranges into bust girth range by applying calculation method for the bust girth design of pressure comfort for CG and the ranges were found to be 7.2 – 10.1 mmHg or 0.96 - 1.35 kPa [71].

Besides, author (Ito, 1995) had also presented pressure ranges that give most comfortable compressive feeling at different parts of the body and gave an assurance that comfortable girdle pressure on most parts of the body should be less than 9.5 mmHg or 1.27 kPa. The finding, nevertheless, also illustrated that at the waist position, higher girdle pressure around 13.2 mmHg or 1.76 kPa could be tolerated [72].

The author (Denton, 1972) defined the pressure beginning of discomfort to be approximately 44.1 – 73.5 mmHg or 5.88 – 9.80 kPa and the comfort zone the normal condition is 14.7 – 29.4 mmHg or 1.96-3.92 kPa depending on the individual condition of the treated body part and body position [73].

However, there are no standardized pressure comfortable range for compression garment on the upper part of the body. The pressure ranges from the literatures could be applied to determine the specific pressure and used as a guideline for calculating reduction factor of the patternmaking for compression garments. In Table 2.1, the optimal of the pressure value range according to the types function garments and body parts was obtained.

Table 2.1 The acceptance of the pressure value range of CG by literatures

Body part	Type	Pressure range		Description: Author
		kPa	mmHg	
Waist	waistband	1.47 - 2.45	11. - 18	Medium range of garment pressure: (Makabe et. al, 1993) [70].
Waist	girdle	1.76	13.2	Comfortable compression feeling of the girdle: (Ito, 1995) [72].
Waist	swimsuit	≤ 0.13	≤ 2.7	Female swimsuit that it will have an influence on the pressure comfort during wearing: (Xu et. al, 2012) [65].
Bust	tight-fitting garments	0.96 -1.35	7.2 – 10.15	Comfort for tight-fitting garments: (Liu et. Al, 2013) [71].
Bust	swimsuit	≤ 1.15	≤ 8.6	Influence on the pressure comfort of female swimsuit during wearing: (Xu et. al, 2012) [65].
Body	tight-fitting garments	1.96-3.92	14.7- 30	Comfort zone of the tight-fitting garments: (Denton,1972) [73].
Body	swimsuit	1 .0	7.5	Optimal effective and safe compression for swimsuit: (Morooka et. al, 2001) [64].
Body	medical application	2.67 - 4.00	20 - 30	The pressure is the best kept for CGs of the medical application: (Partsh et. al, 2015) [53].
Body	post-surgery compression	2.67 - 4.00	20 - 30	Compression therapy from the LIPOELASTIC® company guarantee the required compression ranging: (LIPOELASTIC, 2018) [55]
Lower part	girdle	1.27	9.5	Comfortable compression feeling of the girdle pressure: (Ito, 1995) [72].

2.4 Application of pressure theory on fabric garment

For compression garments production industry in recent years, the use of elastic fabric has widely been accepted for their high stretch ability to exert pressure on the body [6]. Due to their mechanical properties of stretched fabrics, authors Musilová reported that the patternmaking for CG should be calculated by applying regression equations method to find out the tension of fabric stretched that influence a pattern shape and pressure of clothing. Consequently, the magnitude of pressure value of CG on the body can be reduced based on the size of patternmaking, and therefore, the mechanical property of elastic stretched fabric provides the appropriate or specific pressure [27].

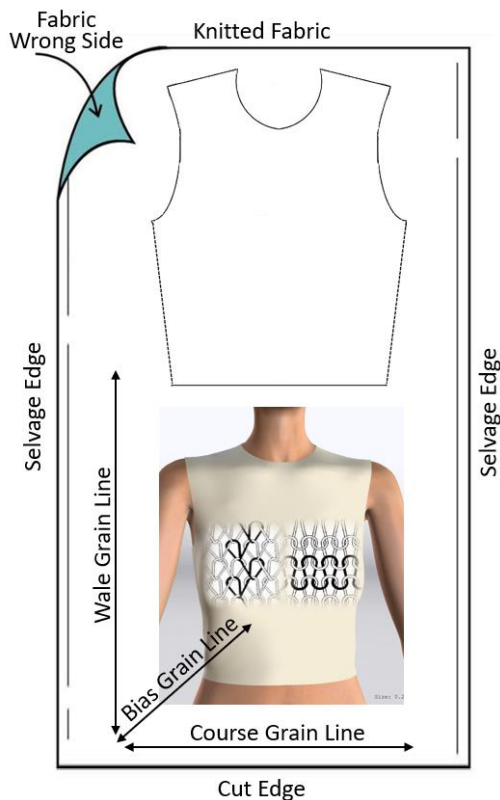


Figure 2.3 Fabric grain lines where the pattern was used the direction for cutting

Fabricating a compression garment with a required specific pressure is important. Pressure exerted by a garment is largely determined by the fabric tension and is influenced by the fabric grain line direction that must be aligned with the stretching direction [74, 6].

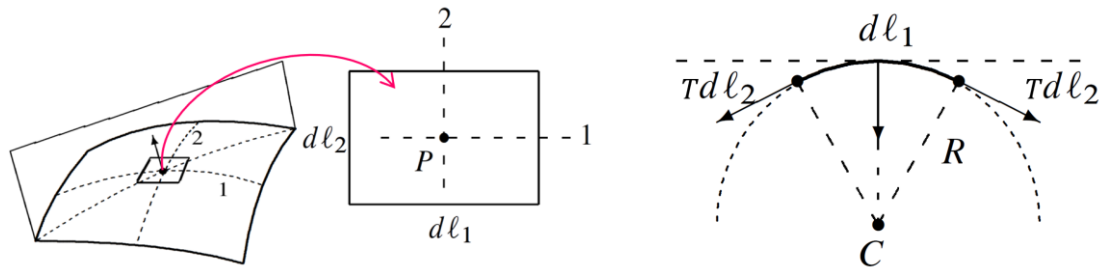
The general, grain line of knitted fabric for producing garment uses in course direction of the knitted fabric in which the direction is aligned to the body circumference [5, 6]. In Figure 2.3, the direction of grain line of knitted fabric including wale, course and bias directions are represented along with the direction of clothing and pattern used for cutting and sewing.

2.4.1 Laplace's law theory

Pierre Simon marquis de Laplace, (1749–1827) a French mathematician [75], who had been making many influential contributions to science of mechanics, a mathematical study of calculus, and a revolutionary theory of probability. Laplace described a mathematical

relationship, Laplace's Law, originally invented to quantify the surface tension of a liquid state in a capillary.

Derivation of the Laplace's law, Laplace explained the pressure discontinuity due to surface tension according to a small rectangle with origin in P and the Z-axis along the normal to the surface in P as shown in the Figure 2.4 (a). The rectangular piece of the surface with sides dl_1 and dl_2 is subject to two tension forces along the 1-direction resulting in a normal force pointing towards the centre of curvature C [6]. The tension forces in the 2-direction contribute analogously to the normal force as shown in the Figure 2.4 (b).



(a) A tiny rectangle aligned with the principal directions [76]

(b) The rectangular piece of the surface with both sides [76]

Figure 2.4 A small rectangle directions and the surface contact acting with the curvature

Surface tension T pulls at this rectangle from all four directions, while the curve of the surface conducts each of these forces not quite like the tangent plane. Considering surface tension acts in the 1-direction with two equally opposite forces directions of magnitude Tdl_2 , each forming a small angle of magnitude $\frac{1}{2}dl_1/R$ with the tangent to the surface in the 1-direction. Projecting both of these forces on the normal can be calculates the total force in the direction of the centre of curvature C_1 as $dF = 2 \cdot Tdl_2 \cdot \frac{1}{2}dl_1 / R = TdA/R$ where $dA = dl_1dl_2$ is the area of the rectangle. Dividing by dA we obtain the excess in pressure on the side of the surface containing the centre of curvature. Then we obtain at the Laplace's law equation for the pressure discontinuity due to surface tension [76].

$$P = T/R \quad (2.1)$$

Where P is the Laplace pressure (Pa), T is the surface tension or wall tension (N.m^{-1}) and R is the principal radii of curvature.

Laplace's law theory is the most common theory for calculating pressure value for CG with assumes the body similar as the cylindrical model. The authors (Kowalski, Mielicka, & Kowalski, 2012) used the Laplace's law theory and assumed the body as the circumference to predict the pressure and design the compression garments [12].

Furthermore, other authors (Kowalski, Mielicka, & Jasinska, 2012) analysed the characteristics of knitted vascular prostheses by mathematical modelling to analysis circumferential longitudinal force depending on the prosthesis pressure and diameter [14].

The authors (Zhao, Li, Yu, Li, & Li, 2017) had also applied Laplace's law theory to help design compression sleeves [18], while authors (Chattopadhyay & Bera, 2017) developed pressure prediction of elastic fabric tube based on energy principle of fabric by load elongation graph. They found that the predicted pressure values on cylindrical model from their testing were to be closer to the actual measured values [19].

2.4.2 Stress in thin-walled pressure vessels

Referring to the Laplace's Law, prediction of wall stress (σ) can be applied to a uniform isotropic hollow cylindrical model [77] as shown in Figure 2.5 (a and b). It is important to note that the thin-walled assumption could be applied in Laplace's Law for compression garment and evidently found in literatures of the authors (Khaburi et. la, 2012) explained the interface pressure of CG generally occur from the circumferential stress of the thin-walled pressure vessels theory where the stress of fabric was stretched along the body circumference [6, 11].

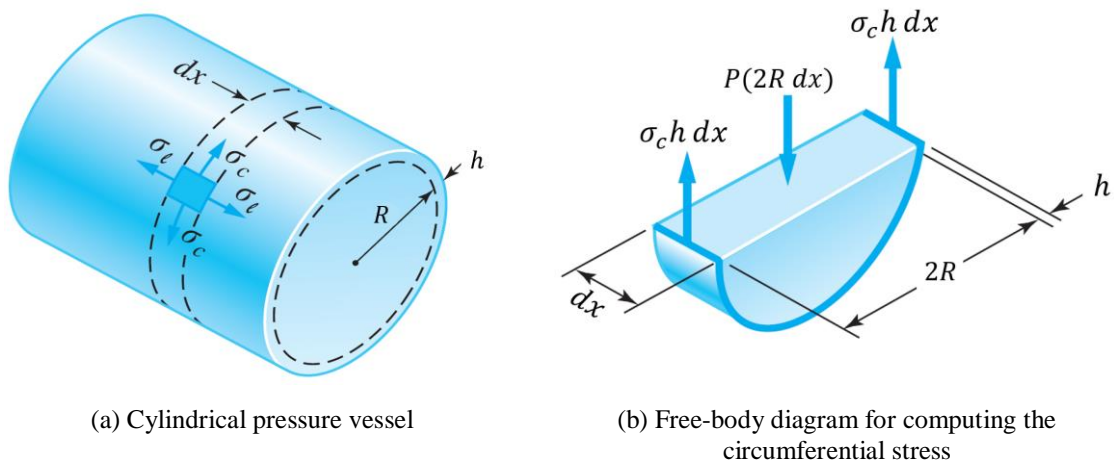


Figure 2.5 The cylindrical vessels free-body diagram of the thin-walled pressure vessels [78]

Consider the cylindrical model of inner radius R and wall thickness h as shown in Figure 2.5 (a), the cylindrical model contains a fluid or gas under pressure P . In this simplified analysis, there is an assumption that the weights of the fluid and the vessel can be neglected when compared to the other forces that act on the vessel. The tensile stresses in the wall that resist the internal pressure are the longitudinal stress σ_l and the circumferential stress σ_c (also known as the hoop stress), as shown in Figure 2.5 (a).

The circumferential stress: Circumferential stress is obtained from the free-body diagram by taking a tiny area of infinitesimal length dx shown in Figure 2.5 (a) and cutting it in half along a diametral plane as shown in Figure 2.5 (b). The fluid isolated by the cuts is considered to be part of the free-body diagram.

The resultant force according to the pressure acting on the diametral plane is $P(2R dx)$, where $2R dx$ is the area of the plane. If we assume the circumferential stress (σ_c) in the wall of the cylinder is constant throughout the thickness (h), then its resultant force is $2(\sigma_c h dx)$. Neglecting the weight of the fluid and the vessel as aforementioned, we find that the equilibrium of vertical forces becomes [78].

$$\sum F = 0 + 2(\sigma_c h dx) - P(2R dx) = 0 \quad (2.2)$$

Which yields for the circumferential stress σ_c [78, 79]:

$$\sigma_c = \frac{PR}{h} \quad (2.3)$$

2.4.3 Related literature reviews on compression garment

Found in various different literatures, many researchers have been applying circumferential stress to predict the interface pressure of the compression garment including (Khaburi, Dehghani, Nelson, & Hutchinson, 2012) who predicted pressure values by making calculation of interface pressure values from thin-walled cylinder theory and thick-walled cylinder theory and on the one hand, they found that the values of pressures estimated by two models were about 1.8% differences with 1.2 mm of fabric thickness and 35 mm of limb radius. On the other hand, for the large cylinder radius of larger than 55 mm, the pressure results were significantly close [11].

Whereas, authors (Macintyre, Baird, & Weedall, 2006) found that the model was able to predict pressure values accurately when cylinders hold longer length of diameters, while the pressures were overestimated when cylinders possess with shorter length of diameters. This predicated that for the prediction of pressure garment, the fabric thickness should be negligible as compared to the human body radius [20].

Interestingly, many researchers aimed to study the pressure garment for prediction of the pressure value of clothing. While the compression garment was investigated to find out the method to achieve specific pressure by reducing the size of circumference of clothing.

Novelty of this research will be focusing on prediction of mathematical modelling of strain value of fabric stretched by determining the specific pressure and the body circumference. At this objective, initial fabric circumference could be calculated and be applied to create sizing of patternmaking for pressure garments.

2.5 Interface Pressure Measurement System

Through this section, information of the compression tester that has been a significant equipment of this experimental testing so called PicoPress® which priduces from Microlab Elettronica Sas in Italy will be introduced. In Figure 2.6, this Pneumatic pressure measurement system is considered as one of the most common types of pressure transducers used to measure the interface pressure under compression of clothing pressure.



Figure 2.6 The PicoPress® devise of the interface pressure measurement system

PicoPress® in Figure 2.6 is a portable pneumatic measuring system fitted with an ultra-thin and flexible sensor. The sensor thickness is 0.2 mm when it is not inflated and 3mm when it is in inflated. The sensor diameter is 50 mm and the device pressure measurement range around 0 – 200 mmHg or 0 – 26.7 kPa. Before the measurement, the sensor is inflated with 2 cc of air by means of electronically controlled syringe integrated in the system [26]. The transducer can be calibrated under the CG and the pressure measured data can be stored on the device or transferred to a computer and the advantage to pressure measurements during dynamic tests [26]. The Picopress® reading the unit of pressure in the medical community is the as millimetre of mercury that is a manometric unit of pressure where 1 mmHg \approx 133.32 Pa or Pascals is SI derived units [79].

Notably, there have been many literatures that applied PicoPress® for making the interface pressure measurement of CG and evidently found that the system is to be very accurate for measurement including the works of:

The authors (Partsch et. al, 2006) who reported that in their thigh compression [25] testing, the pneumatic device had been very beneficial in terms of their financial accessibility and physical features including its size and flexibility [24].

Moreover, in the work of the authors (Mosti et. al, 2008) they found that the linearity and repeatability of this transducer are highly acceptable because PicoPress® had outperformed Kikuhime® and the SIGaT® [26].

The authors (Khaburi et al, 2011) confirmed and indicated that FlexiForce sensors, based on the sensor of piezoresistive (PR) principle, had issued from low preciseness when compared to PicoPress® device. While the sensor produced less errors for measurement the interface pressure values and more agreement with computed pressures [23].

The authors (Chi et.al, 2017) applied the principle of PR sensor to compare between both commercial ready products PicoPress® and Kikuhime® by using the tube cuff model which was wrapped around by the BISCO® HT800 silicone foam. They revealed that PR sensors demonstrated similar performance as PicoPress® [80].

They all agreed that from all manometry-based devices, PicoPress® was determined to have most accuracy with least variations and errors [26, 23, 80, 81]

2.5.1 The effect of the sensor thickness

It could be said that thickness of sensor at a certain extent, does have effect on pressure perturbation which eventually make reading pressure overestimated. The author (Ferguson-Pell, 1980) recommended the ideal interface pressure measurement to use the sensor with thickness no more than 0.5 mm will have no effect on pressure perturbation [82]. However, the pressure readings reported by PicoPress® need to be multiplied with a correction factor according to the thickness that is higher than 0.5 mm. The pressure perturbation is not only caused by the thickness of the sensors only, as inflating the sensor under CG will result in a local stretch for the clothing [6, 83].

The authors (Vinckx et. al, 1990) have studied analytically to analyse the perturbation in the measured pressure when a sensor that is placed under a compression garment applied to a curved surface like the lower limb [22]. They have developed a mathematical model to calculate the perturbation effect due to thickness of sensor which is called the coefficient of pressure perturbation C_{PP} [22] and the schematic of interface pressure perturbation effect under pressure garments as show in Figure 2.7.

$$C_{PP} = \frac{\sin(\frac{\alpha}{2} + \gamma)}{\sin(\frac{\alpha}{2})} \quad (2.6)$$

$$\alpha = \frac{D_S}{R}$$

$$\gamma = \arccos\left(\frac{R}{R+d}\right)$$

Where, d is the sensor thickness in (m), D_S is the sensor diameter in (m), C_{PP} is the coefficient of pressure perturbation, R is the radius in (m).

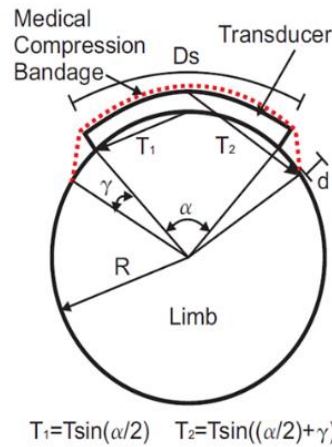


Figure 2.7 Schematic representation of the interface perturbation effect of a sensor placed beneath an extensible bandage over a curved surface [83, 22]

By assuming from the author (Khanburi, 2010) that the small local increase in bandage elongation will result in a linear increase in tension, the perturbation due to the local stretch C_{TP} can be shown to be the following [83]:

$$C_{TP} = \frac{\alpha (R+d)+2((R+d)^2-R^2)}{\alpha R} \quad (2.7)$$

$$\alpha = \frac{D_S}{R}$$

Where, d is the sensor thickness in (m), D_S is the sensor diameter in (m), C_{TP} is the coefficient of pressure perturbation due to local stretch, R is the limb radius in (m).

The total pressure perturbation then can be calculated by the following expression [83]:

$$Total\ Pressure\ Perturbation = C_{PP} \times C_{TP} \quad (2.8)$$

The correction factor for the measured pressure values can be obtained using [83]:

$$Correction\ Factor = \frac{1}{Total\ Pressure\ Perturbation} \quad (2.9)$$

Nevertheless, PicoPress® device also possess some disadvantages as mentioned by [23] that the device overestimated the result of pressure value during the measurement of compression clothing with cylinder model due to the sensor thickness at 3 mm. When the sensor is kept at the fabric area, the radial component of the tension in the fabric increases hence a higher local pressure is measured [22]. They reported that it is necessary to solve perturbation coefficient to find out a real pressure of fabric stretch [6, 84].

2.6 Elastic properties for CG

Elastane (EA) was invented in 1937 while is well known by trade names such as Spandex, Lycra and Dorlastan [85]. Elastane provides permanent elasticity in garments that are required to cling to the body as well as in slight fitted styles offering comfort and shape retention. Elastane has the most elongate tension of textile materials with fibres that can be extended their length and that rebound to their initial length when the tension is slackened. While, higher elastane would demonstrate higher power or resistance to stretch when increasing linear density of elastane into the fabric, the power or resistance would be higher

[86]. Moreover, blends with elastane depend on the type of fabric and the end use for example, 15–40% elastane content used for a body-shaped silhouette or high stretch capacity, such as in swimwear, corsetry or sportswear [85].

2.6.1 Elongation

This is the ultimate elongation of elastic fabric in the particular direction using a predetermined the extensibility [86]. Table 2.2 indicated the extensibility of the elastomeric fabric into three classifications, they can be classified into low, medium and high [8, 9].

Table 2.2 The classification of elastic fibre

Extensibility (%)	Classification of elastic fibre	Application
20% - 150%	low	sportswear
150% - 390%	medium	sportswear or body shaping garments
400% - 800%	high	medical compression garment

The range of extensibility could be helpful to select the fabric utilization due to their application requirement and improve the efficiency of the fabric extensibility for CG on the surface of needed particular areas for stabilizing, compressing, and supporting underlying tissues [87]. The author (Geršak, 2013) reported stretch fabric for CG due to physical exertion by body movement that the simple body movement usually expands around 10% - 50% of extend by skin [88]. Furthermore the elastic recovery is considered to be equally as important as stretching [89, 90, 10] especially when it has a capability in keeping the pressure value of clothing stability.

2.6.2 Structure of Knitted fabrics

Compression garments are commonly fabricated by knitted fabric due to the knitted fabric has better elasticity than a woven fabric owing to an interloped structure. In the knit fabrics when a loop is pulled horizontally it extends by the whole length, whereas a loop when pulled vertically it extends by half its length [91, 92]. Knitted fabric is done by a set of connected loops from a series of yarn in warp or weft direction. Therefore, there are two main types of knitted fabric namely weft knitted fabric and warp knitted fabric [35].

Terms and definitions of knitted structure:

- *Warp knitting:* It is a method of producing a warp knitted by creating loops from each warp formed substantially along the length of the fabric. The feature of each warp thread is fed more or less in line with the direction in which the fabric is operated. Each needle within the knitting width should be fed with at least one separate and individual thread at each course [93].
- *Weft knitting:* It is a method of producing a weft knitted by creating loops from each weft thread that are formed substantially across the width of the fabric. It is characterised by each weft thread is fed more or less at exact angles to the direction in which the fabric is operated. It is able to knit only one thread, but up to 144 threads could be operated within one machine. This method is the more multipurpose of the two in terms of the range of products produced and the type of yarns used [93].
- *Single-jersey fabric:* It is a weft knitted fabric which produces on one set of needles.
- *Interlock:* A combination of two double jersey bindings overlaying in a way that in a wale direction elongated state no heads or feet of the stitches are discernible. On both outer sides, the legs of the right side of the knitted fabric are visible.
- *Purl stitch:* Knitted fabrics with a basic binding in purl stitch show course-wise alternation of the stitch heads on the two outer sides of the fabric. This is achieved by changing the knock-over direction of the stitches off the needles in each course. Purl fabric has high extensibility in all directions.
- *Locknit:* The most popular of wrap knit structure is operated basically with higher than 37 wales per inch and 28 gauges machine. The longer overlap of front bar show in back side of fabric that help to improves the extensibility, cover, opacity, smooth, soft hand and good drapability to the fabric.
- *Course:* A row of loops across the width of the fabric. Courses determine the length of the fabric and are measured as courses per centimetre.
- *Wale:* A column of loops along the length of the fabric. Wales determine the width of the fabric and are measured as wales per centimetre.

- *Stitch density*: The number of stitches per unit area of knitted fabric.
- *Yarn linear density*: It indicates the thickness of the yarn and is normally determined in tex, which is defined as the mass in grams of 1 km of the material. The higher the tex number, the thicker is the yarn and vice versa.

The basic of weft knitted structures is illustrated for its appearance, properties, and end-use applications of single jersey, rib, purl and interlock structures which are summarized in Table 2.3. Weft knitted fabrics are produced commercially for apparel, household and technical products in textile are used for an extremely large array of products ranging from stockings and tight-fitting garment and CG.

Table 2.3 Comparison of appearance and properties of knitted structures [93]

Property	Single jersey	Rib	Purl	Interlock
Appearance	Different on face and back; V-shapes on face, arcs, on back	Same on both sides, like face of plain	Same on both sides, like back plain	Same on both sides, like face of plain
Extensibility				
- <i>Lengthwise</i>	Moderate (10–20%)	Moderate	Very high	Moderate
- <i>Widthwise</i>	High (30–50%)	Very high (50–100%)	High	Moderate
- <i>Area</i>	Moderate–high	High	Very high	Moderate
Thickness	Thicker than plain woven made from same yarn	Much thicker than plain woven	Very much thicker than plain woven	Very much thicker than plain woven
Curling	Tendency to curl	No tendency to curl	No tendency to curl	No tendency to curl
Dimensional stability	Poor	Good	Very good	Very good
Applications	Sportswear, fitting garment	Active sportswear, body sculpturing, medical of CG	Active sportswear, body sculpturing, medical of CG	Active sportswear, body sculpturing, medical of CG

2.6.3 Weight

Definition of fabric weight measurement is the mass unit (g/m^2) and measures according to ASTM D 3776 - 96 standard test method for mass per unit area of fabric [94]. Weight testing is often a prerequisite for subsequent tests of other fabric properties. If fabric weight or dimension is not kept constant, then the test results will not be comparable [95].

2.6.4 Thickness

The thickness of a fabric is one of its fundamental properties and measures according to ASTM D 1777-96 standard test method for thickness of fabric [96]. Thickness measurements are very sensitive to the pressure and specimen size used in the measurement, fabric mm unit is often used as an indicator of thickness [95].

2.6.5 Deformation of elastic fabric

Elastic deformation is one type of deformation which is reversible. when the forces are no longer applied, the object returns to its original shape [97]. It is important for estimating the size of patternmaking that it should understand the deformation of fabric under stretched with different levels due to when fabric is stretched the other side is decreased therefore the deformation has effect when wearing the garment.

The deformation of material depending on the behaviour of fabric size and geometry of the material and the forces applied, various types of deformation may result. Figure 2.8 shows the engineering stress-strain diagram that illustrates the elastic and plastics regions where has the influence on the material deformation.

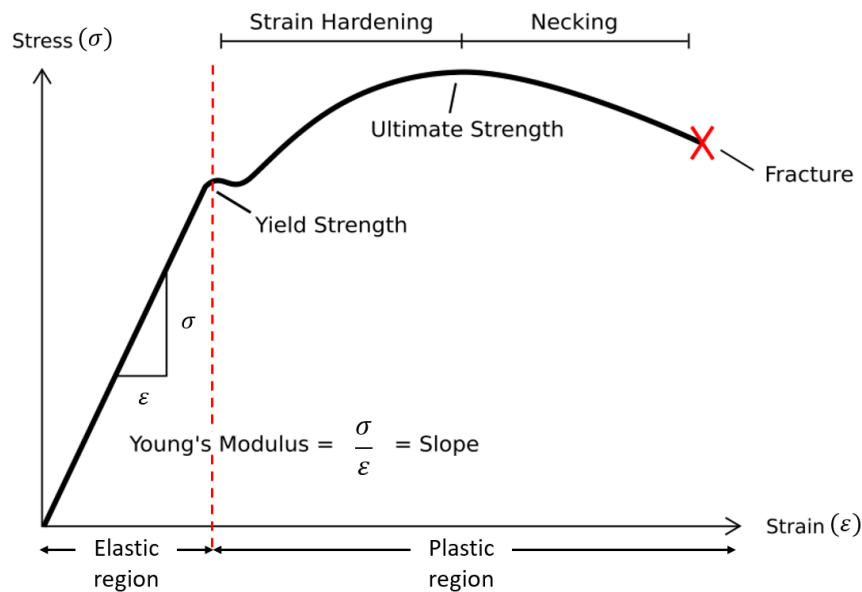


Figure 2.8 Typical stress-strain diagram indicating the various stages of deformation [98].

2.6.5.1 Poisson's ratio: The fundamental properties for studying fabric deformation under loading. When a force system acting on a fabric occurs, the positive strain deformation (dilatation) or extension is in the longitudinal direction where is the direction of the acting force, whilst the transverse deformation (contraction) takes place in the transverse direction [99, 100] as shown in the Figure 2.9 (a and b).

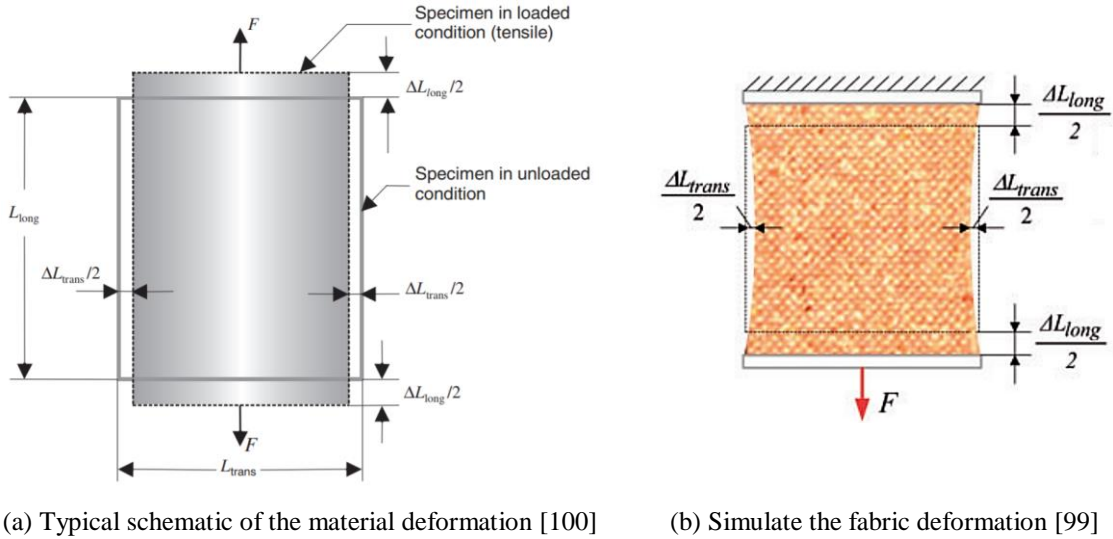


Figure 2.9 Deformation of longitudinal and transversal under tensile loading

The results of the fabric deformations are simultaneous and depend on each fabrics behaviour. Therefore, it is necessary to calculate the magnitude of the fabric deformation decreasing in the transverse deformation in order to plus the fabric loss deformation into the pattern construction when the CG wearing on the body. The material is linearly elastic if the transverse strain (ϵ_{trans}) at any point in a material is proportional to the longitudinal strain (ϵ_{long}) at the same point. The ratio of transverse contraction strain (ϵ_{trans}) to longitudinal or axial strain (ϵ_{long}) in the direction of the applied load force is defined as the Poisson's ratio [97].

2.6.5.2 Longitudinal deformation: as the result of tensile loading, is expressed as strain along the longitudinal axis or specific elongation x and is given in the form [100, 97].

$$\epsilon_{long} = \frac{\Delta L_{long}}{L_{long}} \quad (2.10)$$

where ΔL_{long} is the change in longitudinal direction, that is, in the length, and L_{trans} is the initial length.

2.6.5.3 Transverse deformation: is expressed as strain along the transverse axis or contraction and is given in the form [100, 97].

$$\varepsilon_{trans} = \frac{\Delta L_{trans}}{L_{trans}} \quad (2.11)$$

where ΔL_{trans} is the change in transverse direction, that is, in the width, and L_{trans} is the initial width.

2.6.6 Engineering strain

The Cauchy strain or engineering strain is expressed as the ratio of total deformation to the initial dimension of the material body in which the forces are being applied. The engineering strain (ε) of a material line element or fibre axially loaded is expressed as the change in length (Δl) per unit of the original length (l) of the fabric element.

$$\varepsilon = \frac{\Delta l}{l} = \frac{l_0 - l}{l} \quad (2.10)$$

where ε is the engineering strain, l_0 is the original length of the material and l is the final length of the material.

2.6.7 Engineering stress

Uniaxial stress, this stress is called engineering stress (σ) and is calculated using the original cross-section (A). In engineering applications, structural members experience tiny deformations and can be neglected due to the reduction in cross-sectional area is very small, therefore, the cross-sectional area is assumed constant during deformation.

$$\sigma = \frac{F}{a} \quad (2.11)$$

where F is the applied load and a is the original cross-sectional area.

2.6.8 Tensile strength

The tensile strength of a fabric material is the maximum amount of tensile stress that it can take before failure [97]. For a particular testing, the tensile behaviour result of the elastic knitted fabric is highly non-linear. The authors (Araujo et. al, 2003) reported that in fact, a

careful checking of the loops' characteristic during testing can reveal a two-stage deformation process as shown in the Figure 2.10, presents a typical load-elongation characteristic curve for a weft knitted fabric tested in the walewise direction [101].

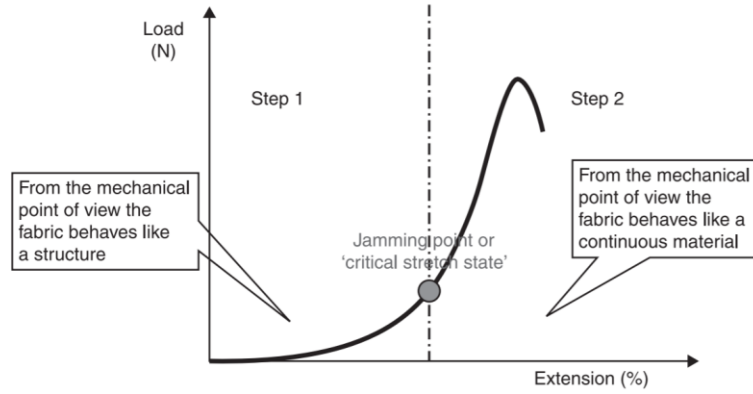


Figure 2.10 Typical load-extension characteristic curve for a weft-knitted fabric [101]

The critical stretch state or jamming state, which is a hypothetical state of deformation. According to the mechanical, in this initial stage of deformation, the fabric behaves like a structure of knitted fabric [101, 102].

2.6.9 Young's modulus and stiffness

Young's modulus: It explains tensile elasticity or the tendency of fabric to deform along an axis when inhibited forces are applied along that axis. The definition of Young's modulus is the ratio of tensile stress (σ) to tensile strain (ε). It is often referred to simply as the elastic modulus [97, 98].

$$E = \frac{\sigma}{\varepsilon} \quad (2.12)$$

Stiffness: This is a property of a structure or component of a structure and hence it is dependent on various physical dimensions. The stiffness of elastic material is measure of the resistance offered by elastic body to deformation. For an elastic body with a single degree of freedom, the stiffness (k) is defined as [97, 98].

$$k = \frac{F}{\delta} \quad (2.13)$$

where F is the applied load on the body and δ is the displacement produced by the force along the same degree of freedom.

The authors (Araujo et. al, 2003) explained the definition of a Young's modulus for the structure encounters some theoretical hindrances. Due to the elastic fabric deformation is non-linear, Hook's law cannot be verified and so it is not possible to consider a Young's modulus. As an alternative, the term stiffness may be used to describe and compare the mechanical behaviour of different elastic fabrics [101].

2.6.10 Elasticity recovery

Elastic recovery is the one of the important performance indicators for compression garments. When a fabric is stretched to a level lesser than breaking strength and is then allowed to recover, the fabric generally does not immediately return to its original state. Its elastic recovery depends on the compression force provided, the length of time that the force is applied and the length of time that the fabric is allowed for recovery [1, 103, 104].

Improving the elastic performance by offering least resistance during garment stretch and they enhance the power by quick recovery due to elastane in the fabric. The fabric stretch recovery tests were carried out according to standard EN 14704-1:2005 (determination of the elasticity of fabrics-strip tests) [105]. The authors (Senthilkumar and Anbumani: 2010) studied the dynamics of elastic knitted fabric for sportswear and was successful results from their design experimental by using speed 500 mm/min and the percentage of extension maximum at 50% [8, 10, 105, 106].

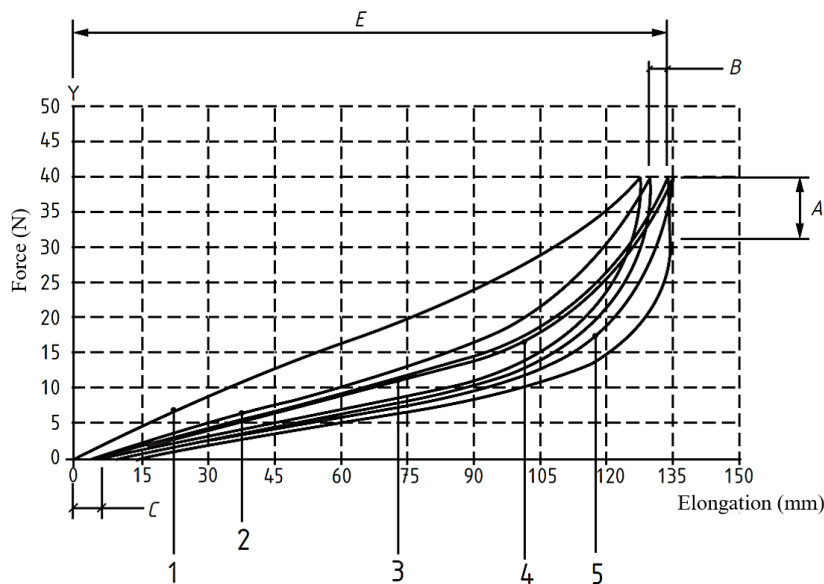


Figure 2.11 Typical cycling graph [100]

In Figure 2.11, a graph typical cycling graph based on standard EN 14704-1:2005 [105] can be analysed for its the elasticity of fabric as follows: (A) is force decay due to the time, (B) is force decay due to exercising (setting the method: fix load per cm width), (C) is unrecovered elongation, (E) is maximum extension, (1) is pre-cycle, (2) is second load cycle, (3) is fifth load cycle, (4) is sixth cycle and (5) fifth unload cycle [105].

The authors (Ilska et. al, 2014) studied the relationship between the force and relative elongation of knitted fabric. In Figure 2.12, the graph of force as a function of absolute elongation in hysteresis loops in the loading and unloading cycle [106, 107] is shown.

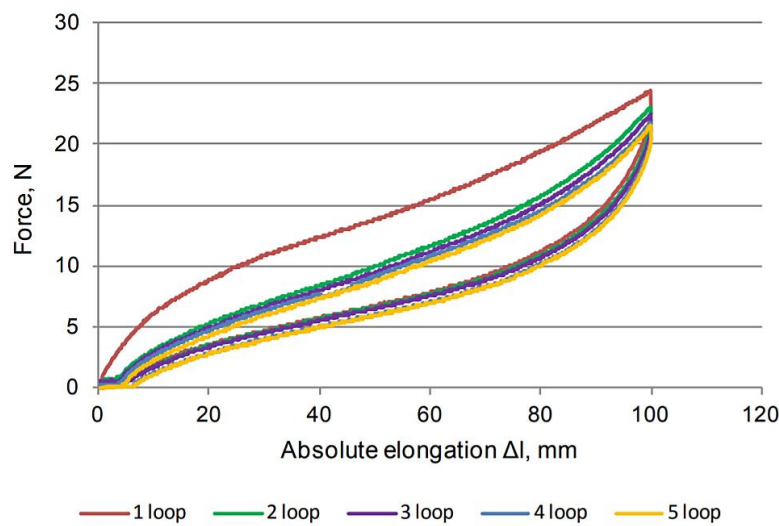


Figure 2.12 Graph of force and elongation in hysteresis loops [106]

2.6.11 Stress relaxation

The stress relaxation is one the effect on compression garments which is used to evaluate the performance of clothing pressure during wearing and the stress in the fabric be able to keep the constant of the pressure over the time. Therefore, relaxation of compression garment is caused by fabric stress relaxation mainly. Fabric stress relaxation refers to the phenomenon that fabric internal stress or tension decayed with the increase of time when fabric extension was constant [104]. The stress required to hold the viscoelastic material at the constant strain will be found to decrease over time in viscoelastic material as in the Figure 2.13 [108]. The elastic fabric problematic of having a viscous and elastic response during applied load therefore it is very important to study and evaluate the elastic fabric performance especially in compression garments [103].

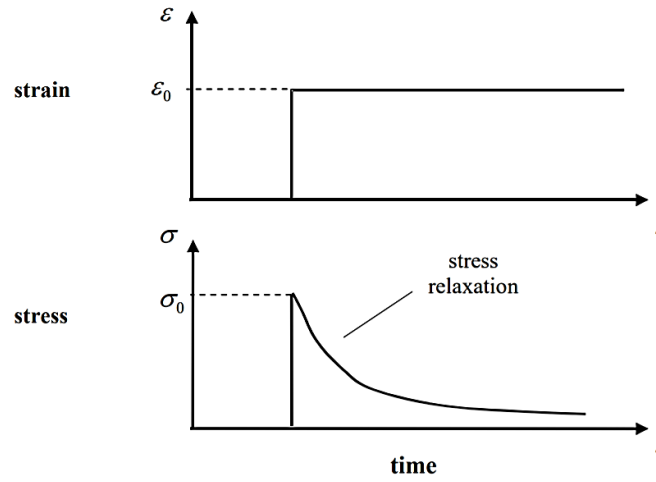


Figure 2.13 Stress response to the stress relaxation test [108]

2.6.12 Dynamic work recovery

The characteristic of stress-strain curve of identical elastic fabric, loading and unloading behaviour of the fabric is almost curvilinear. This fabric is perfectly suitable for CG, it requires stamina and power. But, most of the textile fabrics are non-linear in nature of the viscoelastic deformation, which will produce hysteresis loop as shown in the Figure 2.14.

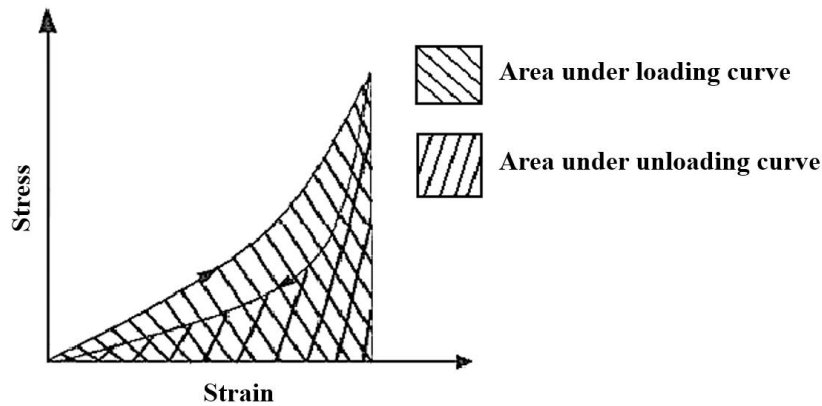


Figure 2.14 Dynamic work recovery [10]

Higher the hysteresis area, the higher will be the energy loss, i.e. lower the fabric stress and strain recovery. The benefit of elastic fabrics has a higher elastic recovery with lower energy loss so that the wearer will get the additional benefit such as improved stamina and power to perform sports activity. In general, elastic textile material will give minimum work energy loss which can be calculated by assessing Dynamic Work Recovery (DWR) [10].

$$DWR \% = \frac{\text{Area under the unloading curve}}{\text{Area under the loading curve}} \times 100 \quad (2.14)$$

Chapter 3 Experimental Materials and Methods

3.1 Materials

The materials for this research represent eight commercially produced knitted fabrics with different types of stretch knitted fabrics were varied in percentages of Polyamide (PA) and Elastane (EA) compositions and structures. Samples S1 – S6 had been being produced by Thailand's Pacific Knitting Factory Co., Ltd. For production of the fabrics, fleecy knitting machine and 4 track single jersey machine of GOANG LIH, model GLF/s-3F-4T, CYL.DIA 32", GAUGE N.P.I. 28 G, Feeders 96F were used with constant knitting speed at 22 rpm. The yarns of knitted fabric of the samples S1 - S6 produced from PA were varied in the linear density of yarns between 44 dtex and 78 dtex while EA were varied in the linear density of yarns at 22 dtex, 33 dtex and 78 detex. Moreover, the samples S7 and S8 with high the EA compositions were supported by garment factories located in Czech Republic and Slovenia. As shown in Table 3.1, characteristics of mentioned elastic knitted fabrics were obtained.

Table 3.1. Elastic knitted fabrics characteristics

Sample	Polyamide		Elastane		Structurer
	(%)	(dtex/ply)	(%)	(dtex/ply)	
S1	90.79	44×2	9.21	22	Single Jersey
S2	87.59	44×2	12.41	33	Single Jersey
S3	74.52	44×2	25.48	78	Single Jersey
S4	94.38	78×2	5.62	22	Single Jersey
S5	92.94	78×2	7.06	33	Single Jersey
S6	83.46	78×2	16.54	78	Single Jersey
S7	72.00	-	28.00	-	Locknit
S8	70.00	-	30.00	-	Interlock

3.2 Methods

Steps in the implementation process to develop the patternmaking method could be divided into three main methods including the making of pattern abscissa, the testing of fabric performance and prediction and investigation of strain value and as shown in Figure 3.1.

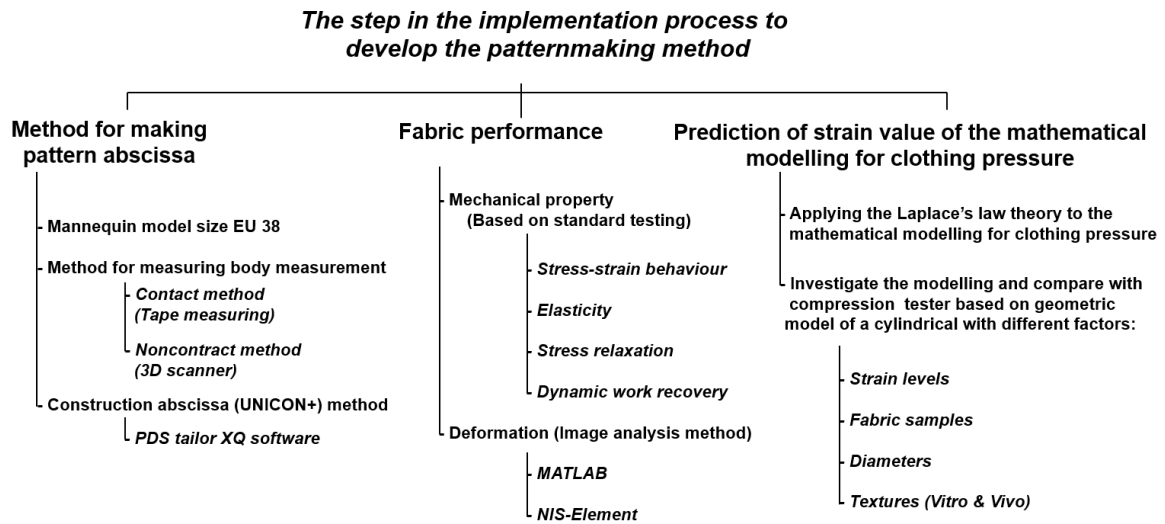


Figure 3.1 A schematic flowchart of the procedure patternmaking development for stretch fabrics

The procedure of the experimental it can be described into 4 phases as flowing:

Phase 1: Patternmaking development method for pressure garments

- Determination of body measurement
- Analysis of patternmaking for pressure garments
 - Determination of the patternmaking modification
 - Determination of the elastic coefficient
 - Applying the elastic coefficient coordinate with standard sizing system
 - Applying the patternmaking method by CAD software

Phase 2: Fabric performance for pressure garments

- Mechanical properties of stretch fabrics
 - Determination of weight per unit area
 - Determination of thickness
 - Determination of wale and course per unit length
 - Determination of strength and elongation properties
 - Determination of stress-strain behaviour
 - Determination of the elasticity
 - Determination of the stress relaxation
 - Determination of dynamic work recovery

- Fabric deformation measurement by image analysis
 - Determination of fabric deformation measurement using MATLAB
 - Concept of gradient deformation tensor

Phase 3: Applying the Laplace's law for GC and evaluating the pressure

- Applying Laplace's law theory to practice on pressure garment
- Prediction of strain value using the mathematical modelling
- Designing experiments to investigate the mathematical modelling with the compression tester
 - Determination of measuring the pressure in vitro model
 - Effect of sensor thickness for measuring the pressure
 - Determination of measuring the pressure in vivo model
- Designing experiment to predict the strain of pressure garments
 - Determination of predicted strain by applying compression tester

Phase 4: Development and application of a novel tensile device

- Designing the novel tensile device
- Determination of the elasticity
- Determination of fabric deformation measurement using NIS-Element

3.3 Patternmaking development method for pressure garments

3.3.1 Determination of body measurement

In this part of the research, female mannequin standard European standard sizing system 38 belonging to the department of Clothing Technology, faculty of Textile Engineering, Technical University of Liberec will be used for measurement in order to input the parameters into the construction abscissa formulas of patternmaking modification. The mentioned mannequin will be applied the body measurement for the experiment in order to analyse and estimate the size of patternmaking for clothing required for specific pressure. Table 3.2 illustrates the obtained parameters of body measurement from the mannequin; meanwhile, those parameters are described in Figure 3.2 as body measurement chart along with mannequin simulated by Optitex 3D software.

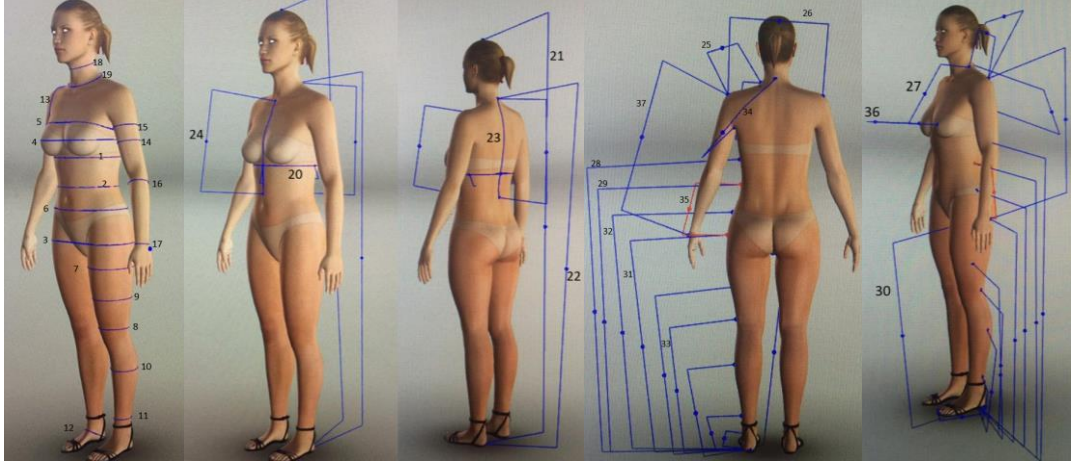


Figure 3.2 The women body measurement chart

Table 3.2 Women body measurements of the mannequin

No.	Girth measurement	Unit: cm.	No.	Length measurement	Unit: cm.
1	Under bust	72.50	20	Size (under bust)	36.00
2	Waist	71.50	21	Height	168.00
3	Hips	96.00	22	Cervical height	141.00
4	Bust	86.60	23	Back waist length from CB	38.00
5	Upper bust	79.00	24	Front waist length from CF	32.50
6	High hip	84.00	25	Shoulder slope	12.50
7	Thigh	52.50	26	Cross shoulders	41.00
8	Knee	34.50	27	Bust height	25.00
9	Low thigh	38.00	28	Under bust height	114.00
10	Calf	35.00	29	Out seam	105.50
11	Ankle	21.50	30	Inseam	79.50
12	Foot Instep	29.00	31	Hip height	85.00
13	Armscye	31.50	32	High hip height	97.00
14	Biceps	27.50	33	Knee height	46.00
15	Upper biceps	27.50	34	Armscye depth	15.00
16	Elbow	23.50	35	Waist to hips	20.00
17	Wrist	15.00	36	Bust point to bust point	20.00
18	Neck	29.00	37	Arm length	57.00
19	Base neck	36.00			

3D body scanning using sense™2 3D scanner for capturing the body figure and dimensions of the mannequin was used as shown in Figure 3.3. The red tiny dots on the body were to determine the important land mark points on the body according to the ISO 8559-1:2017 [109] including shoulder point, back neck point, side neck point, front neck point, bust point, centre chest point, armpit front fold point, armpit back fold point, under bust level and waist level. While the 3D image processed by the blender software would be applied to analyse the body cross section in varied parts of the body as shown in the Figure 3.4.

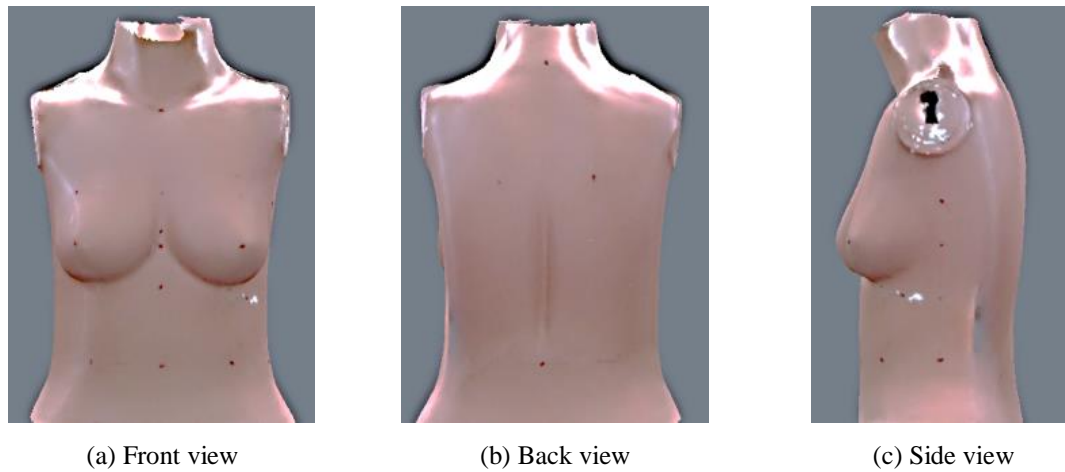


Figure 3.3 The 3D images with point marks using senseTM2 3D scanner

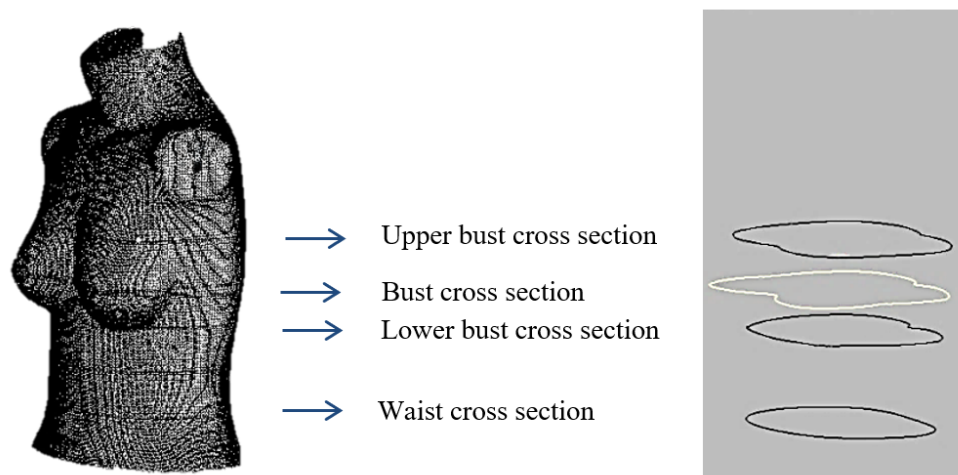


Figure 3.4 The 3D images of body cross sections

3.3.2 Analysis of patternmaking for pressure garments

The initial step to make the patternmaking for pressure garments should be first defining the relationship of the connecting lines between the 2D of construction abscissa and the 3D body measurement that is the fundamental step for developing pattern garment fit for stretch fabrics. According to the relationship between the body measurement and the lines of construction abscissa the concern should be given on various important mark points of 3D body shape in order to set the pattern well fit to the body and for the important mark points, including the shoulder angle, bust, and armhole (armhole) like the conventional block pattern in Figure 3.5 will be showing the relationship between patternmaking and body.

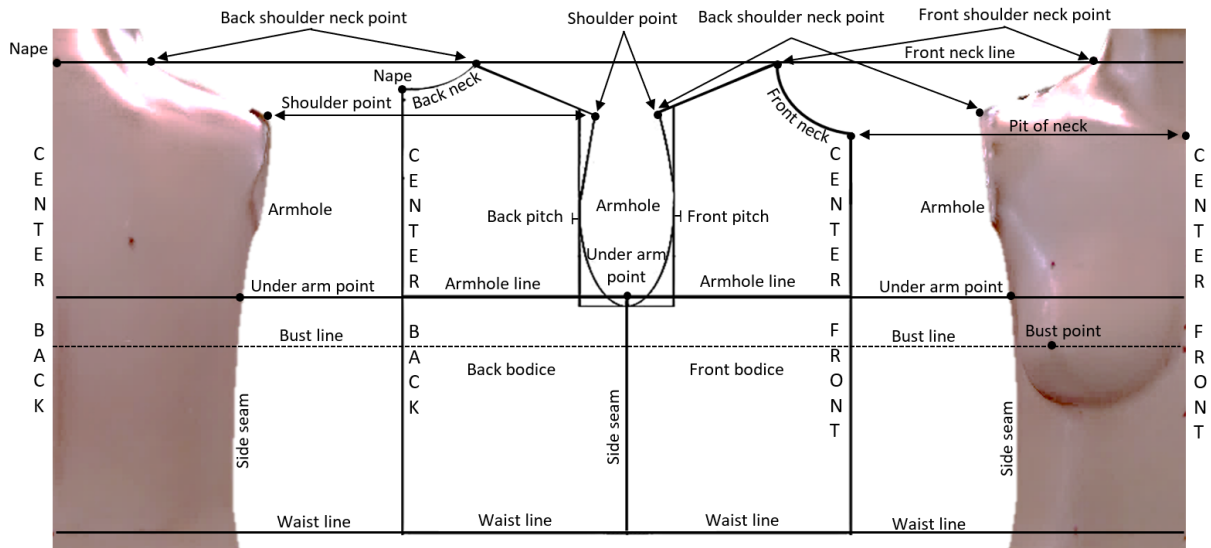


Figure 3.5 Conventional block pattern relationship to the body measurement

3.3.2.1 Determination of the patternmaking modification: The modification of the patternmaking for pressure garment can be defined as the area that may have very possibilities to obtain the pressure value according to compression of clothing. The assumption of the body shape could define by estimating that the patternmaking of body shape size is similar to the cylindrical shape and therefore, the adjustment of patternmaking according to pressure garment only focused on only the body shape that is similar to cylindrical shape would have a great possibility of achieving the pressure value in clothing.

The scientific methodology for developing patternmaking is defined into two parameters for the modification of constructing abscissa formula in different dimensions including the elastic coefficient in width dimension (ECW) and elastic coefficient in length dimension (ECL).

In order to determine the patternmaking in this experiment, a female mannequin is used to define the area on the body for the adjustment of patternmaking which is related to the cylindrical shape as shown in Figure 3.6. The analysis of patternmaking to find out the ECW and ECL on the pressure area is illustrated in yellow.

The essential parameter to help find the ECW is the stress-strain behaviour of stretch fabric. In order to make prediction of the strain value and then the result of predicted strain value would be applied to calculate the ECW. Concerning the ECL it is obtained from the result

of fabric deformation that the experiment used the image processing method for measuring the fabric deformation with different strain levels and then used the statistical regression analysis to make prediction of the ECL.

In Figure 3.6, the pressure area and the relationship between 2D block pattern and 3D body measurement of the pressure area and method are described in order to develop the patternmaking according to pressure requirement.

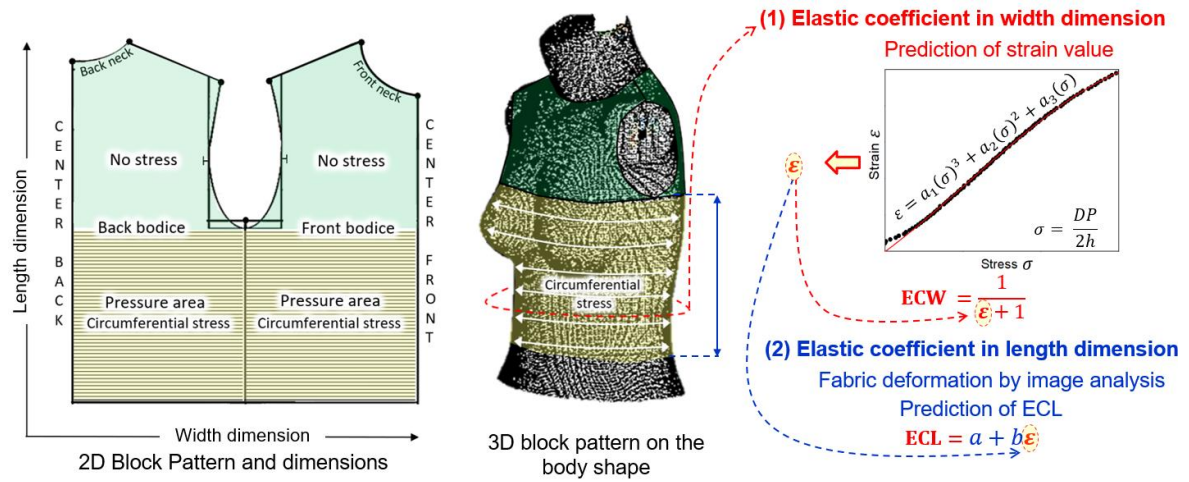


Figure 3.6 Analysis patternmaking for pressure garment based on pressure area

Pressure area zone: This part of the block pattern was related to circumferential stress based on Laplace's law theory and Thin-walled pressure vessel theory and the shape from upper bust to waist was assumed to the cylindrical shape. Therefore, the stress behaviour in fabric was stretched in direction of body circumference as arrows in Figure 3.6. Consequently, the pattern in this part has a direct influence on the fabric deformation when fabric was stretched in one direction; at the same time, the other direction will be shorter when compared to the initial deformation. The pattern construction analysis is to estimate the size during wearing on body whereas, pattern dimension analysis is described below:

- **Width dimension (circumference):** This dimension is a main direction of fabric stretch therefor the existence pressure can be attributed to the degree of fabric stretch. The mathematic modelling was applied to acquire the specific pressure value by equation: $\varepsilon = a_1 \left(\frac{DP}{2h}\right)^3 + a_2 \left(\frac{DP}{2h}\right)^2 + a_3 \left(\frac{DP}{2h}\right)$ and to estimate optimum degree of fabric stretched by strain value.

- Length dimension: it is considered to be given a second priority resulting from the change of deformation degree of fabric stretch in width dimension. During pattern construction, an addition of pattern construction length causes the fabric in width dimension to stretch resulting in the length dimension of fabric to be shorter. To calculate the length dimension, the statistical analysis of predictive deformation changed from individual fabric deformation is applied.

No stress zone: At this certain zone, application of Laplace's law theory had not been conducted. In the experiment as seen in Figure 3.6, pattern was cut at the area of armhole while stress in fabric could not stretch itself in circumference of the body direction and the pattern dimensions analysis is described as follows:

- Width dimension: This dimension of pattern construction was adjusted according to the proportion and balance of patternmaking from a zone of pressure area where decreases the size in width dimension of pattern construction. Therefore, this zone was connected to the pattern construction decreasing and the pattern construction create by designing the armhole curve and shoulder length as shown Figure 3.6.
- Length dimension: this dimension does not have any influence on the fabric deformation change from the fabric stretched and therefore, the length is used in the initial length of block pattern.

3.3.2.2 Determination of elastic coefficient: Referring the human body as similar as the cylindrical model as shown in the Figure 3.7 where illustrates the fabric deformation changed when fabric was stitched without ΔC gap and the fabric was stretched covering on the body. Thus the compression pressure occurs according to the level of strain value, therefore, it can be indicated that the magnitude of the pressure from stretch fabric can determine from fabric strain which can be calculated the circumferential strain by equations (3.1), lateral strain by equation (3.2) and the value of elastic coefficient from the equation (3.3) were used to calculate the elastic coefficient in width and length dimensions by equations (3.4) and (3.5) respectively.

$$\text{Circumferential strain: } \varepsilon_{\text{Circumferential}} = \frac{\Delta C}{C_0} \quad (3.1)$$

$$\text{Lateral strain: } \varepsilon_{\text{Lateral}} = -\frac{\Delta w}{w_0} \quad (3.2)$$

$$\text{Elastic Coefficient: } E_i = \frac{1}{\varepsilon + 1} \quad (3.3)$$

$$\text{Elastic Coefficient in width dimension: } ECW = \frac{1}{\varepsilon_{\text{Circumferential}} + 1} \quad (3.4)$$

$$\text{Elastic Coefficient in length dimension: } ECL = \frac{1}{\varepsilon_{\text{Lateral}} + 1} \quad (3.5)$$

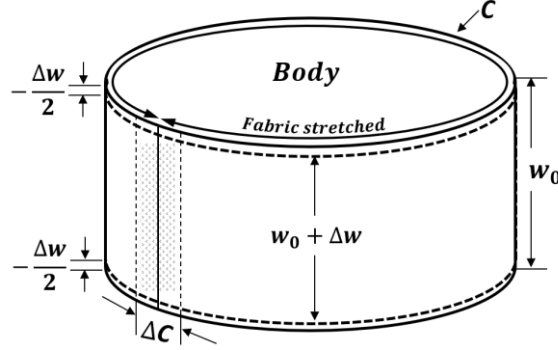


Figure 3.7 The deformation changed of stretch fabric of circumferential and lateral strain

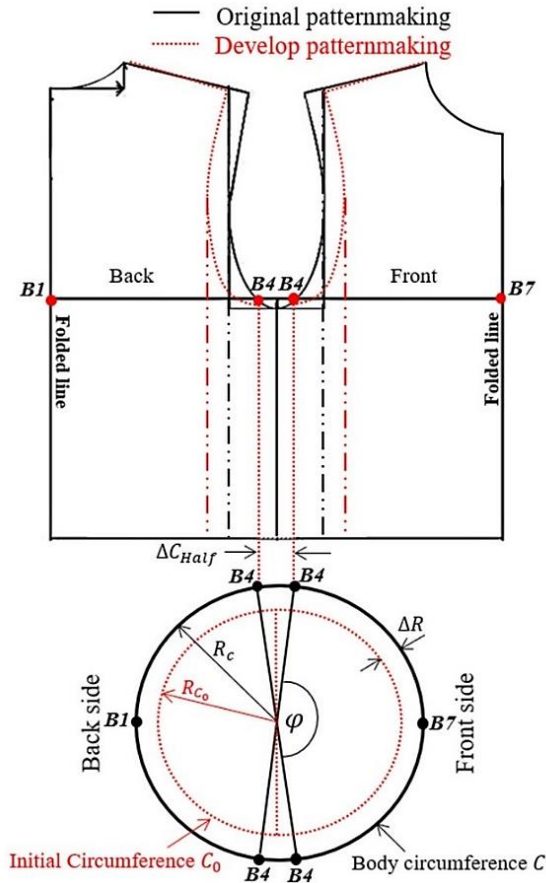


Figure 3.8 Schematic diagram of patternmaking development relate to a circle shape [110]

The initial circumference:

$$C_0 = C \times E_i \quad (3.6)$$

An initial half pattern can be described when $\overline{B1B4} = \overline{B4B7}$ equation can be re-written as follows:

$$\overline{B1B4} = \overline{B4B7} = \frac{C \times E_i}{4} \quad (3.7)$$

Considering the body circumference of pattern relate to a circle circumference:

$$R_{C_0} = R_C \times E_i$$

$$\varepsilon = \frac{\Delta C}{C_0}$$

$$\Delta C_{Half} = \frac{\varepsilon C_0}{2} = R_C(\pi - \varphi)$$

$$\overline{B1B4} = \overline{B4B7} = \frac{R_C(\varphi)}{2} \quad (3.8)$$

Figure 3.8 Referring the mentioned figure, the block pattern construction of female body measurement is represented in black lines and red lines referred to the pattern construction abscissa that has been decreased at bust circumference sizes by strain value and the initial circumference could be calculated by multiplying the elastic coefficient from the equation (3.6). Then the length at bust of pattern construction resulted from the implementation of equations (3.7) while equation (3.8) will be related to cylindrical model as a circle circumference. However, this method represents only a single part of the body circumference and for other parts, circumference could also be calculated.

3.3.2.3 Applying the elastic coefficient coordinate with standard sizing system: In this particular part of the research, propose application of pattern construction development method based on the standard sizing system and the value of elastic coefficient to estimate the size of patternmaking is proposed. In figure 3.9, 2D pattern construction and 3D construction garment are represented to describe two basic steps of calculating construction abscissa including the bust part and the development method of the construction abscissa formula by multiplying the elastic coefficient from the equation (3.9) is as follows:

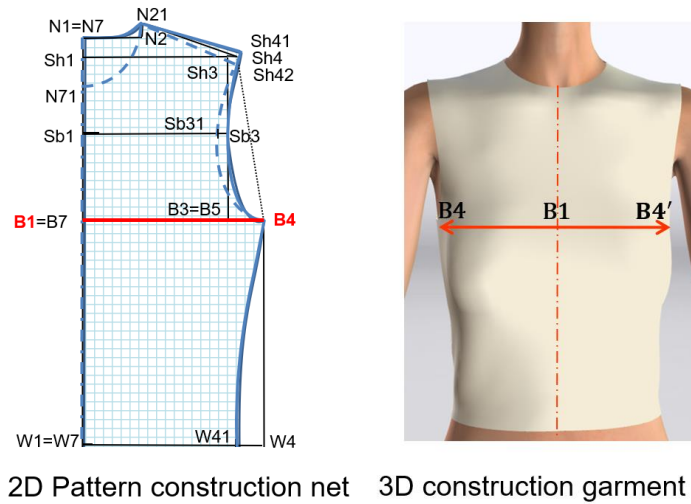


Figure 3.9 Construction abscissa of 2D pattern net and 3D garment

Primary step of construction abscissa

$$\overline{B4B4'} = 0.5 \times B_{Bust}$$

Secondary step of construction abscissa

$$\overline{B1B4} = \left(\frac{\overline{B4B4'}}{2} \right)$$

Construction abscissa development

$$\overline{B1B4} = \left(\frac{\overline{B4B4'}}{2} \right) \times E_i \quad (3.9)$$

Referring to the benefit, this experiment, would essentially help garment industries navigate the suitable way of predicting the size of patternmaking for pressure garment.

3.3.2.4 Applying the patternmaking method by CAD software: The development of pattern construction method for this research was conducted by applying PDS tailor XQ software to create the patternmaking through CAD system. Automatically set up patternmaking depending on standard size which was selected, and the data of the body measurement were calculated and assist in creating the size of pattern construction based on the elastic coefficient. Unikon+ method was applied to PDS tailor XQ software to calculate the construction abscissa under the regression formula from the equations (3.10) and (3.11) and the modification of construction abscissa for stretch fabric by multiplying elastic coefficient was developed by equation (3.12).

Primary step of construction abscissa [27]

$$U_{i(p)} = K_i \times B_i + q_i \mp e_i \quad (3.10)$$

Secondary step of construction abscissa

$$U_{i(s)} = K_i \times U_{i(p)} + q_i \quad (3.11)$$

Construction abscissa development

$$U_{i(s)} = (K_i \times U_{i(p)} + q_i) \times E_i \quad (3.12)$$

Where, U_i is Construction abscissa, K_i is regression coefficient, B_i is body dimension, q_i is absolute term, e_i is easy allowance and E_i is elastic coefficient.

3.4 Fabrics performance for pressure garments

3.4.1 Mechanical properties of stretch fabrics

3.4.1.1 Determination of weight per unit area: The determination of Gram per Square Meter (GSM) is measured according to ASTM D 3776 - 96 standard test methods [94]. Ten samples of width x height (10 cm x 10 cm) were cut and conditioned at the 20 ± 2 °C and

65 ± 5% relative humidity for 24 hours. The samples were weight individually using an electronic weighing balance and the average of ten readings was taken. The weight per square meter area was calculated using the formula given below:

$$\text{GSM} = \frac{w \times 100 \times 100}{\text{area of the sample}} \quad (3.13)$$

3.4.1.2 Determination of thickness: Digital Thickness Gauge M034A was used to determine the thickness of the fabric. Fabric thickness was measured according to standard ISO 5084 the determination of thickness of textiles and textiles products [111]. Ten times readings and the average of ten readings was taken on each sample at different places.

3.4.1.3 Determination of wale and course per unit length: The number of loops in wale per centimetre and course per centimetre were counted using a pick glass from ten different places and the average of ten readings was taken for both wale and course of fabrics respectively.

3.4.1.4 Determination of strength and elongation properties: Testometric universal testing machine was used to test the tensile of stretch fabrics according to standard ISO 13934-1 [112], being selected for inputting into the tensile testing machine experiment include the instrument was based on the principle of CRE (Constant rate of Extension) at 500 mm/min, specimens size (lengthways direction) of (200 x 50) mm, gauge length at (100 ± 1) mm and then samples had been repeated 10 times at the (20 ± 2) °C and (65 ± 5%) relative humidity.

3.4.1.5 Determination of stress-strain behaviour: The stress-strain curve uses the result from the force-elongation behaviour of the experiment of strength and elongation properties is aforementioned to calculate the stress and strain from the equation (3.14) and (3.15) respectively. While the area cross-sectional of fabric is achieved from the fabric width multiplying by fabric thickness as shown in Figure 3.10.

- Definition of stress σ (Pa) is defined as the force per unit area of a material.

$$\sigma = \frac{\text{Force}}{\text{Area cross-sectional}} = \frac{F}{a} \quad (3.14)$$

- Definition of strain ε is defined as extension per unit length.

$$\varepsilon = \frac{l-l_0}{l_0} = \frac{\Delta l}{l_0} \quad (3.15)$$

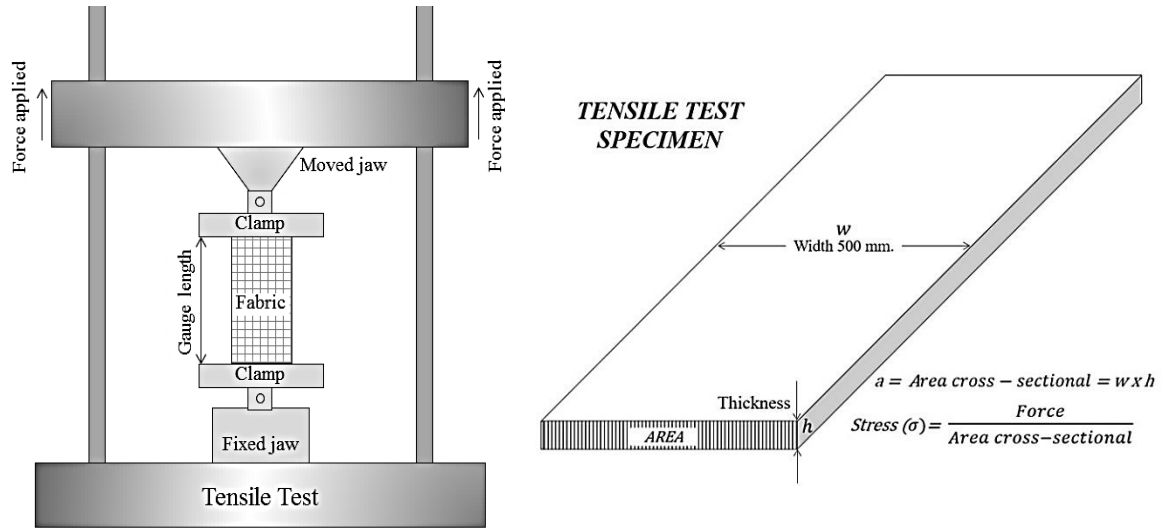


Figure 3.10 Schematic diagram the tensile testing machine

3.4.1.6 Determination of the elasticity: The elasticity of elastic fabric testing according to standard EN 14704-1 strip test [105] for knitted fabrics method A- Strip test specimens of the hysteresis loops obtained from a cyclic tensile test performed on an elastic fabric sample, the specimens 200 mm in length, 50 mm width and the gauge length was 100 mm. The CRE of extension and retraction rate was 500 mm/min. The preparation, pre-conditioning and testing were carried out under standard atmospheric conditions of $(20 \pm 2)^\circ\text{C}$ temperatures and $(65 \pm 5\%)$ relative humidity. Fixed elongation at 50% on each cycle from 1 to 5 cycle times and on the final cycle set CRE testing machine held at the maximum force approximately 60 seconds.

The results of the graph can be calculated force decay due to the time, un-recovered elongation, recovered elongation and elastic recovery as the expressions and calculations of test result:

- *Definition of force decay due to the time:* Loss of force measure over the time when test sample is stretched to a specified elongation or force and held at this position for a given period [105].

$$\text{force decay} = \frac{\text{max force from final cycle} - \text{max force after holding period}}{\text{max force from final cycle}} \times 100 \quad (3.16)$$

- *Definition of un-recovered elongation:* Ratio of un-recovered extension of the test sample after cycling, to a specified force or extension, to its initial length, express as a percentage.
- *Definition of recovered elongation:* Un-recovered elongation expressed as a percentage, subtracted from 100%.
- *Definition of elastic recovery:* Recovered elongation expressed as a percentage of the total elongation.

3.4.1.7 Determination of the stress relaxation: The relaxation procedure of elastic fabrics was investigated by the holed the fabric strain that the test specimens were stretched up to 0.5 with the tensile testing machine and left in this fixed strain for 60 seconds. The values of stress were measured continuously. The experiment had applied the generalized Maxwell model as shown in the Figure 3.11 and standard EN 14704-1 strip test [105] was used for determining method of stress relaxation.

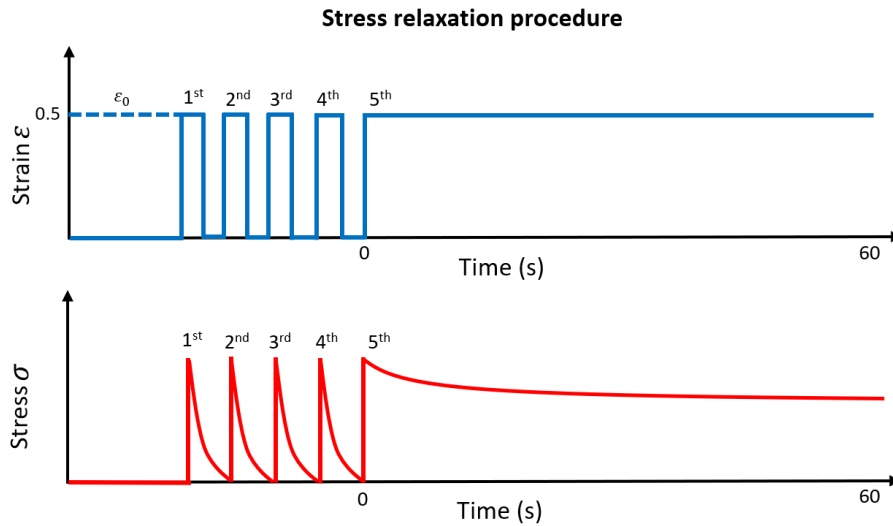


Figure 3.11 The setting method for testing stress relaxation

- *Definition of stress relaxation due to the time:* The loss of stress measure over the time when test sample is stretched to a specified strain or stress and held at this position for a given period.

$$\text{Stress relaxation} = \frac{\text{max stress from final cycle} - \text{max stress after holding period}}{\text{max stress from final cycle}} \times 100 \quad (3.17)$$

3.4.1.8 Determination of dynamic work recovery: The recovery behaviour of fabric or garment is considered to be important in terms of enhancing power of the sports person involved in strenuous sports activity. In general, elastic textile material will give minimum work energy loss which can be calculated by the assessment of the percentage of Dynamic Work Recovery (DWR) as found in equation (3.18).

$$DWR\% = \frac{\text{Area under the unloading curve}}{\text{Area under the loading curve}} \times 100 \quad (3.18)$$

The experiment and specimens were applied with the same procedure of elasticity of elastic fabric testing according to standard EN 14704-1 strip test [105] for knitted fabrics method A- Strip test specimens of the hysteresis loops obtained from a cyclic tensile test. The number of cyclic should be considered for analysis due to the first cycle of the hysteresis loop generally has a huge energy loading area than the other loops. The graph stress-strain curve used for calculating the work energy shown in the Figure 3.12 represented the results of the sample S7 in and also described the area under loading and unloading of dynamic work energy in order to find out the DWR. This experiment uses the hysteresis loops on fifth cycle to calculate the DWR% and comparison.

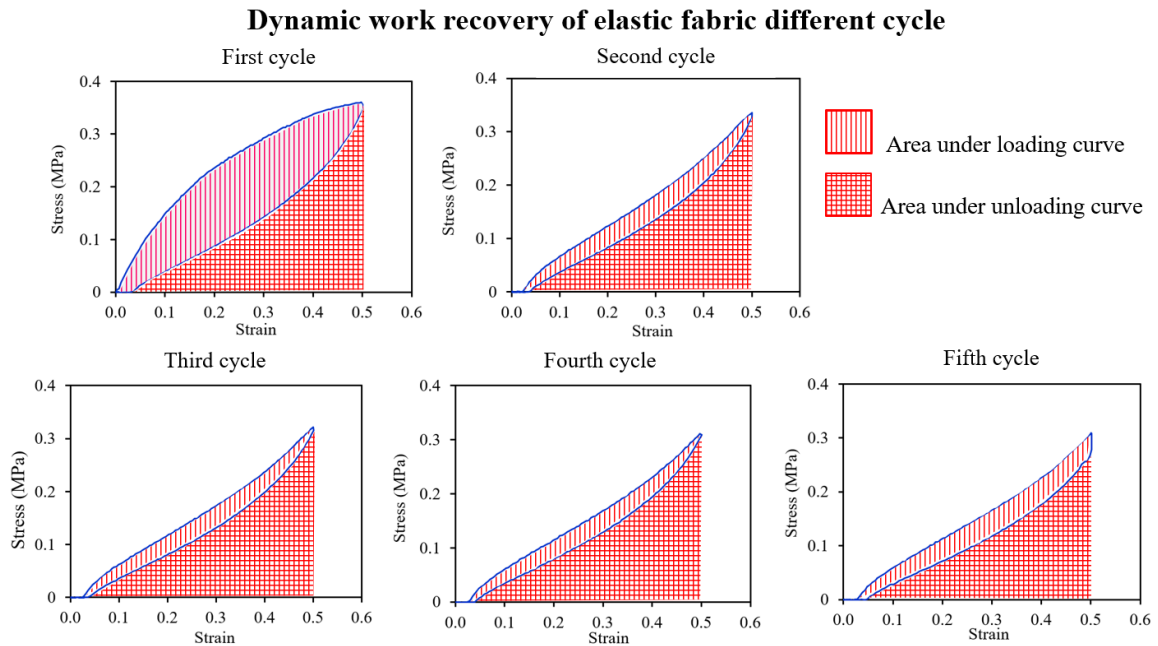


Figure 3.12 Comparative the DWR with different cycle of loading-unloading

3.4.2 Fabric deformation measurement by image analysis

This work presents an investigation on local textile deformations during the tensile testing of stretch fabrics in direction of course using image analysis technique. The grid pattern of black dots was applied on the fabric surface before the test and used as the reference points for image analysis. The concept of gradient deformation tensor employs to estimate the relative displacement of marked points on textile surface under different stretch loading of 10 %, 20 %, 30 % and 40 % extension. Later, the obtained results were validated with simulated images generated by MATLAB image processing tool box. In this way, the image analysis method employs for estimation of deformation properties of elastic knitted fabrics for adequate fitting of garments to the required comfort.

3.4.2.1 Determination of fabric deformation measurement using MATLAB: The elastic fabrics used for the experiment. The specimens cut in course direction with dimensions of (length x width) of 30 cm x 5 cm. The samples condition for 24 hours before actual testing in standard atmosphere of $(20 \pm 2) ^\circ\text{C}$ temperatures and $(65 \pm 5\%)$ relative humidity. The digital image analysis will apply for the standard ISO 13934-1 strip test [112]. The tensile force apply at a speed of 100 mm/min and the gauge length was fixed at 20 cm. For the image acquisition and analysis, the fabric was applied with dot pattern of black colour and the distance between the dots kept at 1 cm both in X axis and Y axis all over the fabric surface. The images of stretched textile specimen were captured by a digital camera with resolution 4000 x 3000 pixels, ISO 200, aperture F 2.2, Shutter Speed 1/15s and distance to camera of 50 cm as shown the Figure 3.13 [113].

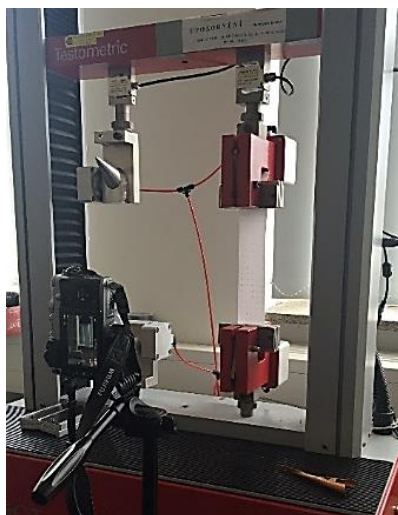


Figure 3.13 Experimental for setup for image analysis

3.4.2.2 Concept of gradient deformation tensor: The concepts of gradient deformation tensor are introduced to quantify the change in shape of infinitesimal line elements in a solid body. Figure 3.14 shows the straight line drawn on the undeformed configuration of a solid. However, after the deformation, the line becomes as a smooth curve.

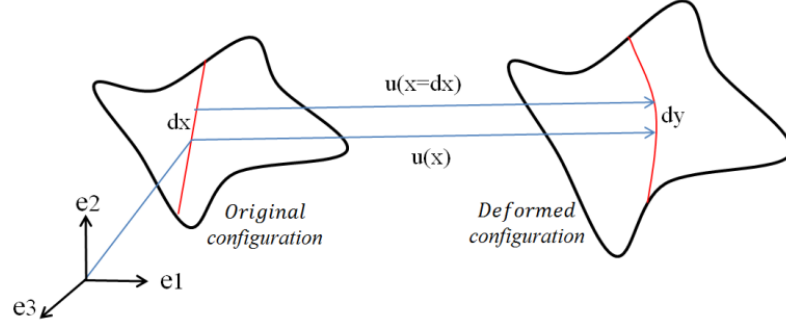


Figure 3.14 Concept of gradient deformation tensor [114]

When we focus attention on a line segment dx , much shorter than the radius of curvature of this curve, the segment would be straight in the undeformed configuration and almost straight in the deformed configuration. Thus, no matter how complex a deformation we impose on a solid, infinitesimal line segments are merely stretched and rotated by a deformation. If we know the displacement field in the solid, we can compute by from the position vectors of its two end points [113].

$$dy_i = x_i + dx_i + u_i(x_k + dx_k) - (x_i + u_i(x_k)) \quad (3.19)$$

Expand $u_i(x_k + dx_k)$ as a Taylor series [113].

$$u_i(x_k + dx_k) \approx u_i(x_k) + \frac{\partial u_i}{\partial x_k} dx_k \quad (3.20)$$

$$dy_i = dx_i + \frac{\partial u_i}{\partial x_k} dx_k = \left(\delta_{ik} + \frac{\partial u_i}{\partial x_k} \right) dx_k \quad (3.21)$$

We identify the term in parentheses as the deformation gradient, so

$$dy_i = F_{ik} dx_k \quad (3.22)$$

In general, deformation gradient tensor is given by

$$F = I + \nabla u$$

or in Cartesian components [113, 114].

$$F_{ik} = \delta_{ik} + \frac{\partial u_i}{\partial x_k} \quad (3.23)$$

$$F = \begin{pmatrix} 1 + u_{11} & u_{12} \\ u_{21} & 1 + u_{22} \end{pmatrix} \quad (3.24)$$

Where ∇u is the displacement gradient tensor, also expressed as $\frac{\partial u_i}{\partial x_k}$ and it is the identity tensor described by the Kronecker delta symbol as follow:

$$\delta_{ik} = \begin{cases} 1, i = k \\ 0, i \neq k \end{cases} \quad (3.25)$$

The acquired digital images were processed to remove the noise and improve the quality of images before calculation of gradient deformation tensor. Figure 3.15 shows the sequence of operations performed for image processing. Segmentation is the process in which an image is divided into constituent objects or regions of similar attributes. Segmentation extracts the desired object of interest from the background. Thresholding is a process of converting a gray-scale input image to a binary image. The purpose of thresholding is to extract those pixels from image which represent an object. In present work ISODATA thresholding was employed [115].

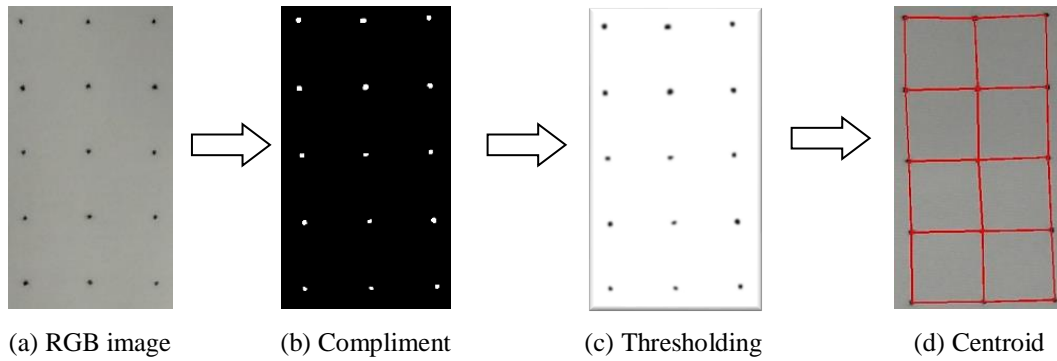


Figure 3.15 Image processing steps [113]

3.5 Applying the Laplace's law for CG and evaluating the pressure

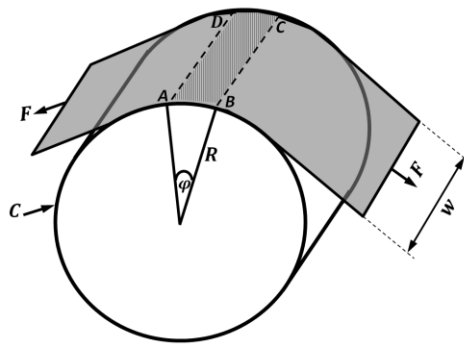
3.5.1 Applying Laplace's law theory to practice on pressure garment

The aim at this part of the experiment is to describe the compression of pressure garment at which fabric was extended during wearing on the body that is based on Laplace's law theory application.

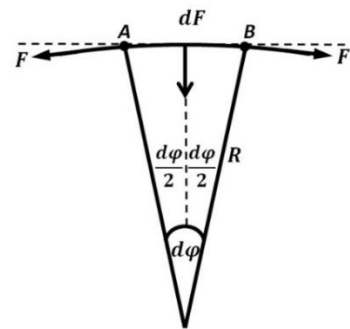
The following assumptions were accepted in the considerations:

1. The relationship between the pressure of compression garment and force by pulling the fabric extended is described by Laplace's Law as shown in equation (3.26).
2. The experiment defined fabric extension in a cylindrical shape as similar to human body shape.
3. The circumferential stress is the focus of the testing; therefore, the ratio of thickness to the centre diameter of the cylinder with very less can be neglected.
4. The relation between stress and strain of elastic fabrics will be determined on the standard of experiment characteristics for the stress-strain phase of the stretch fabric in 5th hysteresis cycles.

By applying Laplace's law, the determination of pressure value requirement for the prediction of strain value of the stretch fabric was conducted. In the testing, the geometric form of the cylinder is assumed to indicate human body figure. Figure 3.16 (a) illustrates the fabric stretch on areas of (A, B, C, D) shown in cylindrical model below and in Figure 3.16 (b), contact pressure was demonstrated on the cylinder with a small element of fabric stretched from position A to B. The force pulls have occurred on fabric at both sides, but curvature of the cylinder surface has created each of these forces unparallel to the tangent plane. In the one-direction force acts with two nearly opposite forces of magnitude is F , each forming a tiny angle of magnitude $F \sin \frac{d\varphi}{2}$ with the tangent to the surface in the one-direction. Projecting of these total force in the direction through of the centre of curvature $dF = 2F \sin \frac{d\varphi}{2} = F d\varphi$ where $dA = R d\varphi w$ is the area of the rectangle (A, B, C, D).



(a) Fabric stretch on the cylindrical model



(b) The pressure contacts on surface area

Figure 3.16 Fabric stretch showing the force directions on the cylindrical model

Pressure P is defined as a measure of the force applied over a unit area. Referring, fabric acts at the small area of the rectangle element in Figure 3.16 (a and b). Finally, adding the contribution from the two-direction we arrive at the Laplace's law for the pressure discontinuity due to force of fabric stretched. It could be observed when dealing with surface tension of stretch fabric, application of Laplace's Law is widely taken part in pressure prediction [6].

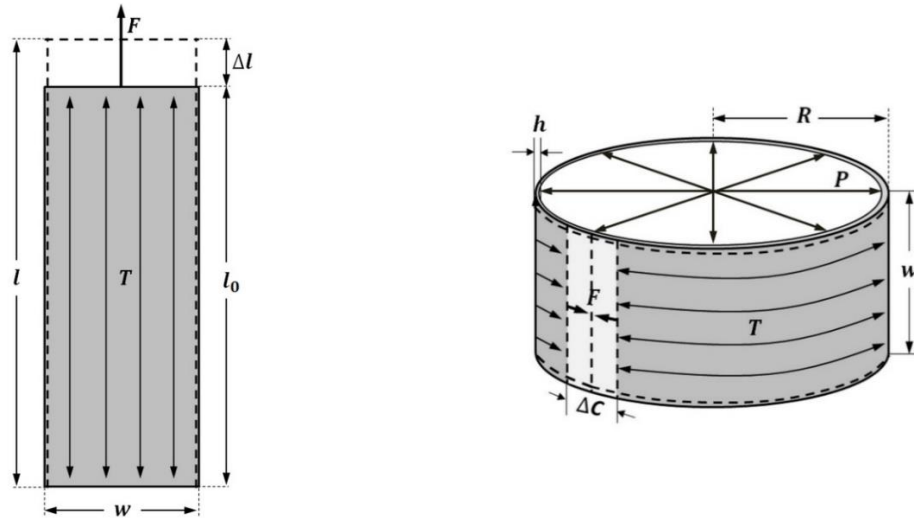
$$P = \frac{dF}{dA} = \frac{Fd\phi}{Rd\phi w} = \frac{F}{Rw} = \frac{Tw}{Rw} = \frac{T}{R} \quad (3.26)$$

In case of considering whole area of cylindrical model, it could be defined that $\phi = 360^\circ$ or 2π as found in the following equation [6]:

$$P = \frac{dF}{dA} = \frac{Fd\phi}{Rd\phi w} = \frac{F2\pi}{R2\pi w} = \frac{Tw2\pi}{Cw} = \frac{T2\pi}{C} \quad (3.27)$$

3.5.2 Prediction of strain value using the mathematical modelling

Referring the tension acting of fabric stretched by tensile testing machine in Figure 3.17 (a) illustrates the loading force F and tension T acting on the fabric and relate to Figure 3.17 (b) represents force F and tension T acting of fabric on cylindrical model. In fact, when fabric extended in the length direction then the other direction will shorter in width direction as shown in the Figure 3.17 (a and b).



(a) Fabric tension acting from tensile strength machine (b) Fabric tension acting on cylindrical model

Figure 3.17 Fabric tension acting on cylindrical model

Stress σ is the ratio of applied force to a cross section area is defined as the force per unit area of a material [6].

$$\sigma = \frac{F}{a} = \frac{Tw}{hw} = \frac{T}{h} \quad (3.28)$$

Applied the tension $T = \sigma h$ from equation (3.28) into the equation (3.27) as follow:

$$P = \frac{\sigma h 2\pi}{c} \quad (3.29)$$

Then it can be applied for calculating the stress σ as related to the fabric which was extended by pulling force and it is so called the circumferential stress [116].

$$\sigma = \frac{DP}{2h} \quad (3.30)$$

The stress–strain data points were fitted with a third-order polynomial function is accurate enough to predict the dependence available of strain ε value at the magnitude of independence available of fabric stress σ . The equation, it can be described with the following the model for prediction equation (3.31).

$$\varepsilon(\sigma) = a_1\sigma^3 + a_2\sigma^2 + a_3\sigma \quad (3.31)$$

Predicted mathematic modelling of circumference stress, substituting independence from equation (3.30) of fabric stress in to the cubic function (3.31) then it obtains the prediction of strain value equation (3.32) as function prediction model of its diameter of the cylindrical model D or diameter of body, pressure P , fabric thickness h and mechanical characteristics of stretch fabric (leading coefficients a_1 , a_2 and a_3) [6].

$$\varepsilon = a_1 \left(\frac{DP}{2h} \right)^3 + a_2 \left(\frac{DP}{2h} \right)^2 + a_3 \left(\frac{DP}{2h} \right) \quad (3.32)$$

3.5.3 Designing experiments to investigate the mathematical modelling with the compression tester

3.5.3.1 Determination of measuring the pressure in vitro model: The experiment on the predictive mathematical modelling method was carried out to find out the pressure values according to the level of strain values of stretched fabric. Conducting an experiment, the strain value of the fabric stretches on the rigid cylindrical model which the model made from Polyvinyl

Chloride (PVC) was used at 0.79 m and 0.505 m circumferences and the initial circumference of the fabric length of was determined from the strain value at 0.1, 0.2, 0.3, 0.4 and 0.5. The initial circumference C_0 was calculated by following equation [6, 110].

$$C_0 = \frac{C}{\varepsilon + 1} \quad (3.33)$$

3.5.3.2 Effect of sensor thickness for measuring the pressure: Regarding results of measured pressure values when measured by the compression tester, measured pressure values were overestimated due to effect of high sensor thickness and therefore, correction factor was then used to eliminate pressure perturbation of sensor thickness effect in the experiment.

Concerning the usage of compression tester PicoPress®, it could be found that when thickness was 0.2 mm, no inflation occurred, however; in case of 3.00 mm, inflation did occur significantly [26, 23]. With this reason, predictive modelling should be applied on the particular area of the sensor. Concerning sensor determination, sensor diameter is D_s 50.00 mm where the area of sensor contacts on fabric and creates the angle φ by radius of the cylindrical model as shown in the Figure 3.18.

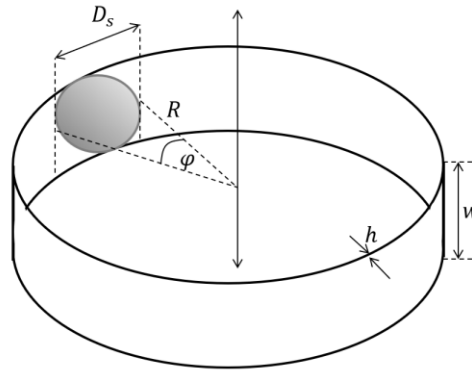


Figure 3.18 The sensor area of compression tester [6]

The pressure value on the sensor can be applied from the equation (3.26) and used the tension $T = \sigma h$ and using the length of fabric stretch of the diameter of a sensor D_s to obtain the equation (3.34) and the stress value by the equation (3.35) [6].

$$P = \frac{F}{A} = \frac{F\varphi}{R\varphi w} = \frac{Tw\varphi}{D_s w} = \frac{T\varphi}{D_s} = \frac{\sigma h \cdot \varphi}{D_s} \quad (3.34)$$

$$\sigma = \frac{D_s P}{h \cdot \varphi} \quad (3.35)$$

The functional equation can be applied by substituting the fabric stress at the sensor area σ_s from equation (3.35) in to the function (3.31) to predict the strain value on the area of sensor of compression tester by equation (3.36) [6].

$$\varepsilon(\sigma_s) = a_1 \left(\frac{D_s P}{h \cdot \varphi} \right)^3 + a_2 \left(\frac{D_s P}{h \cdot \varphi} \right)^2 + a_3 \left(\frac{D_s P}{h \cdot \varphi} \right) \quad (3.36)$$

Due to the thickness of the PicoPress® sensor itself when measuring compression, an overestimation of pressure had occurred as shown in the Figure 3.19. Thus, to eradicate the problem, a reduction of the over stress will be taken part in order to unravel the overestimation [83]. As proposed by [22] in the model, equation (3.37) was applied to estimate the pressure perturbation or coefficient of pressure perturbation (C_{PP}).

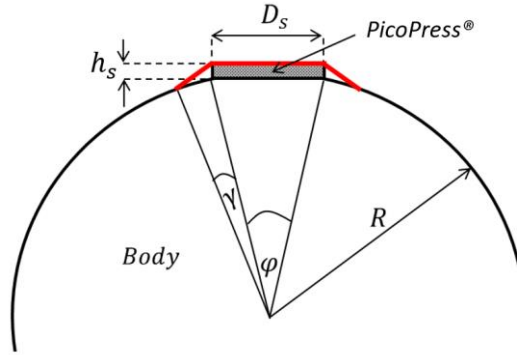


Figure 3.19 The sensor of compression tester acting under fabric stretched on the cylindrical model [6]

$$C_{PP} = \frac{\sin(\frac{\varphi}{2} + \gamma)}{\sin(\frac{\varphi}{2})} \quad (3.37)$$

$$\varphi = \frac{D_s}{R}$$

$$\gamma = \arccos\left(\frac{R}{R+h_s}\right)$$

Concerning the sensing area of the PicoPress® sensor, the probe was shown as in a circular shape in the model as shown in the Figure 3.18 while the stress area as mentioned in equation (3.38) represents the local area of sensor diameter D_s and sensor width w . In fact, it is a

necessity to determine the coefficient of pressure perturbation due to local stretch C_{TP} under the sensor as shown in the following equation (3.39) [6]:

$$P = \frac{F}{A} = \frac{F\varphi}{R\varphi w} = \frac{\sigma h w \varphi}{D_s w} \quad (3.38)$$

$$C_{TP} = \frac{\sigma h w \varphi / D_s w}{\sigma h w \varphi / \pi \left(\frac{D_s}{2}\right)^2} = \frac{\pi D_s^2}{4 D_s w} \quad (3.39)$$

The total pressure perturbation then can be calculated by [84].

$$\text{The total pressure perturbation} = C_{PP} \times C_{TP} \quad (3.40)$$

Where C_{PP} is coefficient of pressure perturbation due to sensor dimension and C_{TP} is coefficient of pressure perturbation due to local stretch.

The correction factor for the measuring the pressure values can be applying by following Khaburi, Dehghani-Sanij, Nelson and et al. [83] equation:

$$\text{Correction factor} = \frac{1}{\text{The total pressure perturbation}} \quad (3.41)$$

The equation (3.41) was used for calculating the correction factor of the compression tester PicoPress® in order to get the actual pressure results for this experiment.

3.5.3.3 Determination of measuring the pressure in vivo model: The experiment was used the same procedure of measuring the compression pressure with rigid cylindrical model. Conducting an experiment, the strain value of the fabric stretch on the thigh part of the human body was used at 0.505 m circumferences which the thigh shape assumed as a cylinder shape. The initial circumference of fabric length was determined from the strain value at 0.1, 0.2, 0.3, 0.4 and 0.5. were calculated by equation (3.33).

3.5.4 Designing experiment to predict the strain of pressure garments

3.5.4.1 Determination of predicted strain by applying compression tester: The experiment was conducted to determine fabric strain at 0.1, 0.2, 0.3, 0.4 and 0.5 and compression tester PicoPress® was then used for measurement. The actual pressure results could be calculated the strain values from the predictive modelling from the equation (3.33). Afterwards, strain

value results from the modelling were compared with the strain values and results were determined.

3.6. Development and application of a novel tensile measurement device

This part is to develop a new the tensile measurement device for testing the value of weight and elongation of elastic fabric. Due to the high expense of standard tensile testing such as Testometric materials testing machines, a device should be designed and developed in order to help solve the problem and meanwhile, this device could also be helping the researcher measuring accuracy of fabric elongation by weight. Thus, a new tensile measurement device could help and solve the solution for estimating the size of pattern construction for pressure garments.

3.6.1 Designing the novel tensile device

The tensile measurement device was invented by Ing. Blažena Musilová, Ph.D. and Mr. Gerhard Geisler who produced the device and added the functions system for testing as shown the Figure 3.20. Sketched by Mr. Gerhard Geisler, 10 manual functions of tensile measurement device are shown as follows:

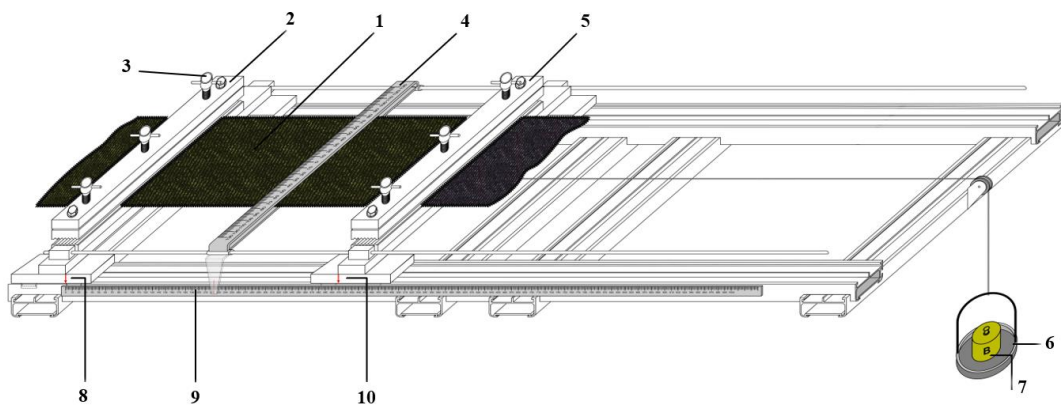


Figure 3.20 The Schematic design of the tensile measurement device

1. *Fabric specimen*: The specimen test could be applied very larger size for testing and the maximum is 20 cm.
2. *Fixed jaw*: The jaw could be used for fixed and holding one side of specimen.
3. *Fixed screw*: The screw helps holding the specimen tightly.

4. *Scale measurement width*: The ruler scale makes its measurement in centimetre unit and measurement of specimen width could be changed in accordance to displacement and deformation.
5. *Moved jaw*: The jaw is connected to cable and tray to load up the weight. The jaw can be moved depending on the weight and stretch ability of the specimen without friction on the mobile roller.
6. *Tray*: Tray is used to input the weight.
7. *Standard weight*: Weight that is used for measurement in the experiment.
8. *Initial mark*: The mark that starts from 0 centimetre.
9. *Scale measurement length*: The ruler scale makes its measurement in centimetre unit and measurement of specimen length could be changed in accordance to displacement depending on the length.
10. *End mark*: The mark can be used for indicating the final length of any specimen change.

3.6.2 Determination of the elasticity

The experimental design of the manual tensile testing device as shown in Figure 3.21 was referred to the elasticity of elastic fabric testing according to standard EN 14704-1 strip test. The specimens were cut 200 mm in length, 50 mm width and the gauge length 100 mm. The loading was assessed by weight instead of pulling force. The weight starts from zero and additional 250 g of weight is added in every step of weight calibration and length of fabric is measured until the fabric elongation reaches 50% on each cycle from 1 to 5 cycle times.

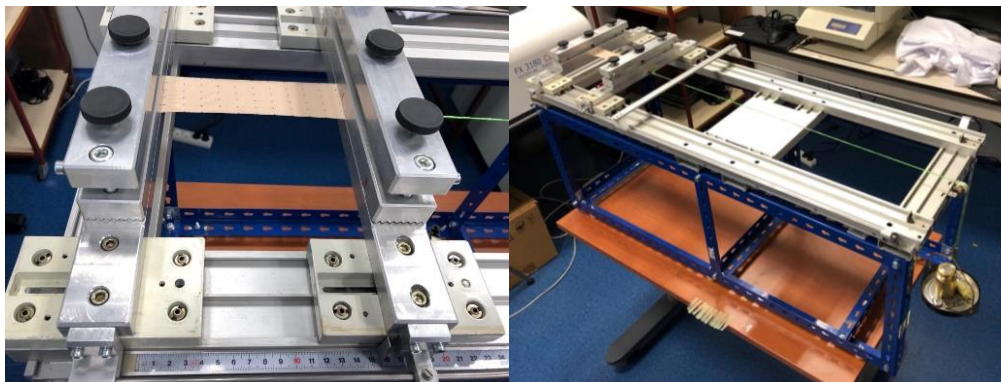
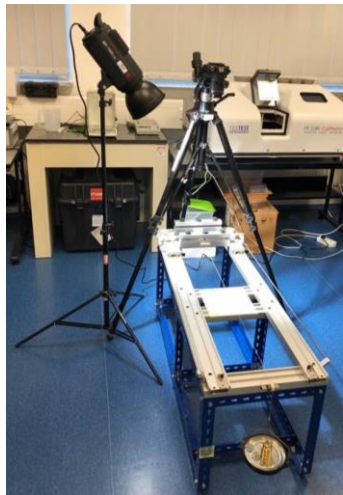


Figure 3.21 The experimental design and testing of manual tensile testing device

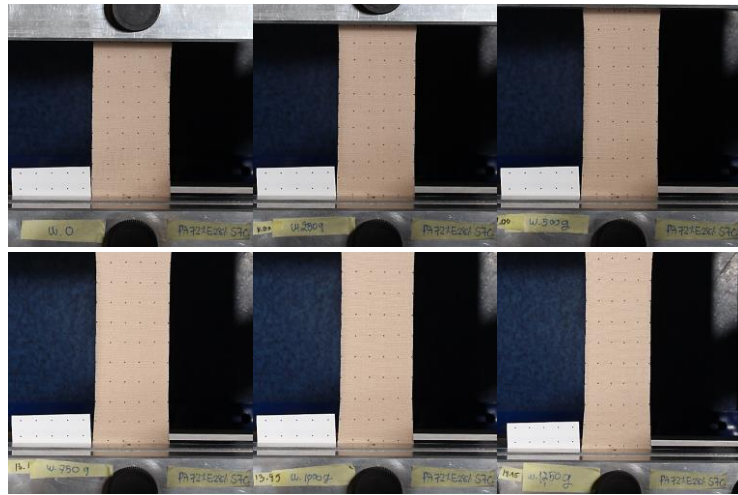
3.6.3 Determination of fabric deformation measurement using NIS-Element

The experiment of image analysis using NIS-Element software used the specimens were cut in with dimensions 200 mm in length, 50 mm width and the gauge length was 100 mm. For the image acquisition and analysis, the specimen was applied with black dot pattern and the distance between the dots kept at 1 cm both in X axis and Y axis all over the fabric surface.

The setting method as shown in Figure 3.22 (a) images of fabric specimen were captured by a digital camera with resolution 4000 x 3000 pixels, ISO 200, aperture F 2.2, Shutter Speed 1/15s and distance between camera and specimen was 70 cm and the sequences of deformed images at every step of the weight 250 g of specimen elongation are shown in Figure 3.22(b) and then the results were validated with calibration images generated by Nikon NIS-Elements - Imaging Software.



(a) Camera and lighting set up for the experiment



(b) The fabric deformation by images from sample S7

Figure 3.22 The experimental design for capturing the images from manual tensile testing device

Chapter 4 Results and Discussion

4.1 Mechanical properties of elastic fabrics suitable for CGs

4.1.1 Preliminary testing of elastic fabrics to obtain preliminary data of fabrics

Preliminary data results for GSM, thickness, stitch density of wale and course per unit length, fibre composition of Polyamide (PA) and Elastane (EA), fineness of yarn and structure of knitted fabrics were determined as per standard testing methods shown in the Table 4.1.

Table 4.1 Elastic knitted fabric characteristics

Sample	GSM (g/m ²)	Thickness (mm)	Wale per cm.	Course per cm.	PA (%) (dtex/ply)	EA (%) (dtex/ply)	Structure
S1	215.21 (±0.017)	0.55 (±0.004)	24 (±0.196)	35 (±0.196)	90.79 (44×2)	9.21 (22)	Single jersey
S2	218.18 (±0.011)	0.55 (±0.005)	24 (±0.261)	35 (±0.261)	87.59 (44×2)	12.41 (33)	Single jersey
S3	260.47 (±0.012)	0.50 (±0.004)	21 (±0.196)	39 (±0.261)	74.52 (44×2)	25.48 (78)	Single jersey
S4	270.87 (±0.012)	0.60 (±0.005)	19 (±0.196)	32 (±0.196)	94.38 (78×2)	5.62 (22)	Single jersey
S5	305.14 (±0.01)	0.61 (±0.004)	19 (±0.196)	35 (±0.196)	92.94 (78×2)	7.06 (33)	Single jersey
S6	318.49 (±0.01)	0.57 (±0.004)	19 (±0.196)	34 (±0.196)	83.46 (78×2)	16.54 (78)	Single jersey
S7	319.66 (±0.01)	0.79 (±0.006)	21 (±0.392)	36 (±0.523)	72.00	28.00	Locknit
S8	310.00 (±0.007)	0.64 (±0.005)	20 (±0.392)	38 (±0.392)	70.00	30.00	Interlock

Note: “±” is the upper and lower 95% confidence interval of the mean

4.1.2 Physical testing for performance and serviceability of fabrics

4.1.2.1 Force and elongation characteristics: The results of tensile testing were experimented according to standard ISO 13934-1 [112]. In Figure 4.1 (a, b and c) will be representing the graph of relationship of force-elongation among eight sample tests in three directions including wale, course and bias respectively.

Figure 4.1 (a, b and c) illustrates the characteristics of force-elongation in wale, course and bias directions respectively. The maximum force when compares with the same structure of single jersey from samples (S1 - S6), samples (S4 - S6) are characterized as a group with high yarn count number of PA (Polyamide: 78 dtex, 2 plies) and the maximum force was

considered higher than the low yarn count group of PA (Polyamide: 44 dtex, 2 plies) as found in sample (S1 -S3). Overall, it could be assumed that the size of yarn count in the samples (S1-S6) with single jersey structure had very much influence on the magnitude of force value, the bigger yarn count is the higher maximum force value and vice versa. Moreover, the biggest size of elastane yarn count (78 dtex) also shows higher maximum force in the groups of samples (S3) and (S6). According to the interlock structure of the sample (S8), result of maximum force value had shown similar results with single jersey structure in group with high yarn count number of PA in samples (S4 - S6). Apart from that, locknit structure does have the highest force value in wale and course directions.

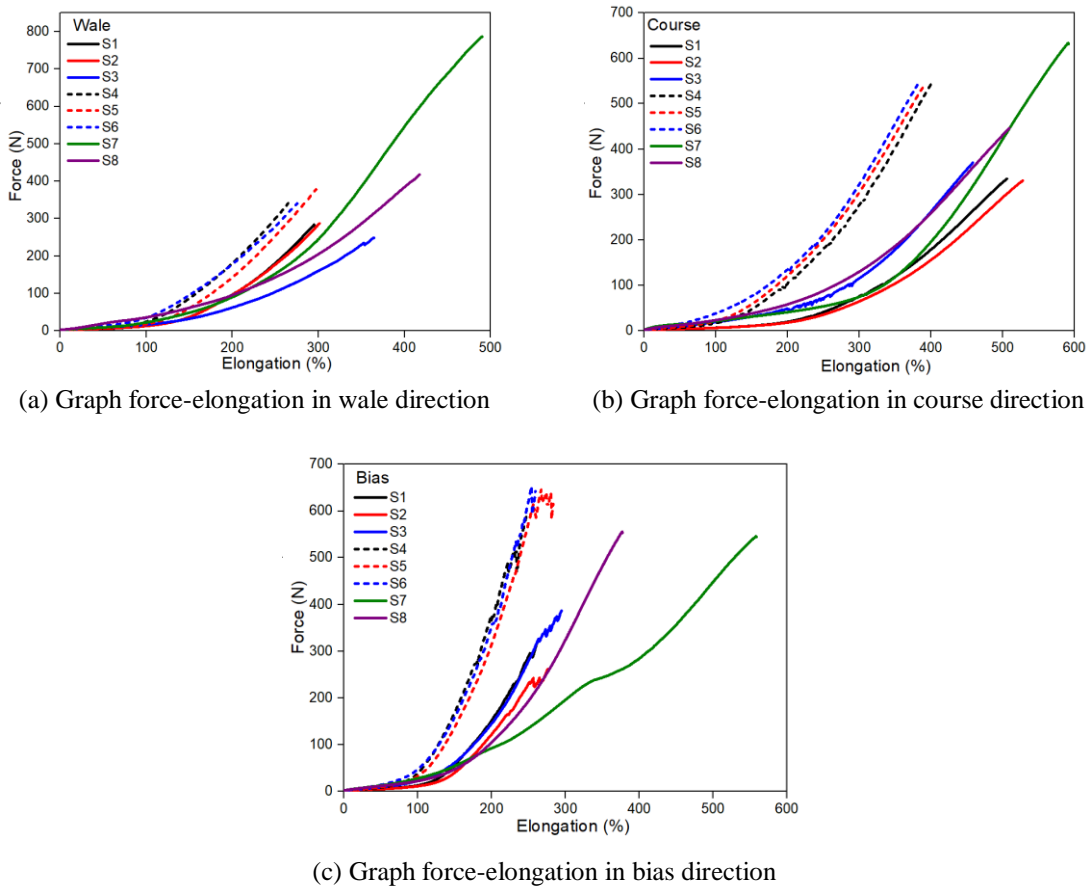


Figure 4.1 Graphs of force-elongation characteristics in different directions

When considering the extensibilities of the knitted fabric in Figure 4.1 (a, b and c), the results of extensibilities in group of single jersey structure found that the small number of yarn count group of the sample (S1 – S3) is higher the percentage of elongation in direction of wale and course than a big group of yarn count of the sample (S4 – S6). Meanwhile, in the fabric directions, it could be found that in course direction, there was the highest efficacy extension in fabric stretched up to 400% as shown in Figure 4.1 (b). Obviously, the locknit

structure illustrates the percentage of elongation approximately 500% - 600% which seems to have an extreme extensibility when compared to the single jersey structure and interlock one. Overall, types of knitted structure and fabric direction signified an influence on the performance of extensibility. When mentioning the fabric direction, course direction has outperformed the wale and bias directions and thus, the course direction is rather suitable for pattern construction along the body circumference.

Table 4.2 illustrates the results of maximum force and elongation of elastic fabrics. The indicated point on the graphs at the maximum force can be considered as a highest point. Overall, it was observed that locknit structure work done, and efficiency possessed higher extensibility values than single jersey and interlock of knitted fabrics structures when compared.

Table 4.2 Elastic knitted fabrics characteristics of maximum force and elongation at fracture

Sample	Wale		Course		Bias	
	Max. force (N)	Elongation (%)	Max. force (N)	Elongation (%)	Max. force (N)	Elongation (%)
S1	279.89 (± 17.077)	295.87 (± 6.852)	333.18 (± 3.941)	495.68 (± 3.941)	301.64 (± 14.183)	280.71 (± 11.922)
S2	283.57 (± 9.329)	301.24 (± 3.709)	323.37 (± 10.213)	511.12 (± 9.643)	260.18 (± 7.716)	280.35 (± 4.454)
S3	249.38 (± 10.970)	361.63 (± 3.191)	366.72 (± 4.656)	450.85 (± 9.723)	381.23 (± 13.876)	295.03 (± 7.270)
S4	347.70 (± 13.605)	263.63 (± 8.824)	535.10 (± 15.483)	392.24 (± 11.151)	574.21 (± 16.289)	254.45 (± 8.882)
S5	374.12 (± 19.712)	296.05 (± 8.423)	537.07 (± 18.843)	392.20 (± 6.326)	633.32 (± 23.889)	263.57 (± 11.492)
S6	342.80 (± 14.428)	279.88 (± 9.955)	542.06 (± 9.490)	378.29 (± 4.247)	643.20 (± 18.580)	255.74 (± 3.998)
S7	795.54 (± 17.034)	498.14 (± 8.355)	612.48 (± 11.175)	583.95 (± 3.937)	519.77 (± 18.591)	547.07 (± 7.411)
S8	412.92 (± 10.525)	412.63 (± 9.850)	437.37 (± 7.979)	503.64 (± 4.936)	534.55 (± 15.808)	364.81 (± 8.879)

Note: " \pm " is the upper and lower 95% confidence interval of the mean

4.1.2.2 Stress and strain behaviour: Referring results of force-elongation curves, they were then calculated the stress-strain as shown in Figure 4.2 (a, b and c) and the comparative results of Ultimate Tensile Strength (UTS) or tensile strength, strain and Young's modulus were obtained as illustrated in Table 4.3.

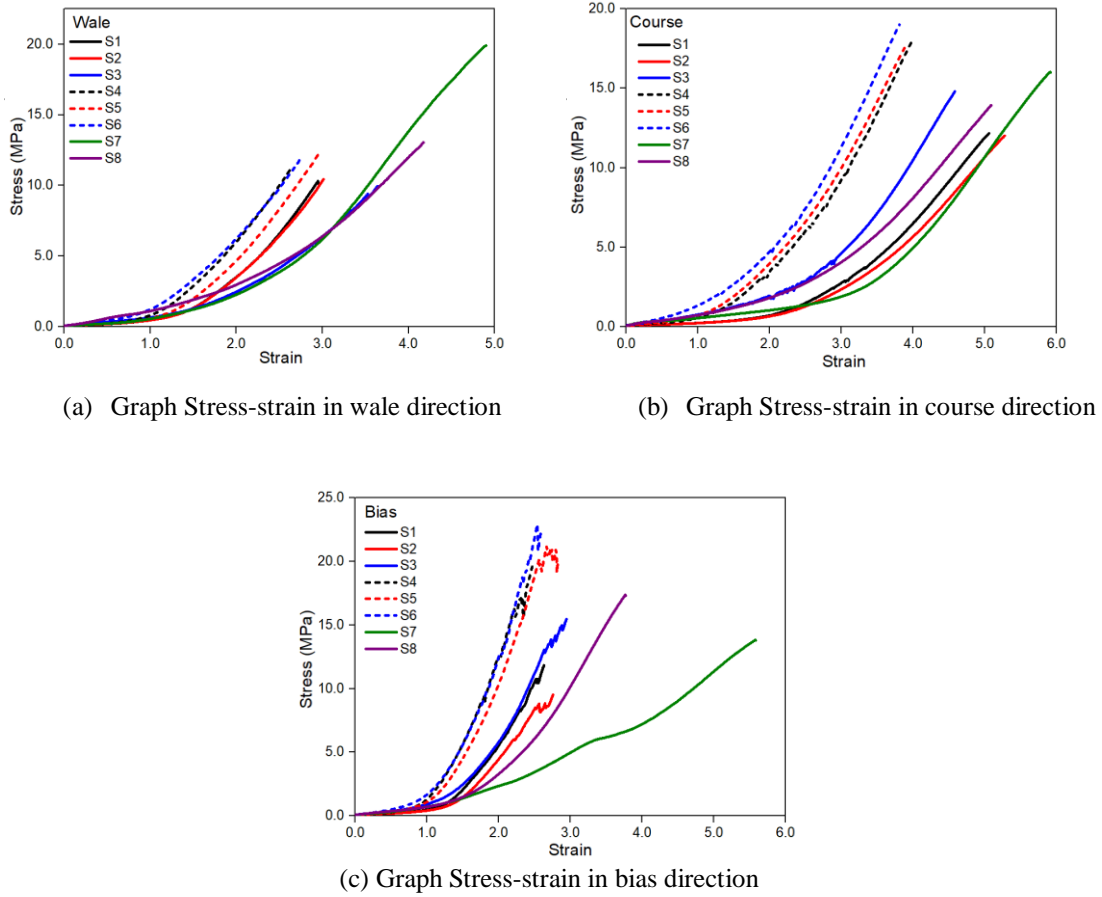


Figure 4.2 Graphs Stress-strain different directions of 8 samples

The graphs in Figure 4.2 (a, b and c) illustrates the stress-strain curves in wale, course and bias directions. The results were analysed in accordance to the fabric structure and the samples of single jersey structure (S1 -S6) were compared with different yarn count of elastane at the number 22 dtex (black), 33 dtex (red) and 78 dtex (blue) and constant yarn count of Polyamide at 44 dtex (line) and 78 dtex (dash line) as shown in the graphs. It could be found that the number of yarn count of elastane has a significant influence on the stress value when yarn count number of elastane has higher stress value.

When considering the knitted fabric structures in Figure 4.2 (a, b and c), containing an excellent extensibility especially in course direction, sample (S7) in locknit structure obtaining strain values almost reaches to 6.0 in course direction. While the directions of wale and bias are considered to perform outstanding in stretching which is almost double the single jersey and interlock ones.

Table 4.3 The properties of UTS, strain and Young's modulus with difference directions

Sample	Wale			Course			Bias		
	UTS (MPa)	Strain	Young's modulus (MPa)	UTS (MPa)	Strain	Young's modulus (MPa)	UTS (MPa)	Strain	Young's modulus (MPa)
S1	10.18 (± 0.621)	2.96 (± 0.069)	3.44 (± 0.183)	12.12 (± 0.143)	4.96 (± 0.087)	2.45 (± 0.057)	10.97 (± 0.516)	2.81 (± 0.119)	3.92 (± 0.276)
S2	10.31 (± 0.33)	3.01 (± 0.037)	3.42 (± 0.079)	11.76 (± 0.371)	5.11 (± 0.096)	2.30 (± 0.065)	9.46 (± 0.281)	2.80 (± 0.045)	3.38 (± 0.151)
S3	9.98 (± 0.439)	3.62 (± 0.032)	2.76 (± 0.102)	14.67 (± 0.186)	4.51 (± 0.097)	3.25 (± 0.039)	15.25 (± 0.555)	2.95 (± 0.073)	5.17 (± 0.106)
S4	11.59 (± 0.453)	2.64 (± 0.088)	4.40 (± 0.107)	17.84 (± 0.516)	3.92 (± 0.112)	4.55 (± 0.030)	19.14 (± 0.543)	2.54 (± 0.089)	7.54 (± 0.438)
S5	12.27 (± 0.646)	2.96 (± 0.084)	4.14 (± 0.110)	17.61 (± 0.618)	3.92 (± 0.063)	4.49 (± 0.121)	20.76 (± 0.783)	2.64 (± 0.115)	7.90 (± 0.477)
S6	12.03 (± 0.506)	2.80 (± 0.100)	4.30 (± 0.120)	19.02 (± 0.333)	3.78 (± 0.042)	5.03 (± 0.050)	22.57 (± 0.652)	2.56 (± 0.040)	8.83 (± 0.243)
S7	20.14 (± 0.431)	4.98 (± 0.084)	4.04 (± 0.028)	15.51 (± 0.283)	5.84 (± 0.039)	2.66 (± 0.040)	13.16 (± 0.471)	5.47 (± 0.074)	2.40 (± 0.054)
S8	12.90 (± 0.329)	4.13 (± 0.098)	3.13 (± 0.006)	13.67 (± 0.249)	5.04 (± 0.049)	2.71 (± 0.026)	16.70 (± 0.494)	3.65 (± 0.089)	4.58 (± 0.067)

Note: " \pm " is the upper and lower 95% confidence interval of the mean

4.1.2.3 Elasticity: The results of hysteresis loops obtained from a cyclic tensile test were performed on an elastic fabric sample according to standard EN ISO 14704-1 [105]. The experiment was determined the limit of patternmaking allow for reduction size of patternmaking at the maximum 50% of the actual size of block pattern.

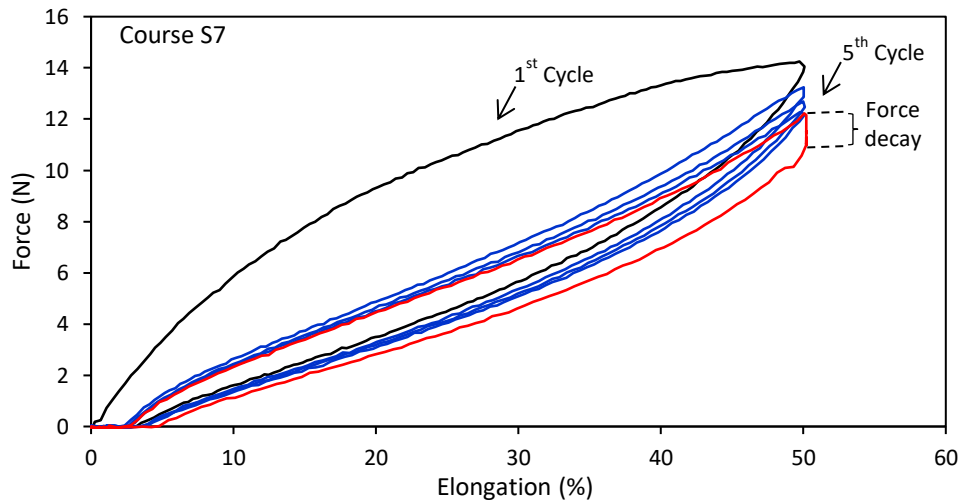
**Figure 4.3** The hysteresis loops 5th cycle of S7 in course direction

Figure 4.3 illustrated the hysteresis loops of the sample S7 in course direction and obviously, at the 1st loading, there was an extremely high force value. Due to the inertia in fabric, the effect on friction among yarns in course and wale directions at the first time has occurred.

While after first loading, the friction was less and the results of force values were very close ones and thus, this research will be aiming at finding out the relationship between force and elongation at the 5th cycle to calculate the stress-strain results for development patternmaking method. After the experimental testing, it could be found that there was force decay over the time while the hysteresis loops graph results indicated that there were both recovered and un-recovered elongation. The results of elastic recovery calculation are given below in Table 4.4. The graphs of comparative force decay and elastic recovery are given in the Figure 4.4 (a and b) respectively.

Table 4.4 The elasticity properties of knitted fabrics in course direction

Sample	Wale			Course		
	Force decay over time (%)	Un-recovered elongation (%)	Elastic recovery (%)	Force decay over the time (%)	Un-recovered elongation (%)	Elastic recovery (%)
S1	10.86 (± 0.395)	8.34 (± 0.043)	91.66 (± 0.043)	13.12 (± 0.389)	10.23 (± 0.165)	89.77 (± 0.165)
S2	13.66 (± 0.336)	7.71 (± 0.382)	92.29 (± 0.382)	13.88 (± 0.179)	9.89 (± 0.207)	90.11 (± 0.207)
S3	9.33 (± 0.680)	6.62 (± 0.101)	93.38 (± 0.101)	9.75 (± 0.466)	8.58 (± 0.446)	91.42 (± 0.446)
S4	17.23 (± 0.288)	10.97 (± 0.211)	89.03 (± 0.211)	18.38 (± 0.354)	12.94 (± 0.242)	87.06 (± 0.242)
S5	13.84 (± 0.318)	9.81 (± 0.197)	90.19 (± 0.197)	14.58 (± 0.352)	11.33 (± 0.408)	88.67 (± 0.408)
S6	11.66 (± 0.311)	8.33 (± 0.111)	91.67 (± 0.111)	14.43 (± 0.586)	9.29 (± 0.360)	90.71 (± 0.360)
S7	10.46 (± 0.348)	6.41 (± 0.209)	93.59 (± 0.209)	9.17 (± 0.565)	7.84 (± 0.192)	92.16 (± 0.192)
S8	8.70 (± 0.781)	10.27 (± 0.262)	89.73 (± 0.262)	7.58 (± 0.573)	10.72 (± 0.201)	89.28 (± 0.201)

Note: “ \pm ” is the upper and lower 95% confidence interval of the mean

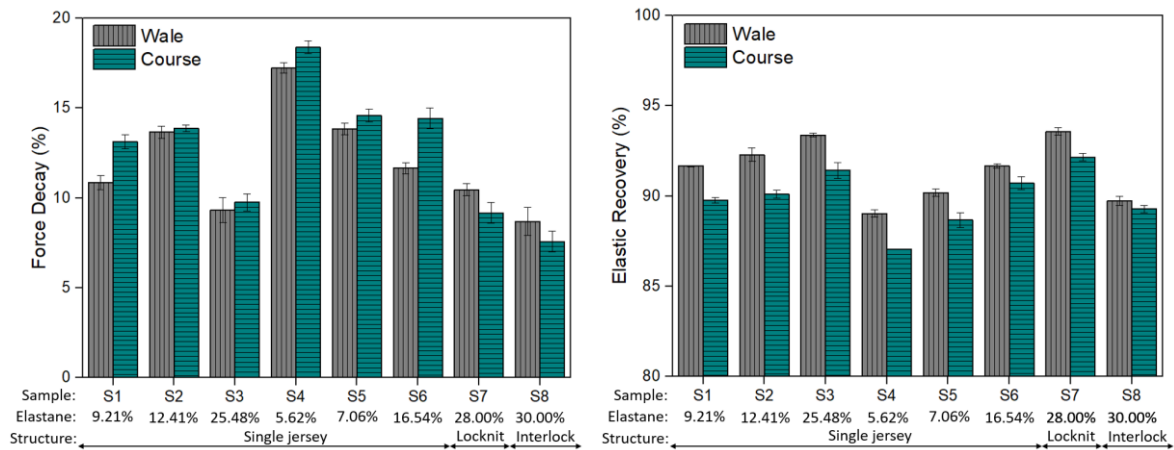


Figure 4.4 Graphs comparative the influence of elastane composition on force decay and elastic recovery

In this section, One-way ANOVA is analysed and the selected value of significance for all statistical tests in the study shall be 0.05. Analysis of different combination of factors is presented in Table 4.5. Analysing factors used for calculations are percentage of elastane of the fabric, force decay and elastic recovery. The One-way ANOVA statistic results were found that the percentage of elastane has significantly influenced on the percentage of elastic recovery ($F_{\text{Critical}} < F_{\text{Statistic}}$) and ($P < 0.05$). Whilst, percentage of force decay has insignificantly been affected by the percentage of elastane. The statistical analysis indicated that the group of the percentage elastane, force decay over the time and elastic recovery are significantly different.

Table 4.5 The One-way ANOVA analysis of influence effect of the elastane on force decay and elasticity

Factor	$F_{\text{Statistic}}$	F_{Critical}	Significant ($F_{\text{Critical}} < F_{\text{Statistic}}$)	P-Value	Significant ($P < 0.05$)
Elastane (%) Force decay (%)	3.2664	4.1709	Insignificant	0.0808	Insignificant
Elastane (%) Elastic recovery (%)	941.8839	4.1709	Significant	3.23E-24	Significant
Elastic recovery (%) Force decay (%)	7688.4973	4.1709	Significant	1.01E-37	Significant
Elastane (%) Force decay (%) Elastic recovery (%)	908.3073	3.2043	Significant	4.21E-37	Significant

4.1.2.4 Stress relaxation: Stress relaxation is considered as one of the main factors that may take an effect on compression garment. Concerning the time of stretching, when the fabric is stressed over time stress in fabric will decrease. This standardized according to standard EN ISO 14704-1 [105] experiment was conducted to fix strain at 0.5 in the fifth cycle that could hold the elongation period up to 60 seconds. The results of stress value were compared and expressed in Figure 4.5.

When considered single jersey structure, the group of Polyamide yarn count 44 dtex of the sample (S1 - S3) by varying yarn count of elastane at number 22 dtex (black), 33 dtex (red) and 78 dtex (blue). It was found that the stress value is rather higher when yarn count of elastane is higher as found in S3, S2 and S1 from high to low respectively. Furthermore, the group of Polyamide yarn count 78 dtex of the samples (S4 – S6) also illustrated that the stress values did have influence on elastane yarn count, and the stress values are considered from high to low in S6 (78 dtex), S5 (33 dtex) and S4 (22 dtex) respectively.

When making comparison of the stress relaxation values, the results showed that when stress value was at first 10 seconds, the values seemed to go downward dramatically and then slightly decreased when reached the 30th second and the stress value was almost at steady state until reached the 60th second. Therefore, based from the findings, stress relaxation is should be considered in order to help the fabric keep constant the pressure value during wearing on the body.

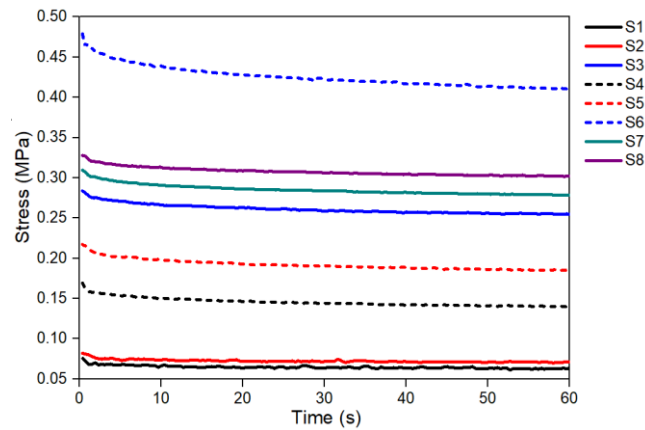


Figure 4.5 Comparative the stress relaxation over the time

Overall, high stress values are suitable for compression garments as found in samples S6, S8, S7 and S3 while low stress values of the samples S5, S4, S2 and S1 are suitable for sportswear due to its lower pressure when compared to compression garment. The results of initial stress and final stress values were calculated to find out the stress relaxation are given below in Table 4.6.

Table 4.6 The stress relaxation and stress performance between initial and final holding strain at 0.5

Sample	Initial stress holding (Pa)	Final stress holding over the time (Pa)	Stress relaxation (%)
S1	68,625.45 (± 844.033)	59,621.82 (± 522.580)	13.12 (± 0.389)
S2	80,174.55 ($\pm 1,517.523$)	69,047.27 ($\pm 1,295.204$)	13.88 (± 0.179)
S3	281,440.00 ($\pm 2,055.217$)	254,000.00 ($\pm 1,714.076$)	9.75 (± 0.466)
S4	175,400.00 ($\pm 3,119.077$)	143,146.67 ($\pm 1,957.123$)	18.38 (± 0.354)
S5	219,087.21 ($\pm 3,749.497$)	187,147.54 ($\pm 3,104.075$)	14.58 (± 0.352)
S6	479,803.51 ($\pm 3,686.624$)	410,526.32 (± 494.010)	14.43 (± 0.586)
S7	306,734.18 ($\pm 1,879.029$)	278,602.53 (± 145.853)	9.17 (± 0.565)
S8	335,025.00 ($\pm 15,818.426$)	309,625.00 ($\pm 14,916.356$)	7.58 (± 0.573)

Note: “ \pm ” is the upper and lower 95% confidence interval of the mean

4.1.2.5 Dynamic work recovery: Analysis of dynamic elastic behaviour is an objective evaluation of stretch and recovery performance of elastic knitted fabrics. The analysis of this dynamics will help engineer improve performance of sportswear and compression garment.

The results of hysteresis loops at fifth cycle from eight samples were analysed then calculated to determine the DWR% as shown in Figure 4.6. It could be described from the results depicted in the graphs that there is a significant difference between the area under loading and area under unloading. Therefore, the lack of energy inside the hysteresis loop is the energy loss in fabric.

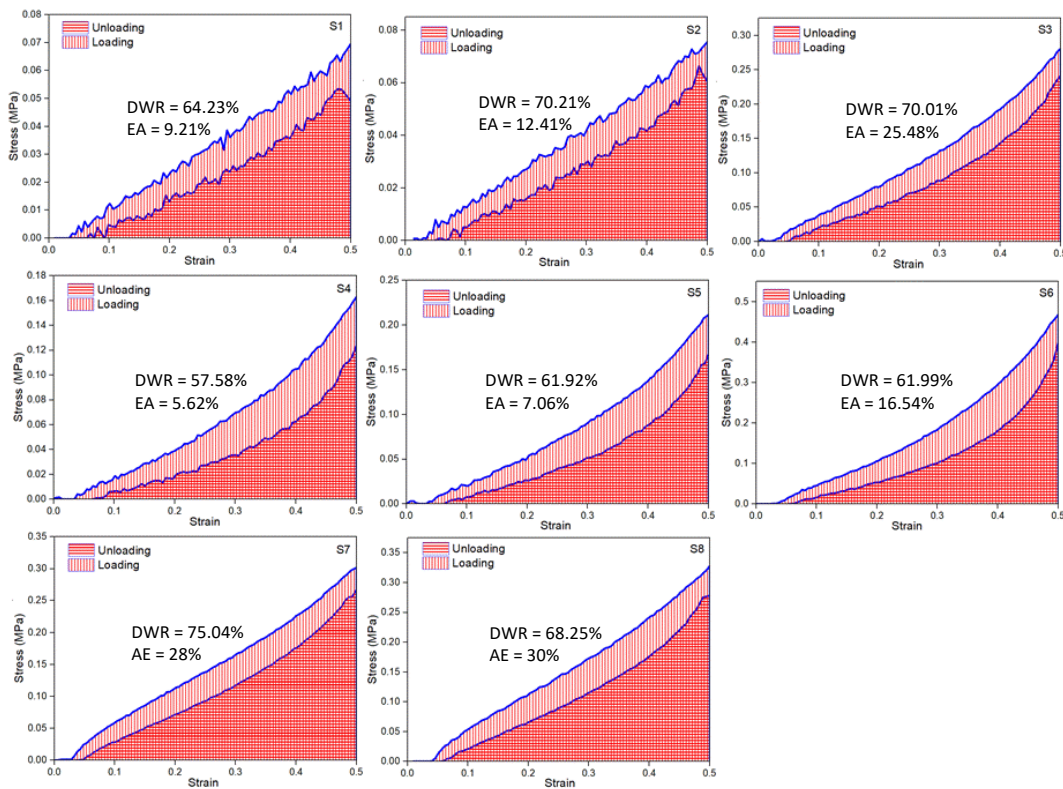


Figure 4.6 Graphs of Dynamic Work Recovery at the fifth cycle of eight samples

The results of dynamic work recovery were obtained the energy between area under loading and unloading and then were calculated for the DWR % as illustrated in Table 4.7. When considering grate dynamic recovery DWR % of sample S7 at 75.04%. has it could be found that the sample is considered to have high elastane composition at 28%, and in the meantime, samples S2, S3 and S8 have elastane composition at 12.41%, 25.48% and 30.00% while DWR% was at 70.21%, 70.01% and 68.25% respectively. In sample S4, has lowest elastane of 5.62% lowest DWR% of 57.85% were revealed. And thus, it could be concluded that the

percentage of elastane might be helping for adjustment to improve the performance of fabric recovery and value of DWR% could be used for further improvement on clothing function such as active sportswear for athletes and CGs.

Table 4.7 The results of fabric energy between loading-unloading and DWR%

Sample	Area under loading curve (Unit: Energy per unit volume)	Area under unloading curve (Unit: Energy per unit volume)	DWR (%)
S1	15,347.51 (±41.972)	9,868.77 (±18.876)	64.23 (±0.120)
S2	17,364.61 (±34.237)	12,191.84 (±18.890)	70.21 (±0.193)
S3	57,207.02 (±62.307)	40,048.89 (±42.903)	70.01 (±0.128)
S4	30,244.90 (±77.251)	17,413.48 (±55.905)	57.58 (±0.177)
S5	39,600.96 (±88.840)	24,519.91 (±31.470)	61.92 (±0.140)
S6	83,571.97 (±94.929)	51,829.44 (±32.361)	61.99 (±0.062)
S7	69,071.64 (±61.568)	51,828.46 (±30.250)	75.04 (±0.071)
S8	73,008.53 (±93.681)	49,826.90 (±38.883)	68.25 (±0.066)

Note: “±” is the upper and lower 95% confidence interval of the mean

4.2 Characterization of stretch fabric tensile deformation by image analysis

This novel experiment presented the digital image analysis technic by MATLAB for the measurement of local deformations of knitted fabrics. The image analysis approach was selected to calculate the gradient deformation tensor under the extension ranging from 10 % to 40 % in course direction of knitted fabric. The gradient deformation tensors were obtained by the analysis of movements of dots painted on the specimen. In this way, the outcome of this work will help predict the deformation of the lateral strain and will be applied to calculate appropriate the ECL of pattern construction for compression garment.

4.2.1 Validation of results with simulated images

In order to ensure the accuracy of calculated gradient deformation tensor values, the results were validated with simulated images generated by MATLAB image processing tool box. The deformation tensor is obtained by [113, 114]:

$$F = \begin{pmatrix} 1 + u_{11} & u_{12} \\ u_{21} & 1 + u_{22} \end{pmatrix}$$

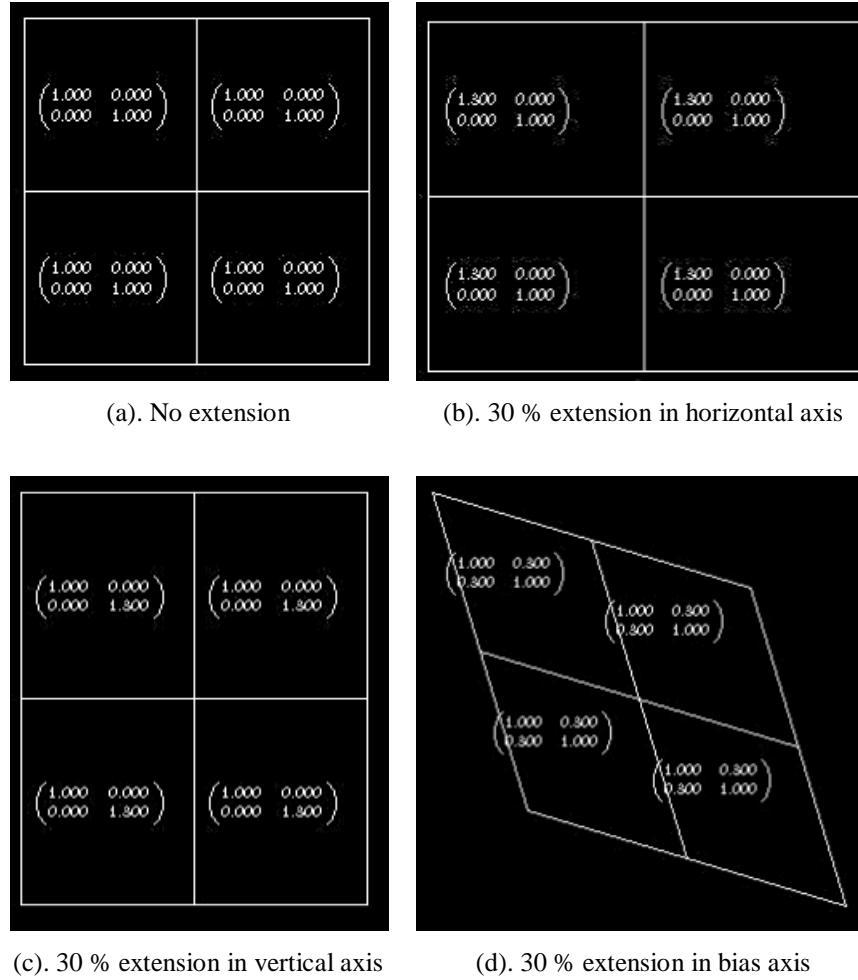


Figure 4.7 Simulated images from MATLAB image processing toolbox [113]

Figure 4.7 (1-d) shows the simulated images without extension, 30 % extension in horizontal, vertical and bias axis respectively. The simulated images show that the gradient tensor deformation values also change in similar percentage with respect to the applied extension. This successfully validated the concept of image analysis for determination of elastic distribution properties of fabrics.

4.2.2 Fabric deformation image was extended by tensile testing machine

The in this experimental testing, fabric was extended in the vertical axis as shown in Figure 4.7 (c). In order to make an evaluation of fabric deformation, fabric sample. The Cartesian components of $(1 + u_{11})$ describe the deformation of distance changed in width or shrink direction and $(1 + u_{22})$ describe the deformation of distance changed in length or extended of fabric direction.

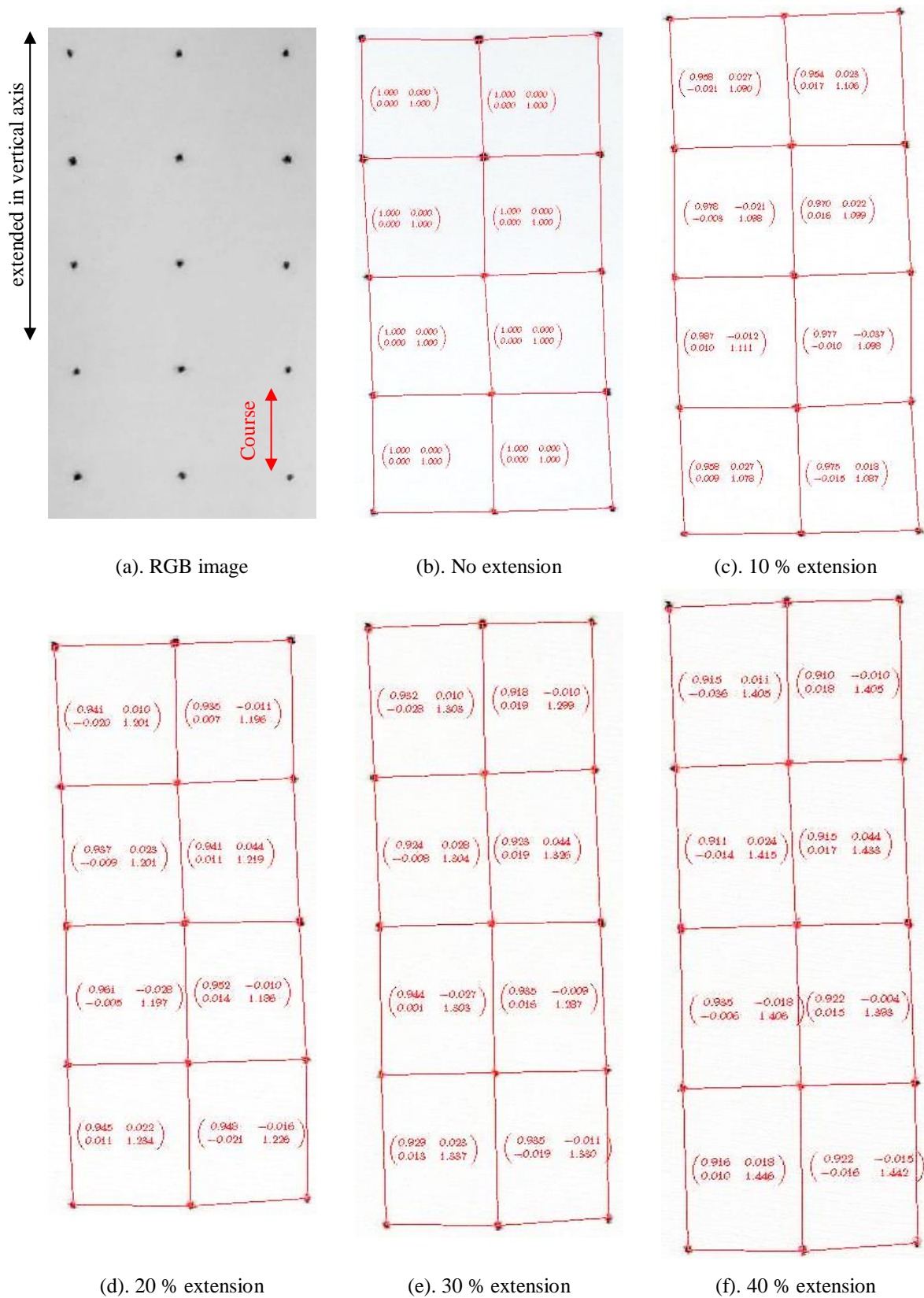
Gradient deformation tensor in course direction:**Figure 4.8** Gradient deformation tensor for course direction by tensile testing machine

Figure 4.8 (a-f) shows the calculated values of gradient deformation tensor for 0 %, 10 %, 20 %, 30 % and 40 % extension in course direction of knitted fabric of the sample S6. It is clear that the images got stretched along with the points marked on them under different extension. The calculated gradient deformation tensor values were also found to change in similar percentage for each case, which proved to have accurate estimation of image analysis and the results are obtained as shown in Table 4.8.

Table 4.8 Results of gradient tensor deformation in vertical direction

Dimension	Deformation (cm)			
	Strain 0.1	Strain 0.2	Strain 0.3	Strain 0.4
Width	0.970 (± 0.008)	0.945 (± 0.006)	0.930 (± 0.006)	0.918 (± 0.006)
Length	1.096 (± 0.007)	1.207 (± 0.012)	1.311 (± 0.012)	1.418 (± 0.013)

Note: “ \pm ” is the upper and lower 95% confidence interval of the mean

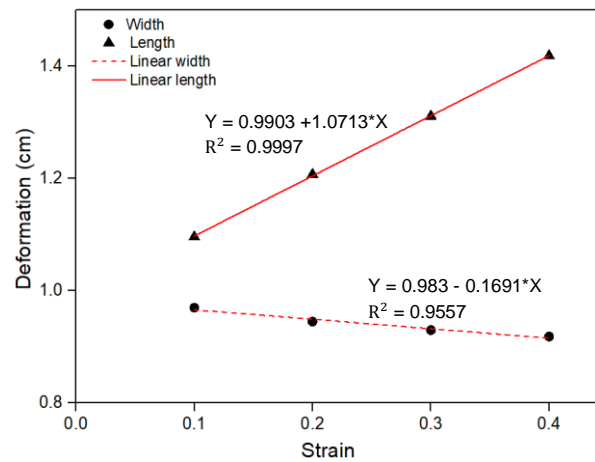


Figure 4.9 Deformation behaviour of stretch fabric of the sample S6

The deformation distribution between length and width of stretch fabric is given in Figure 4.9. It was found that the length was higher when the extended level was higher while width of fabrics was shrunk when fabrics extended. The One-way ANOVA statistic results were found that the deformation of fabric extended in course direction was significant different at the ($F_{\text{Significance}} < 0.05$) are given in Table 4.9.

Table 4.9 Prediction of extension deformation behaviour of knitted fabrics using different fabrics directions

Equation: $Y = a + b \cdot X$		Value	Standard Error	Adj R-Square	$F_{\text{Statistic}}$	$F_{\text{Significance}}$	Significant ($F_{\text{Significance}} < 0.05$)
length	Intercept	0.9903	0.0028	0.9997	11111.18	8.99E-05	Significant
	Slope	1.0713	0.0102				
width	Intercept	0.9830	0.0057	0.9557	65.7948	0.0149	Significant
	Slope	-0.1691	0.0209				

4.2.3 Comparison of fabric deformation with Engineering stress and True stress

The deformation image results under fabric stretched in width was obtained and then being applied by predictive equation ($Width_{Predicted} = 0.983 - 0.1691 \times Strain_{Experiment}$) of the sample S6 to calculate the actual width under the strain level from the tensile testing experiment in order to find out True Stress (TS).

The predictive results of actual width were done and successful to calculate TS is calculated by the actual width of fabric based on strain level and they were compared with Engineering stress (ES) is calculated by the initial width of fabric as shown in Figure 4.10. It was found that TS and ES had close values under the strain level 0 - 0.2 but they are slightly different in terms of TS stress which was a bit higher than ES from strain 0.2 - 0.4. The results could be confirmed that under the strain level of fabric stretched when compared stress values between TS and ES, it is acceptable to use ES instead of TS and the application of the image analysis was successful and evident enough to prove the stress values.

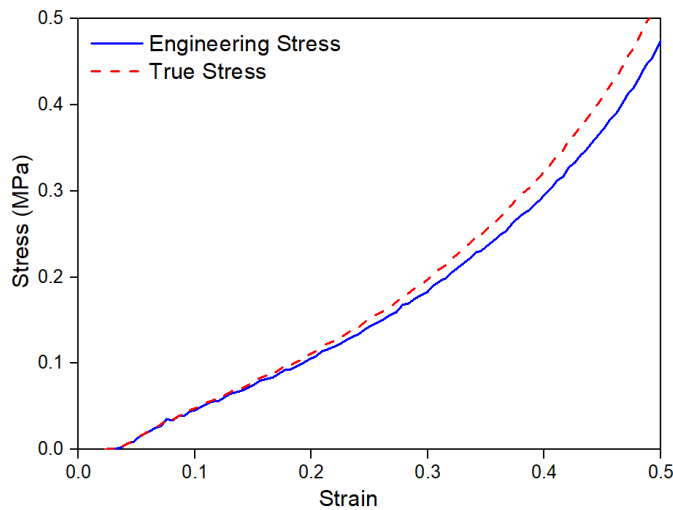


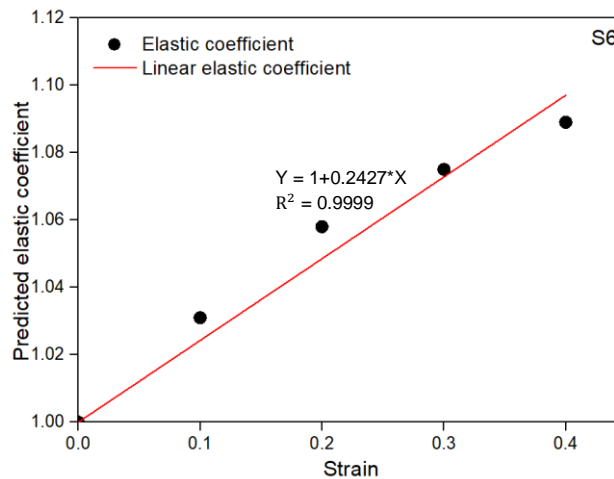
Figure 4.10 The comparative the stress values between TS and ES

4.2.4 Prediction of elastic coefficient of ECL from fabric deformation

Regarding results of the mean values in width dimension in Table 4.8 by image analysis, they were used to calculate the later strain and elastic coefficient as given in Table 4.10 and then further predicted to determine the elastic coefficient as shown in Figure 4.11.

Table 4.10 Fabric deformation of later strain and elastic coefficient

Strain	Width (cm)	Lateral strain = $-\frac{\Delta w}{w}$	Elastic Coefficient = $\frac{1}{\epsilon_{Lateral}+1}$
0.1	0.970	- 0.030	1.031
0.2	0.945	- 0.055	1.058
0.3	0.930	- 0.070	1.075
0.4	0.918	- 0.082	1.089

**Figure 4.11** The prediction of elastic coefficient of the sample S6

The predictive of elastic coefficient are significant ($F_{\text{Significance}} < 0.05$) as given in Table 4.11 and these predicted equations were done and successful which was helpful enough to find out the ECL in order to calculate and estimate the accurate size of pattern construction under the strain level.

Table 4.11 Prediction of elastic coefficient ECL

Predicted the elastic coefficient							
Equation: Y= a + b*X		Value	Standard Error	Adj R-Square	F _{Statistic}	F _{Significance}	Significant (F _{Significance} <0.05)
Elastic coefficient	Intercept	1	-	0.9999	107,848	5.158E-10	Significant
	Slope	0.2427	0.0131				

4.3 Application of Laplace's law pressure theory on pressure for garments

This research has been conducted to develop mathematical models to predict the strain value of fabric based on Laplace's law theory. The experiment was designed in accordance to the strain values with different of the strain levels of stretched fabric in order to make an investigation of the pressure value in garments.

4.3.1 Applying the mathematic modelling for prediction of the strain value

Referring to the elastic behaviour results from the previous experiment, they will be applied to the actual mechanical characteristic from stress-strain curves at the 5th cycle to predict the modelling and find out the dependent variable of strain value.

Due to the direction of course is the directly effect on fabric stretched according to the fabric grain line of clothing production. Course direction is normally used in the body circumference way and therefore this direction was used for greatly extended along to the body circumference. Due to this reason the experiment was considered particularly in course direction to predict the mathematic modelling.

Figure 4.12 shows the elastic behaviour of the elastic fabrics between the predicted strains (dependent variable) at the magnitude of the fabric stress (independent variable) from standard EN 14704-1. The results were predicted in the strain values by statistical analysis of 3rd order polynomial fitting-lines which are given on Table 4.12.

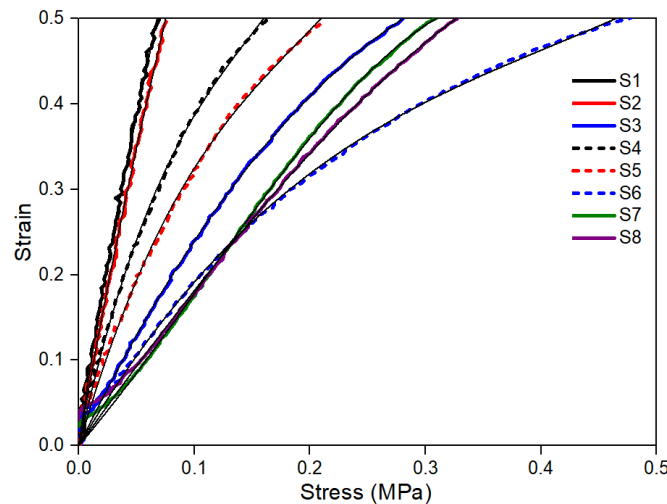


Figure 4.12 The actual mechanical characteristic from stress-strain curves of eight samples

Evidently, sample S6 displayed results with highest stress value that could reach to 0.5 MPa at 0.5 of strain value and therefore the sample is applicable for use in CG. On the other hand, the result of the samples S1 and S2 possessed lesser stress values of 0.1 MPa at the strain 0.5 and hence, these fabrics are inappropriate for the high pressure use in CG particularly when they cause a decrease in the size of patternmaking.

In Table 4.12, the statistical analysis indicates that the 3rd order polynomial function of the cubic model are a good fit for the data, the Adjusted R-Square values over 98%, P-value ($F_{\text{Significance}} < 0.05$) are all significant and P-value ($P < 0.05$) for the cubic coefficients are significant.

Table 4.12 The coefficients of the 3rd order polynomial fitting-lines

Equation $\varepsilon = a_1\sigma^3 + a_2\sigma^2 + a_3\sigma$		Value	Standard Error	P-value	Adj. R-Square	$F_{\text{Significance}}$	Significant ($F_{\text{Significance}} < 0.05$)
S1	a_1	3.45E-16	1.39E-16	0.0148	0.9986	4.93E-131	Significant
	a_2	-6.05E-11	1.27E-11	7.22E-06			
	a_3	9.90E-06	2.78E-07	5.15E-56			
S2	a_1	1.14E-16	8.84E-17	0.0491	0.9880	1.17E-135	Significant
	a_2	-2.71E-11	8.93E-12	0.0031			
	a_3	8.05E-06	2.15E-07	3.92E-57			
S3	a_1	1.29E-18	1.07E-18	1.97E-87	0.9886	2.49E-153	Significant
	a_2	-3.90E-12	3.92E-13	3.50E-16			
	a_3	2.78E-06	3.35E-08	0.0334			
S4	a_1	6.27E-17	8.58E-18	1.02E-10	0.9881	2.79E-138	Significant
	a_2	-2.86E-11	1.81E-12	8.10E-28			
	a_3	6.10E-06	8.99E-08	1.00E-79			
S5	a_1	2.97E-17	4.00E-18	5.41E-11	0.9883	1.56E-139	Significant
	a_2	-1.71E-11	1.10E-12	1.57E-27			
	a_3	4.66E-06	7.10E-08	1.11E-79			
S6	a_1	3.47E-18	3.32E-19	1.84E-17	0.9886	1.71E-144	Significant
	a_2	-4.26E-12	2.04E-13	3.61E-37			
	a_3	2.31E-06	2.95E-08	5.54E-88			
S7	a_1	-8.92E-18	7.78E-19	2.64E-19	0.9885	6.22E-155	Significant
	a_2	2.87E-12	3.19E-13	3.40E-14			
	a_3	1.58E-06	3.09E-08	2.88E-68			
S8	a_1	-1.52E-18	1.15E-18	0.0494	0.9874	3.23E-128	Significant
	a_2	-6.08E-13	5.00E-13	0.0277			
	a_3	1.89E-06	5.17E-08	3.19E-54			

The polynomial function equations from Table 4.12 were used to perform the analysis of modelling results of the strain value of stretch fabric depending on their pressure and diameter of the cylindrical model by ORIGIN[®]9.1 software as shown in Figure 4.13 (a, b, c, d, e and f). The fabric samples of S3, S4, S5, S6, S7 and S8 owing to their fabric stretch properties possessed high stress values as applicable for prediction the strain and the mathematical modelling was used from the prediction equation (3.32)

$$\varepsilon = a_1 \left(\frac{DP}{2h} \right)^3 + a_2 \left(\frac{DP}{2h} \right)^2 + a_3 \left(\frac{DP}{2h} \right)$$

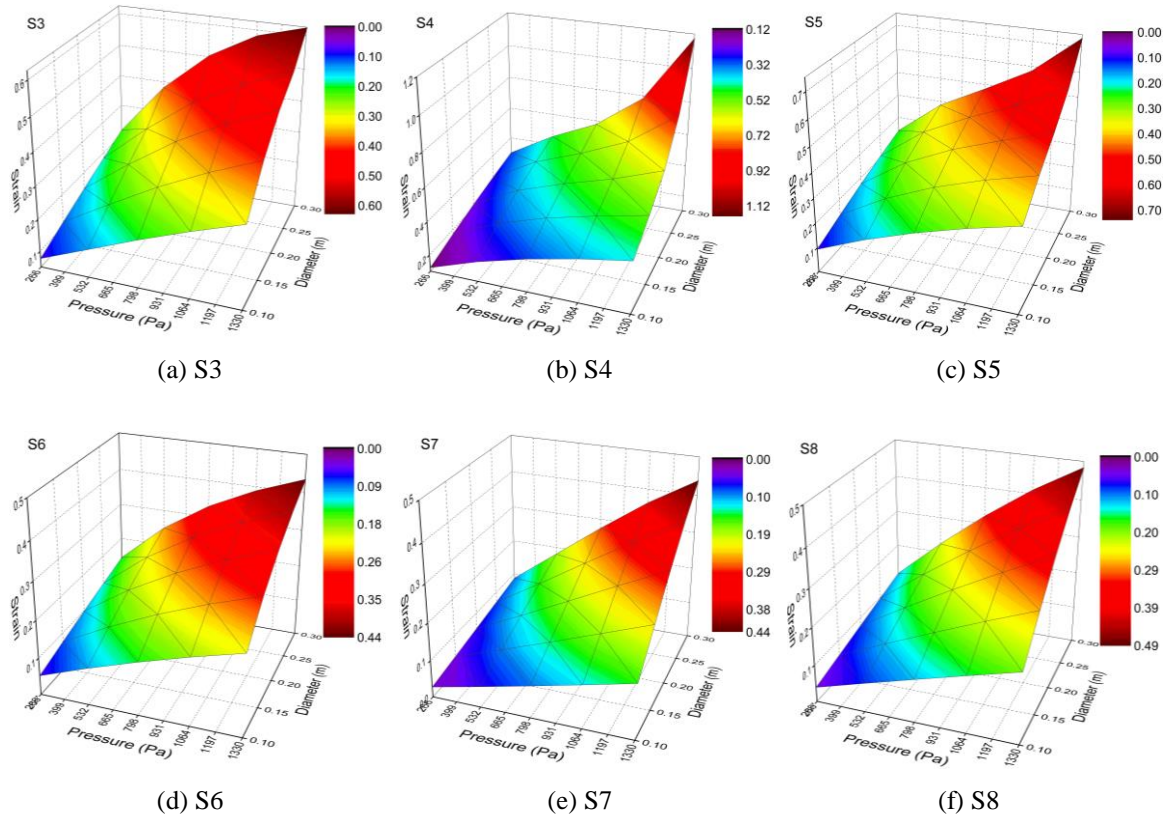


Figure 4.13 The stretch fabric effect of pressure and diameter on the strain

Based on stress-strain curves of experiment shown in Figure 4.13 it could be found that the strain values were changed due to characteristic of fabrics stretched. Considering at the pressure 1,066 Pa for determining and the range of diameters at 0.22 - 0.28 referring to diameter of female human body the strain value was predicted of the S6, S7 and S8 found that the maximum strain values are less than 0.5. Thus, a good performance of elastic fabric to produce the high compression garment should be considered.

4.3.2 Evaluation of mathematical modelling of pressure garments

The experiment was designed to investigate the predictive modelling application based on Laplace's law theory that accuracy enough to find out the pressure values and strain values of stretched fabric. Additionally, the correction factor was introduced to get rid of the pressure perturbation from sensor thickness effect.

4.3.2.1 Measurement of pressure garments in vitro model: Conducting an experiment, the strain value of the fabric stretches on the rigid cylindrical model which made from PVC was used at 0.79 m circumference the fabric length was applied to determine the strain value by

cylindrical circumference at 0.1, 0.2, 0.3, 0.4 and 0.5. In Table 4.13, 4.14, 4.15 and 4.16, the results of pressure values are represented with different methods. The sample S3, S4, S5 and S6 were calculated to obtain their stress values as shown in the second column and then further predicted to the determine pressure value in the third column. Finally, the numbers from fourth and fifth column were compared for the pressure values by compression tester PicoPress®.

Table 4.13 Comparison of S3 pressure values between predicted pressure and measured pressure

Strain ϵ	$\sigma = 802226\epsilon^3 - 52934\epsilon^2 + 379857\epsilon$		Measured pressure (PicoPress®)	
	Stress σ (Pa)	Predicted pressure (Pa); $P = \frac{\sigma 2h}{D}$	(mmHg)	(Pa)
0.1	38,258.59	152.06	2.10 (± 0.196)	279.97 (± 26.131)
0.2	80,271.85	319.05	4.00 (± 0.292)	533.28 (± 38.953)
0.3	130,853.14	520.08	5.90 (± 0.196)	786.59 (± 26.131)
0.4	194,815.82	774.31	8.00 (± 0.506)	1,066.56 (± 67.469)
0.5	276,973.25	1,100.85	12.00 (± 0.292)	1,599.84 (± 38.953)

Note: “ \pm ” is the upper and lower 95% confidence interval of the mean

Table 4.14 Comparison of S4 pressure values between predicted pressure and measured pressure

Strain ϵ	$\sigma = 516049\epsilon^3 + 52508\epsilon^2 + 163053\epsilon$		Measured pressure (PicoPress®)	
	Stress σ (Pa)	Predicted pressure (Pa); $P = \frac{\sigma 2h}{D}$	(mmHg)	(Pa)
0.1	17,346.43	68.94	1.10 (± 0.196)	146.65 (± 26.131)
0.2	38,839.31	154.37	2.20 (± 0.261)	293.30 (± 34.841)
0.3	67,574.94	268.58	4.10 (± 0.196)	546.61 (± 26.131)
0.4	106,649.62	423.89	6.20 (± 0.261)	826.58 (± 34.841)
0.5	159,159.63	632.59	8.20 (± 0.261)	1,093.22 (± 34.841)

Note: “ \pm ” is the upper and lower 95% confidence interval of the mean

Table 4.15 Comparison of S5 pressure values between predicted pressure and measured pressure

Strain ϵ	$\sigma = 609694\epsilon^3 + 116938\epsilon^2 + 207991\epsilon$		Measured pressure (PicoPress®)	
	Stress σ (Pa)	Predicted pressure (Pa); $P = \frac{\sigma 2h}{D}$	(mmHg)	(Pa)
0.1	22,578.17	109.48	1.90 (± 0.196)	253.31 (± 26.131)
0.2	51,153.27	248.04	2.90 (± 0.196)	386.63 (± 26.131)
0.3	89,383.46	433.42	6.10 (± 0.196)	813.25 (± 26.131)
0.4	140,926.90	683.35	8.10 (± 0.196)	1,079.89 (± 26.131)
0.5	209,441.75	1,015.58	11.00 (± 0.292)	1,466.52 (± 38.953)

Note: “ \pm ” is the upper and lower 95% confidence interval of the mean

Table 4.16 Comparison of S6 pressure values between predicted pressure and measured pressure

Strain ϵ	$\sigma = 2E+06\epsilon^3 - 88045\epsilon^2 + 450182\epsilon$		Measured pressure (PicoPress®)	
	Stress σ (Pa)	Predicted pressure (Pa); $P = \frac{\sigma 2h}{D}$	(mmHg)	(Pa)
0.1	46,137.75	209.05	3.10 (± 0.196)	413.29 (± 26.131)
0.2	102,514.60	464.49	6.10 (± 0.196)	813.25 (± 26.131)
0.3	181,130.55	820.70	11.40 (± 0.320)	1,519.85 (± 42.671)
0.4	293,985.60	1,332.05	16.90 (± 0.352)	2,253.11 (± 46.906)
0.5	453,079.75	2,052.91	23.00 (± 0.292)	3,066.36 (± 38.953)

Note: “ \pm ” is the upper and lower 95% confidence interval of the mean

The results of the predicted pressure values and measured pressure values were compared as shown in the Figure 4.14 (a-d). It could be observed from the results that the measured pressure values are over estimating. Due to this reason, the compression tester PicoPress® might be having some negative effects during measuring on the pressure perturbation.

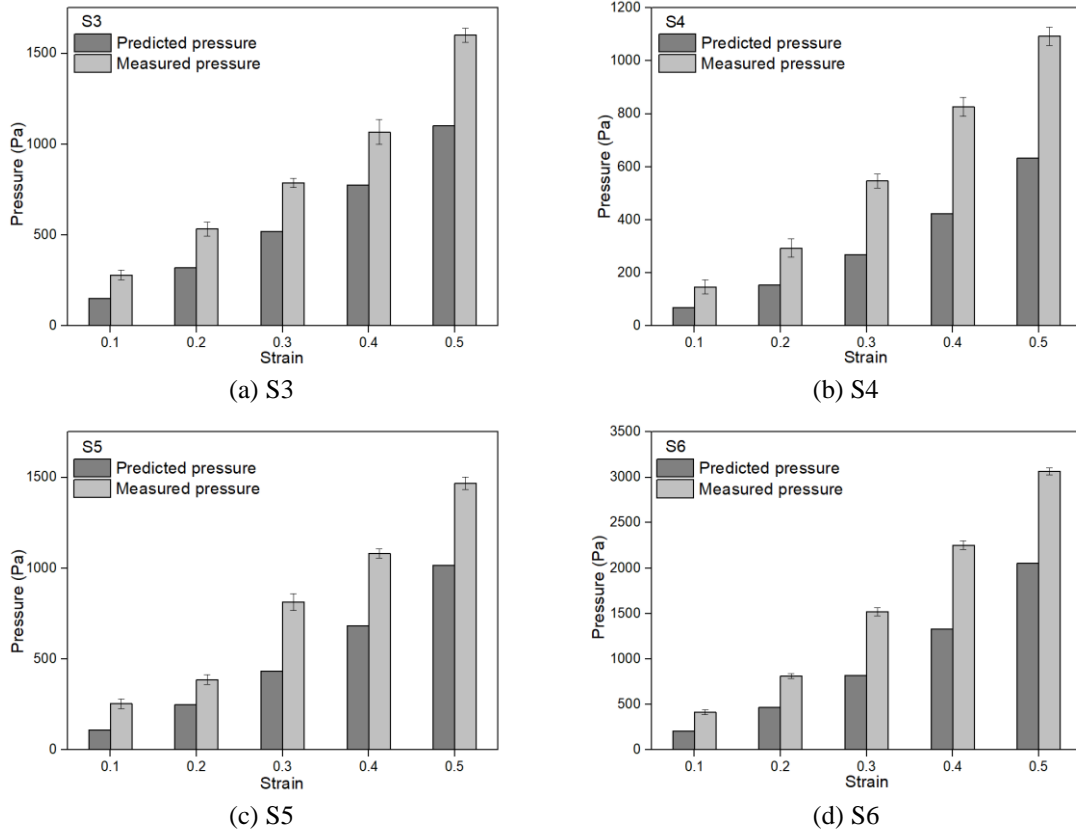


Figure 4.14 Comparison of pressure values between predicted pressure and measured pressure

4.3.2.2 The effect of the sensor thickness in vitro model: In this particular part of the experiment, the compression tester PicoPress® was used for measuring the interface pressure under the fabric stretch. The effect of the sensor thickness measured on the rigid cylindrical model is shown in the Figure 4.15.

$$C_{PP} = \frac{\sin\left(\frac{22.93^\circ}{2} + 12.39^\circ\right)}{\sin\left(\frac{22.93^\circ}{2}\right)} = 2.03$$

$$\varphi = \frac{0.05}{0.1258} = 0.4 = 22.93^\circ$$

$$\gamma = \arccos\left(\frac{0.1258}{0.1258 + 0.003}\right) = 12.39^\circ$$

$$C_{TP} = \frac{3.14 \times 0.05^2}{4 \times 0.05 \times 0.05} = 0.785$$

$$\text{Correction factor} = \frac{1}{2.03 \times 0.785} = 0.628$$

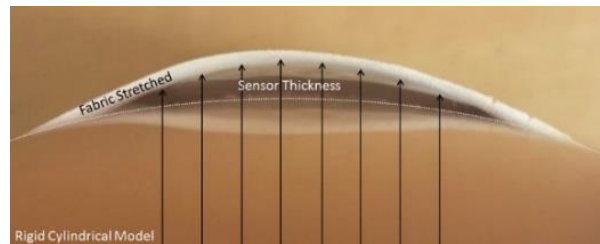


Figure 4.15 Effect of sensor thickness under fabric stretched on rigid cylindrical model

According to in Figure 4.16, the graph represents the effect of sensor thickness using PicoPress® and thus the correction factor for calculating from equation (3.41) is 0.628 by sensor thickness (h_s) 0.003 m, sensor diameter (D_s) 0.05 m and the circumference of the cylindrical model (C) 0.79 m and body radius (R) 0.126 m. The graph of effect of thickness, it is very clearly seen that the pressure perturbation effect will not occur when the thickness sensor is lesser than 0.00025 m. On the other hand, the thickness increase, the pressure perturbation become increasing continuously. While the correction factor dramatically decreases during the thickness starts from 0.00025 m to 0.0035 m subsequently the correction factor decreases gradually.

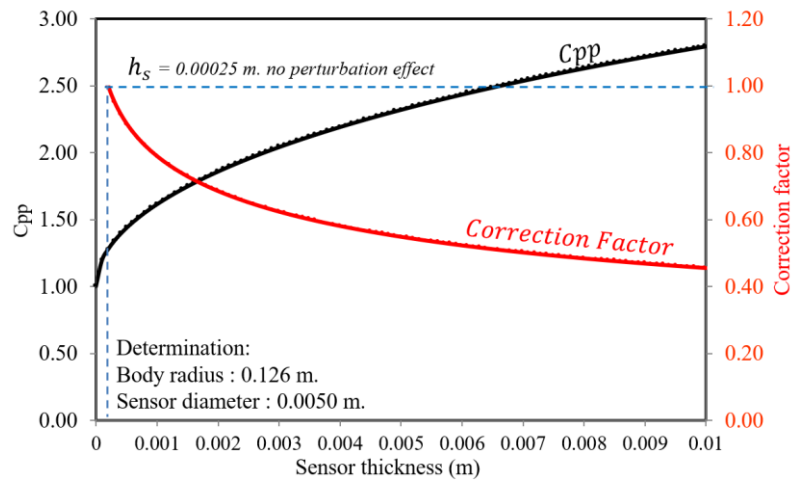


Figure 4.16 Effect of sensor thickness between correction factor and C_{pp} [6]

In Table 4.17, 4.18, 4.19 and 4.20 represent the results of pressure values obtained from different methods of pressure values (Predicted pressure, Measured pressure and Corrected measured pressure) shown in samples S3, S4 S5 and S6. The measured pressure were then multiplied with the correction factor by 0.628 to get the actual pressure which is so called the corrected measured pressure and the results will be compared as illustrated in mentioned tables.

Table 4.17 Comparison of S3 pressure values in three different methods at 0.79 m circumference

Strain ϵ	Predicted pressure (Pa)	Measured pressure (Pa)	Correction factor	Corrected measured pressure (Pa)
0.1	152.06	279.97 (± 26.131)	0.628	175.82
0.2	319.05	533.28 (± 38.953)	0.628	334.90
0.3	520.08	786.59 (± 26.131)	0.628	493.98
0.4	774.31	1,066.56 (± 67.469)	0.628	669.80
0.5	1,100.85	1,599.84 (± 38.953)	0.628	1,004.70

Note: “ \pm ” is the upper and lower 95% confidence interval of the mean

Table 4.18 Comparison of S4 pressure values in three different methods at 0.79 m circumference

Strain ϵ	Predicted pressure (Pa)	Measured pressure (Pa)	Correction factor	Corrected measured pressure (Pa)
0.1	68.94	146.65 (± 26.131)	0.628	92.10
0.2	154.37	293.30 (± 34.841)	0.628	184.19
0.3	268.58	546.61 (± 26.131)	0.628	343.27
0.4	423.89	826.58 (± 34.841)	0.628	519.09
0.5	632.59	1,093.22 (± 34.841)	0.628	686.54

Note: “ \pm ” is the upper and lower 95% confidence interval of the mean

Table 4.19 Comparison of S5 pressure values in three different methods at 0.79 m circumference

Strain ϵ	Predicted pressure (Pa)	Measured pressure (Pa)	Correction factor	Corrected measured pressure (Pa)
0.1	109.48	253.31 (± 26.131)	0.628	159.08
0.2	248.04	386.63 (± 26.131)	0.628	242.80
0.3	433.42	813.25 (± 26.131)	0.628	493.98
0.4	683.35	1,079.89 (± 26.131)	0.628	678.17
0.5	1,015.58	1,466.52 (± 38.953)	0.628	937.72

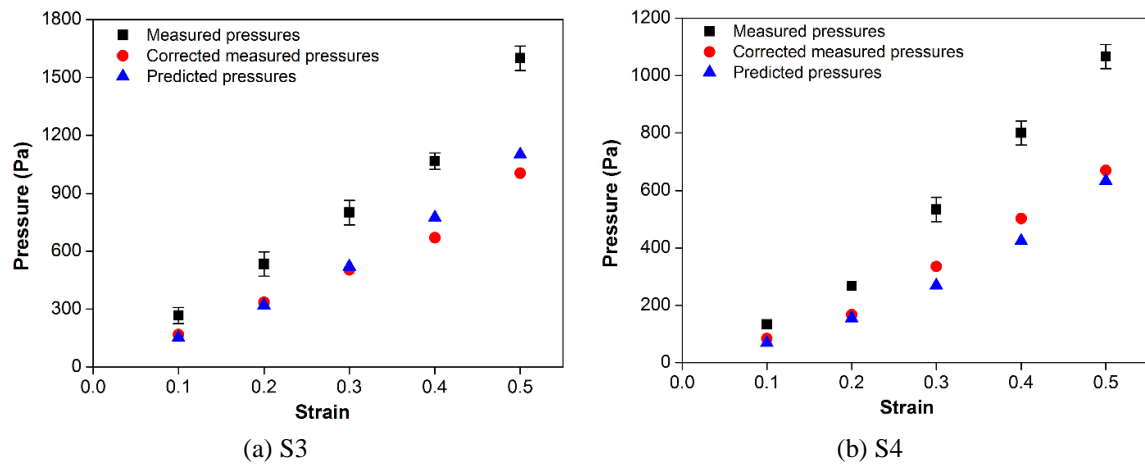
Note: “ \pm ” is the upper and lower 95% confidence interval of the mean

Table 4.20 Comparison of S6 pressure values in three different methods at 0.79 m circumference

Strain ϵ	Predicted pressure (Pa)	Measured pressure (Pa)	Correction factor	Corrected measured pressure (Pa)
0.1	209.05	413.29 (± 26.131)	0.628	251.17
0.2	464.49	813.25 (± 26.131)	0.628	510.72
0.3	820.70	1,519.85 (± 42.671)	0.628	954.46
0.4	1,332.05	2,253.11 (± 46.906)	0.628	1,414.95
0.5	2,052.91	3,066.36 (± 38.953)	0.628	1,925.67

Note: “ \pm ” is the upper and lower 95% confidence interval of the mean

Figure 4.17 (a, b, c and d) shows the comparison of pressure values obtained from three methods of calculation which are compared with different strain values of the circumference at 0.79 m.



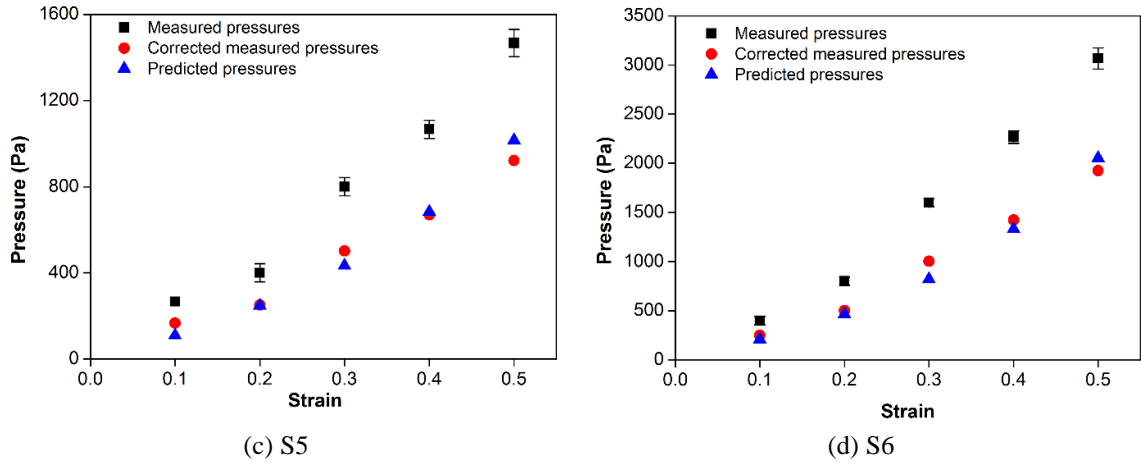


Figure 4.17 Comparison of the pressure values methods with the circumference at 0.79 m. [6]

Apparently, the corrected measured pressure values as illustrated in the graphs are very close to the ones predicted pressure values. While the means of the measured pressure values by PicoPress® illustrate that those pressure results are the highest values when compared with another two methods.

4.3.2.3 Measurement of pressure garments with different circumferences: Relating to the experiment aforementioned, same method was applied but the circumference was decreased from 0.79 m to 0.505 m. The body radius (R) 0.0804 m was then calculated by applying correction factor at 0.712 that was explained to calculate the correction factor below [6]. The results of sample S3, S4, S5 and S6 are shown in Table 4.21, 4.22, 4.23 and 4.24 respectively.

$$C_{PP} = \frac{\sin(\frac{35.65^\circ}{2} + 15.41^\circ)}{\sin(\frac{35.65^\circ}{2})} = 1.79$$

$$\varphi = \frac{0.05}{0.0804} = 0.62 = 35.65^\circ$$

$$\gamma = \arccos\left(\frac{0.0804}{0.0804 + 0.003}\right) = 15.41^\circ$$

$$C_{TP} = \frac{3.14 \times 0.05^2}{4 \times 0.05 \times 0.05} = 0.785$$

$$\text{Correction factor} = \frac{1}{1.79 \times 0.785} = 0.712$$

Table 4.21 Comparison of S3 pressure values in three different methods at 0.505 m circumference

Strain ε	Predicted pressure (Pa)	Measured pressure (Pa)	Correction factor	Corrected measured pressure (Pa)
0.1	237.93	413.29 (± 26.131)	0.712	294.26
0.2	499.20	679.93 (± 26.131)	0.712	484.11
0.3	813.76	1,093.22 (± 34.841)	0.712	778.38
0.4	1,211.54	1,626.50 (± 34.841)	0.712	1158.07
0.5	1,722.47	2,159.78 (± 52.261)	0.712	1528.27

Note: “ \pm ” is the upper and lower 95% confidence interval of the mean

Table 4.22 Comparison of S4 pressure values in three different methods at 0.505 m circumference

Strain ε	Predicted pressure (Pa)	Measured pressure (Pa)	Correction factor	Corrected measured pressure (Pa)
0.1	107.88	306.64 (± 39.591)	0.712	218.32
0.2	241.54	413.29 (± 26.131)	0.712	294.26
0.3	420.24	786.59 (± 26.131)	0.712	560.05
0.4	663.24	1,213.21 (± 26.131)	0.712	863.81
0.5	989.80	1,599.84 (± 38.953)	0.712	1,139.09

Note: “ \pm ” is the upper and lower 95% confidence interval of the mean

Table 4.23 Comparison of S5 pressure values in three different methods at 0.505 m circumference

Strain ε	Predicted pressure (Pa)	Measured pressure (Pa)	Correction factor	Corrected measured pressure (Pa)
0.1	171.30	279.97 (± 26.131)	0.712	199.34
0.2	388.10	413.29 (± 26.131)	0.712	294.26
0.3	678.16	933.24 (± 38.953)	0.712	664.47
0.4	1,069.22	1,613.17 (± 26.131)	0.712	1,148.58
0.5	1,589.05	1,999.80 (± 38.953)	0.712	1,423.86

Note: “ \pm ” is the upper and lower 95% confidence interval of the mean

Table 4.24 Comparison of S6 pressure values in three different methods at 0.505 m circumference

Strain ε	Predicted pressure (Pa)	Measured pressure (Pa)	Correction factor	Corrected measured pressure (Pa)
0.1	327.10	679.93 (± 46.906)	0.712	484.11
0.2	726.78	1,359.86 (± 34.841)	0.712	968.22
0.3	1,284.13	2,546.41 (± 46.906)	0.712	1,813.05
0.4	2,084.23	3,359.66 (± 65.181)	0.712	2,392.08
0.5	3,212.13	4,252.91 (± 60.972)	0.712	3,028.07

Note: “ \pm ” is the upper and lower 95% confidence interval of the mean

In Figure 4.18 (a, b, c and d), the graphs illustrated the comparison results of pressure values of the pressure correction and pressure prediction methods which are very close when correction factor was calculated. In this part of the experiment, it could be proven that the mathematical modelling to predict the pressure based on Laplace’s Law and the correction factor are applicable for making precise estimation of pressure in vitro model.

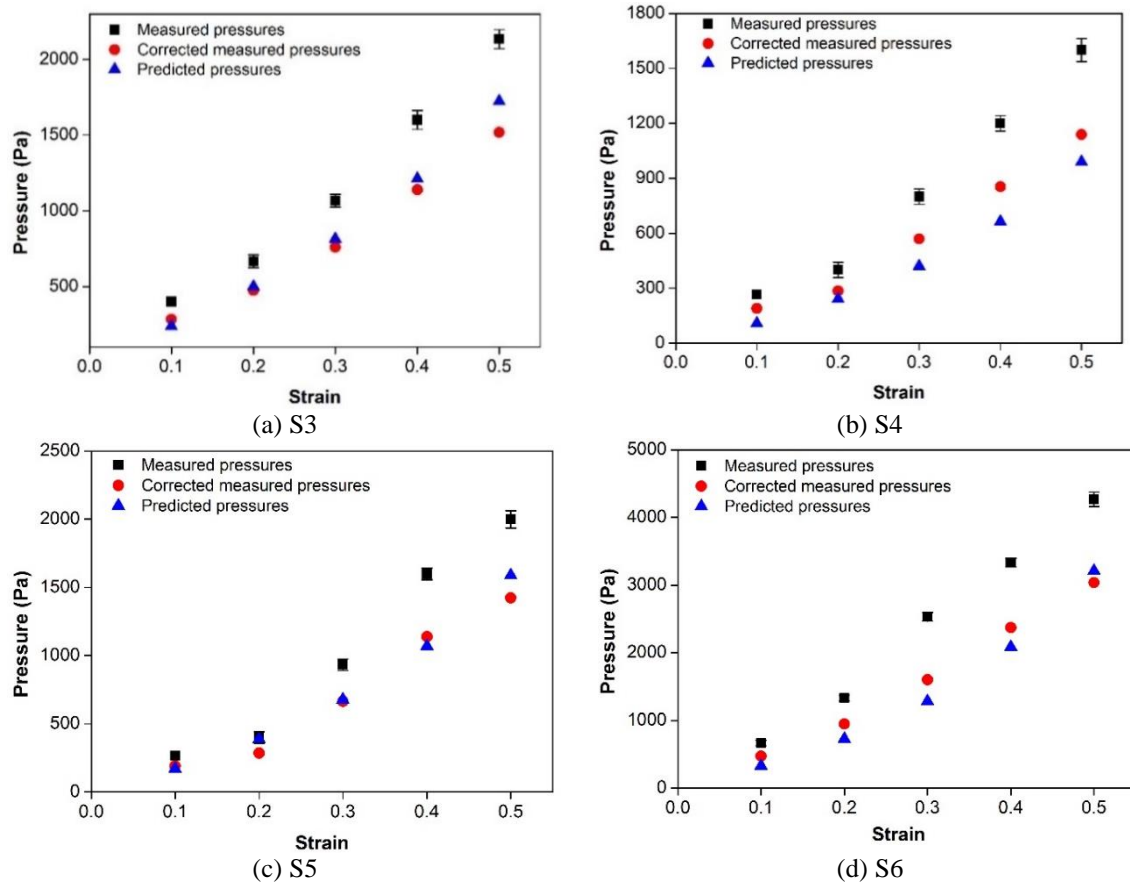


Figure 4.18 Comparison of the pressure values methods with the circumference at 0.505 m. [6]

4.3.2.4 Measurement of pressure garments in vivo model: Relating to the experiment above, same method was applied at the circumference 0.505 m and correction factor at 0.712. The experiment used rigid cylindrical model as shown in the Figure 4.19 (a) and a real human body at thigh part similar to the cylindrical shape were compared to find out pressure values measured by PicoPress® in Figure 4.19 (b).



(a) Measurement of pressure value in vitro model



(b) Measurement of pressure value in vivo model

Figure 4.19 Measurement of pressure values between vitro model and vivo model [6]

The result of pressure value comparison of sample S6 between the model of vitro and vivo was shown in Table 4.25. The experiment had been conducted by measuring each strain level with standing position 30 times. Additionally, predicted pressure and corrected measured pressure in vitro model were compared with the measured pressure in vivo model.

Table 4.25 Comparison of pressure values with different models between vitro and vivo of sample S6

Strain ϵ	Pressure (Pa)		
	Predicted pressure (Predictive modelling)	Corrected measured pressure (Vitro model)	Measured pressure (Vivo model)
0.1	327.10	484.11	399.96 (± 38.953)
0.2	726.78	968.22	799.92 (± 38.953)
0.3	1,284.13	1,813.05	1,599.84 (± 38.953)
0.4	2,084.23	2,392.08	2,266.44 (± 38.953)
0.5	3,212.13	3,028.07	3,066.36 (± 55.088)

Note: “ \pm ” is the upper and lower 95% confidence interval of the mean

Interestingly, pressure values of the soft tissue surface (vivo) at the thigh part show close results to the predicted pressure values and corrected measured pressures of the rigid body as shown the Figure 4.20. It could have been assumed that skin human body was soft and unessentially an influence on the pressure perturbation of sensor thickness during measurement.

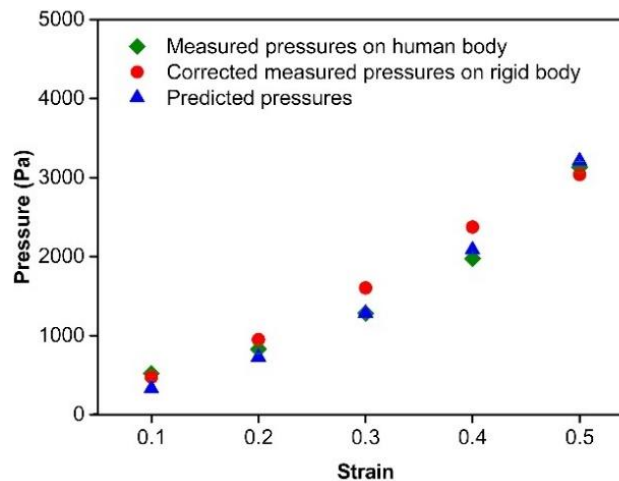


Figure 4.20 Comparison of S6 pressure values with different models between vitro and vivo [6]

Regarding the results, finding out the influence of the pressure perturbation according to the sensor thickness was successful when measuring interface pressure with the rigid cylindrical model (vitro). While soft tissue surface of the skin human body (vivo) showed that its pressure values were evidently close with the predicted modelling and thus, it could be concluded that pressure perturbation had no the effect on skin human body when measured by PicoPress[®] at 3.00 mm. sensor thickness.

4.3.3 Evaluation of mathematical modelling for prediction of the strain value

The objective of this experiment was to design the method that could be used for investigating the prediction of the strain value on the mathematical modelling. The strain value of fabric stretch is the main factor to develop the patternmaking for CG and therefore, the experiment was then carried out to find out the strain values of stretched fabric from the measured pressure by PicoPress®. Moreover, the correction factor also was computed to get rid of the pressure perturbation from sensor thickness effect.

Conducting an experiment, the strain value of the fabric stretch in vitro model was used at 0.79 m circumference with similar method. The fabric length was used for determining the strain value by cylindrical circumference at 0.1, 0.2, 0.3, 0.4 and 0.5. In Table 4.26, 4.27, 4.28 and 4.29 the results of predicted strain values of the sample S3, S4, S5, and S6 from the corrected measure pressure at 0.79 m circumference were presented.

Table 4.26 Comparison of S3 strain values between experimental strain and predicted strain

Strain ϵ	Corrected measured pressure (Pa)	Stress σ ; $\sigma = \frac{D_s P}{h \cdot \varphi}$ (Pa)	Predicted Strain ϵ $\epsilon = 1.29\text{E-}18\sigma^3 - 3.9\text{E-}12\sigma^2 + 2.78\text{E-}06\sigma$	Error (%)
0.1	175.82	44,306.64	0.11	-10.00
0.2	334.90	84,394.80	0.21	-3.81
0.3	493.98	124,482.96	0.29	3.96
0.4	669.80	168,789.60	0.36	8.92
0.5	1,004.70	253,184.40	0.47	5.04

Table 4.27 Comparison of S4 strain values between experimental strain and predicted strain

Strain ϵ	Corrected measured pressure (Pa)	Stress σ ; $\sigma = \frac{D_s P}{h \cdot \varphi}$ (Pa)	Predicted Strain ϵ $\epsilon = 6.27\text{E-}17\sigma^3 - 2.86\text{E-}11\sigma^2 + 6.1\text{E-}06\sigma$	Error (%)
0.1	92.10	19,341.00	0.11	-7.74
0.2	184.19	38,679.90	0.20	1.61
0.3	343.27	72,086.70	0.31	-4.87
0.4	519.09	109,008.90	0.41	-1.58
0.5	686.54	144,173.40	0.47	5.42

Table 4.28 Comparison of S5 strain values between experimental strain and predicted strain

Strain ϵ	Corrected measured pressure (Pa)	Stress σ ; $\sigma = \frac{D_s P}{h \cdot \varphi}$ (Pa)	Predicted Strain ϵ $\epsilon = 2.97\text{E-}17\sigma^3 - 1.71\text{E-}11\sigma^2 + 4.66\text{E-}06\sigma$	Error (%)
0.1	159.08	32,859.15	0.14	-35.71
0.2	242.8	50,152.13	0.19	2.78
0.3	493.98	102,035.21	0.33	-9.67
0.4	678.17	140,081.02	0.40	0.28
0.5	937.72	193,692.98	0.48	4.62

Table 4.29 Comparison of S6 strain values between experimental strain and predicted strain

Strain ϵ	Corrected measured pressure (Pa)	Stress σ ; $\sigma = \frac{D_s P}{h \cdot \phi}$ (Pa)	Predicted Strain ϵ $\epsilon = 3.47\text{E-}18 \sigma^3 - 4.26\text{E-}12 \sigma^2 + 2.31\text{E-}06 \sigma$	Error (%)
0.1	251.17	55,521.79	0.12	-15.72
0.2	510.72	112,896.00	0.21	-5.74
0.3	954.46	210,985.89	0.33	-10.11
0.4	1,414.95	312,778.42	0.41	-2.99
0.5	1,925.67	425,674.42	0.48	4.19

The results of predictive strain values are very close to the strain value were fixed from experiment and it was found that the predicted strain at 0.1 are not accurate enough for estimation possessing high errors around (-7.74% to -35.71%). While the predictive strain range 0.2 - 0.5 are considered to be more precise. The results represented clearly that the predicted strain values after taking account of correction factor of the pressure perturbation are close to the strain values.

Figure 4.21 indicates the correlation of the strain value between the predicted strain versus experimentally determined strain level at the cylindrical model of 0.79 m circumference. It can be seen that the correlation of the predicted strain and experimental strain of samples S3, S4, S5 and S6 are found to be well correlated with adjusted coefficients of determination 0.9948, 0.9896, 0.9807 and 0.9865 respectively in Table 4.30. This indication of the predictive strain mathematical modelling involving pressure and body diameter parameters can be used for making estimating the strain for CG accurately.

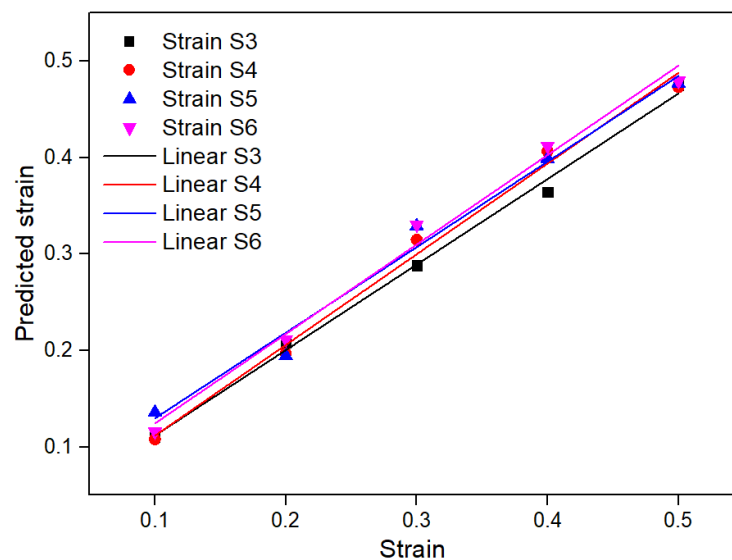
**Figure 4.21** The correlation of predicted strain VS experimental strain of sample S3, S4, S5 and S6

Table 4.30 The correlation of predicted strain VS experimental strain of sample S3, S4, S5 and S6

Correlation of the strain from predicted strain and experimental strain							
Equation: $Y = a + b \cdot X$		Value	Standard Error	Adj R-Square	F _{Statistic}	F _{Significance}	Significant (F _{Significance} < 0.05)
S3	Intercept	0.0230	0.0106	0.9948	770.0957	1.03E-4	Significant
	Slope	0.8862	0.0319				
S4	Slope	0.0177	0.0159	0.9896	380.6864	2.94E-4	Significant
	Slope	0.9398	0.0482				
S5	Intercept	0.0410	0.0206	0.9807	203.9023	7.44E-4	Significant
	Slope	0.8868	0.0621				
S6	Intercept	0.0316	0.0180	0.9865	293.5320	4.33E-4	Significant
	Slope	0.9271	0.0541				

4.4 Performance of novel tensile measurement device

4.4.1 Measurement of fabric properties by novel tensile measurement device

The experimental of a novel tensile measurement device was considered successful and the results of loading from the calibration weight and elongation in Table 4.31 were obtained from the length of fabric extended from five times cycle loading.

Table 4.31 The fabric extension values of sample S6 with different weights and cycle loading

Weight (g)	Elongation (mm)				
	1 st cycle	2 nd cycle	3 rd cycle	4 th cycle	5 th cycle
0	0.00	0.00	0.00	0.00	0.00
250	102.50	112.50	113.00	113.50	113.50
500	113.50	125.50	127.00	127.50	128.00
750	123.00	135.50	136.50	138.00	138.50
1,000	131.50	142.50	143.50	145.00	145.50
1,250	141.00	148.50	149.50	150.50	151.00
1,500	150.00	153.00	154.50	155.00	155.00

Referring, the sample S6 results in Table 4.31 were compared with the elasticity of elastic fabric testing according to standard EN 14704-1 strip test between loading and percentage elongation as shown in Figure 4.22 (a).

Furthermore, the sample S6 results from the fifth cycle was then calculated to find out the predictive polynomial fitting line of the strain value and also were compared with standard tensile testing in Figure 4.22 (b).

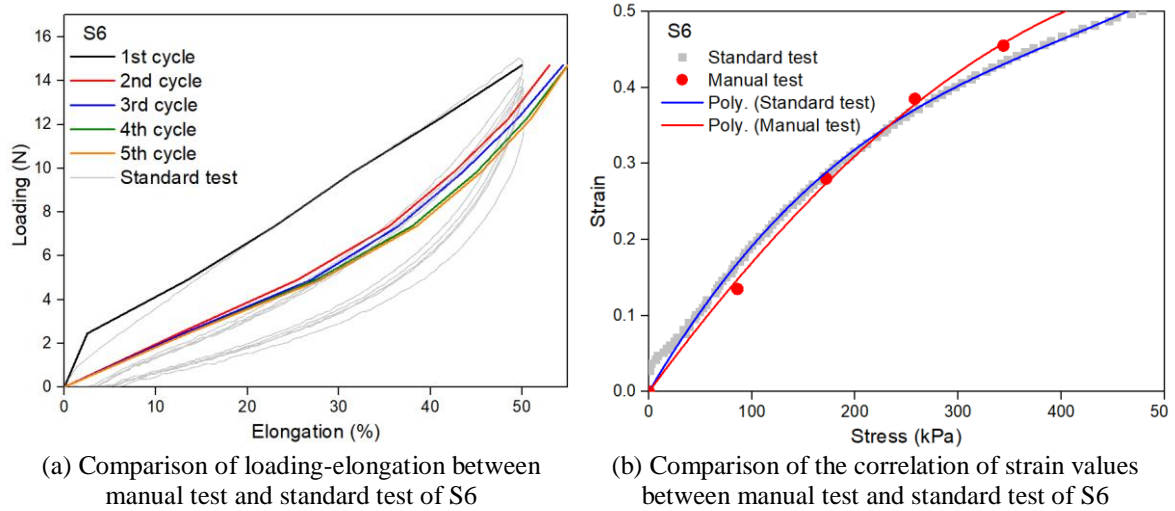


Figure 4.22 Comparison of fabric property results of sample S6 between manual test and standard test

It can be seen in Figure 4.22 (b) that the correlation lines between manual test and standard test were very close to one another and the strain predicted results were found to have very strong correlation when making coefficient adjustment of determination from manual tensile testing at 0.9994 and standard test at 0.9886 as illustrated in Table 4.32.

Table 4.32 The correlation of the strain prediction of the sample S6 with different testing devices

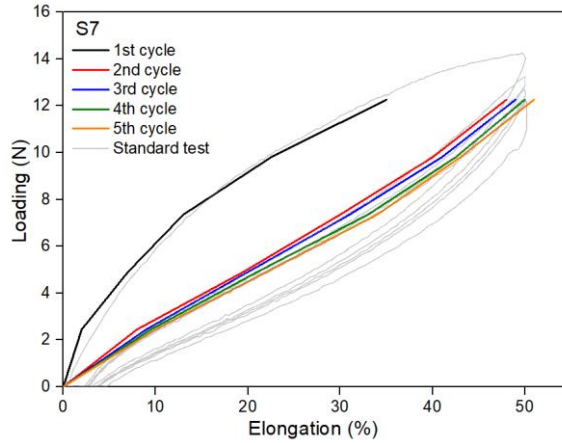
Equation: $Y = a + B1 * x + B2 * x^2 + B3 * x^3$		Value	Standard Error	Adj R-Square	F _{Statistic}	F _{Significance}	Significant (F _{Significance} < 0.05)
Standard test	a	0	-	0.9886	40955.63	1.71E-144	Significant
	B1	2.31E-6	2.95E-08				
	B2	-4.37E-12	2.04E-13				
	B3	3.47E-18	3.32E-19				
Manual test	a	0	-	0.9994	4533.51	1.62E-7	Significant
	B1	1.84E-6	1.09E-7				
	B2	-1.4E-12	6.21E-13				
	B3	-2.1E-19	8.36E-19				

In table 4.33 experimental results of sample S7 was obtained and were plotted in graph as shown Figure 4.23 (a) in order to compare the fabric characteristic of loading-elongation curves between manual test and standard test. It could be concluded from the result that loading-elongation curves with different cycles from manual test contained close values to the standard test ones.

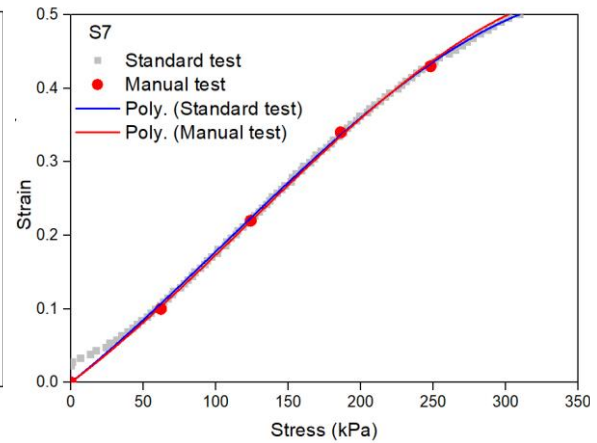
Consequently, in Figure 4.23 (b) the predicted stain of polynomial fitting line from manual test was very close to the standard test and the correlation matched well to the adjusted coefficient of determination at 0.9985 and 0.9997 as described in Table 4.34.

Table 4.33 The fabric extension values of sample S7 with different weight and cycle loading

Weight (g)	Elongation (mm)				
	1 st cycle	2 nd cycle	3 rd cycle	4 th cycle	5 th cycle
0	0.00	0.00	0.00	0.00	0.00
250	102.00	104.00	105.00	105.00	107.00
500	114.00	117.00	118.50	118.50	120.50
750	127.00	130.00	133.50	133.00	134.50
1,000	141.00	143.50	145.50	146.50	148.50
1,250	151.00	153.50	154.50	156.50	158.50



(a) Comparison of loading-elongation between manual test and standard test of S7



(b) Comparison of the correlation of strain values between manual test and standard test of S7

Figure 4.23 Comparison of fabric property results of sample S7 between manual test and standard test**Table 4.34** The correlation of the strain prediction of the sample S7 with different testing devices

Equation: $Y = a + B1 * x + B2 * x^2 + B3 * x^3$		Value	Standard Error	Adj R-Square	F _{Statistic}	F _{Significance}	Significant (F _{Significance} < 0.05)
Standard test	a	0	-	0.9985	90619.08	6.22E-155	Significant
	B1	1.58E-06	3.09E-08				
	B2	2.87E-12	3.19E-13				
	B3	-8.92E-18	7.78E-19				
Manual test	a	0	-	0.9997	8489.57	2.17E-6	Significant
	B1	1.49E-06	1.14E-07				
	B2	3.45E-12	1.08E-12				
	B3	-9.53E-18	2.37E-18				

Based from the results obtained from sample S6 and S7, it could be found that the results from a novel tensile measurement device are very close to the standard ones and thus, conclusion could be drawn that manual tensile testing device is considerably applicable for testing measurement on elongation of fabric stretched by using the calibration weight instead. Additionally, with its low cost and high accuracy in fabric stretched measurement, this device is considered very beneficial.

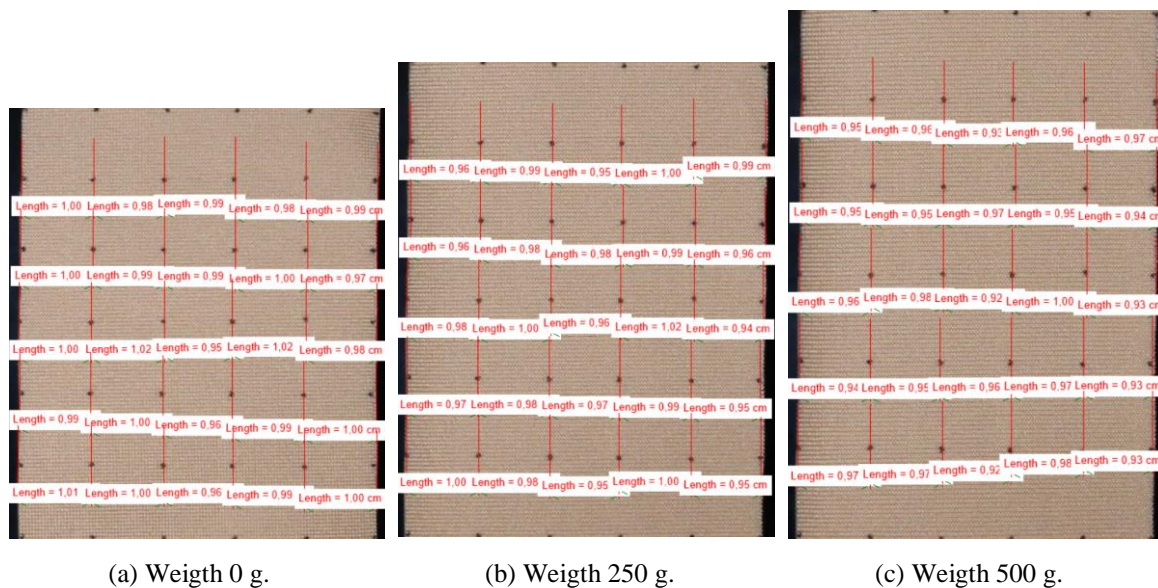
4.4.2 Fabric deformation image by manual tensile testing

The image analysis results were done by NIS-Elements software which is used to calibrate the deformation of fabric stretched under the different weight interval 250 g. The experiment put its emphasis on the fabric deformation appearing at the width dimension (lateral strain). The results of the strain value obtained from fabric extension, width from fabric reduction and elastic coefficient in length dimension ECL of S6, S7 and S8 are shown in Table 4.35.

Table 4.35 The results of fabric deformation in strain, width and elastic coefficient

Weight (g)	Sample S6			Sample S7			Sample S8		
	Strain	Width (cm)	ECL	Strain	Width (cm)	ECL	Strain	Width (cm)	ECL
0	0.000	1.00 (± 0.007)	1.000	0.000	1.00 (± 0.007)	1.000	0.000	1.00 (± 0.006)	1.000
250	0.130	0.968 (± 0.008)	1.033	0.070	0.976 (± 0.008)	1.020	0.010	0.996 (± 0.008)	1.004
500	0.280	0.935 (± 0.005)	1.070	0.200	0.954 (± 0.008)	1.053	0.250	0.987 (± 0.009)	1.013
750	0.380	0.924 (± 0.006)	1.082	0.340	0.931 (± 0.009)	1.075	0.380	0.98 (± 0.007)	1.020
1,000	0.450	0.908 (± 0.007)	1.101	0.480	0.921 (± 0.006)	1.087	0.480	0.968 (± 0.007)	1.033
1,250	0.510	0.894 (± 0.008)	1.118	0.580	0.904 (± 0.008)	1.111	-	-	-

In figure 4.24 (a-f), illustration of images processing results of the sample S7 with different weight at interval 250 g form 0 – 1,250 g is shown.



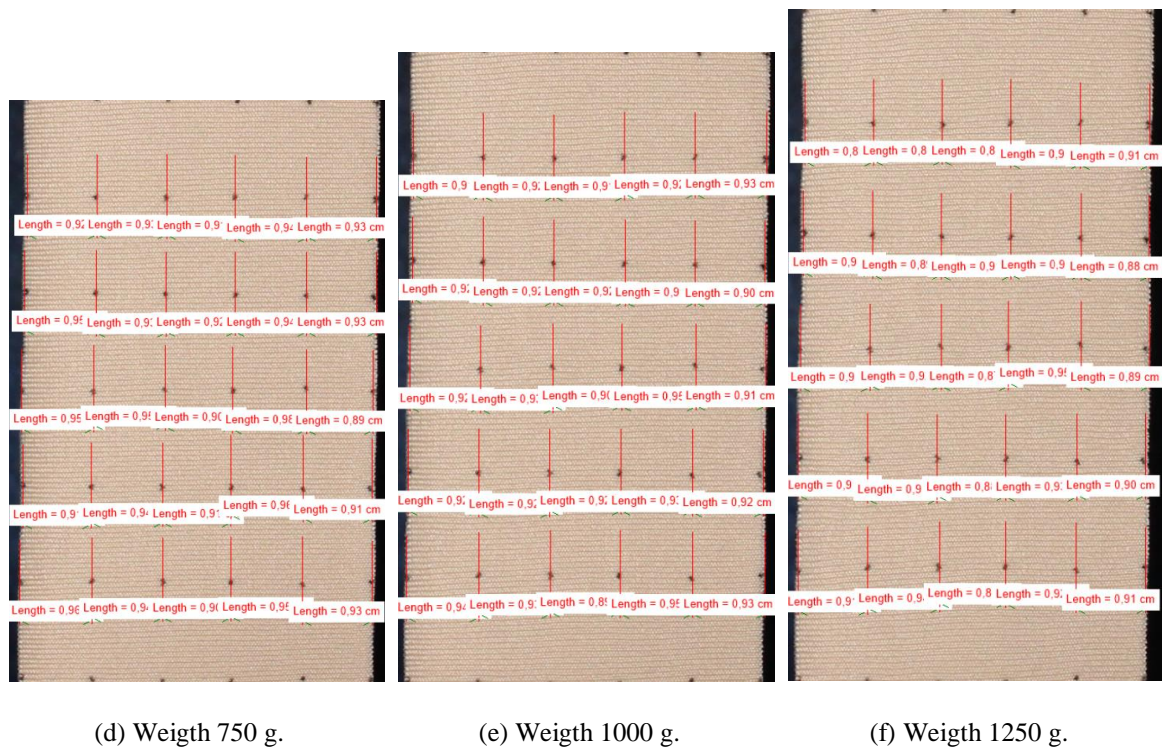


Figure 4.24 The fabric deformation of the sample S7

The image analysis results of fabric length and width can be applied to help predict the ECL of samples S6, S7 and S8 by using statistical analysis as shown in Figure 4.25. The graph illustrates the obtained linear regressions which are found to be well correlated with adjusted coefficient of determination at 0.9998, 0.9993 and 0.9999 respectively in Table 4.36.

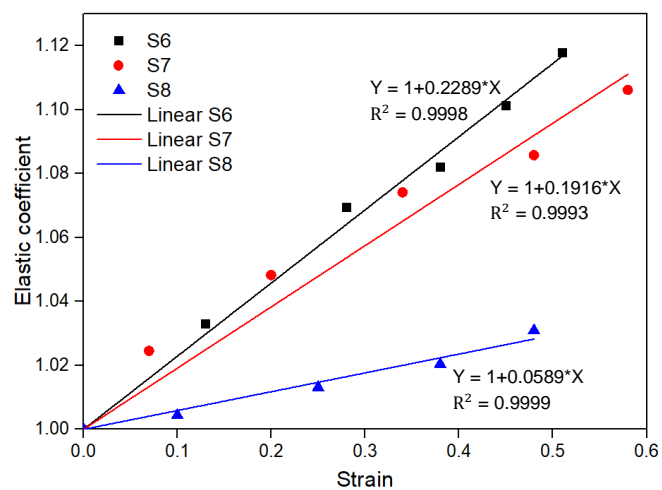


Figure 4.25 The prediction of the elastic coefficient (ECL) of sample S6, S7 and S8

Table 4.36 Prediction of elastic coefficient by linear regression of samples S6, S7 and S8

Equation: $Y = a + b \cdot X$		Value	Standard Error	Adj R-Square	F _{Statistic}	F _{Significance}	Significant (F _{Significance} < 0.05)
S6	Intercept	1	-	0.9998	5.003E5	1.07E-13	Significant
	Slope	0.2289	0.0044				
S7	Intercept	1	-	0.9993	9.156E4	7.48E-12	Significant
	Slope	0.1916	0.0100				
S8	Intercept	1	-	0.9999	1.324E6	3.42E-12	Significant
	Slope	0.0589	0.0029				

4.5 Defining patternmaking development procedure for stretch fabrics

The final part of the research emphasizes to develop the method how to modification the size of patternmaking method for stretch fabrics. Through the experiments, the researcher has integrated the knowledge to predict the strain value based on the factors are the body diameter and specific pressure required. The main key factor to estimate the size of patternmaking is the elastic coefficient of ECW and ECL where can be calculated from the predicted stain and then the patternmaking size will be appraised.

4.5.1 Body measurement

During procedures of the measurement, senseTM2 3D scanner was applied to create 3D image of female mannequin and blender software was then used to analyse and process the accurately size of the body cross section at main different parts of the female body for the creation of patternmaking as shown in Figure 4.26 (a).

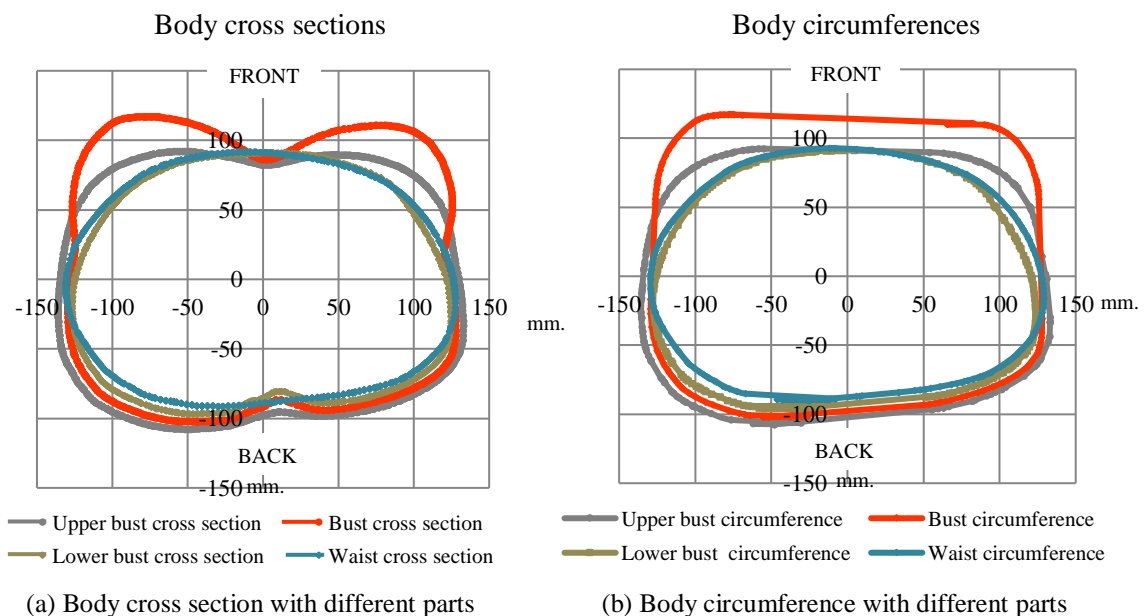


Figure 4.26 The graphs of cross sections and circumferences with different parts of the body

Figure 4.26 (b) the body circumferences were used for prediction of the strain value in order to calculate the size of patternmaking of this experiment.

However, at the point of body cross sections in Figure 4.26 (a), clear curves were found to be occurring and this could lead to a big advantage in terms of analysing the pressure of clothing at the specific area of the body.

4.5.2 Investigation of elastic fabric performance

The results of circumference (C) in the different parts of the body from Figure 4.26 (b) were used to calculate the body diameter (D) for the predicted strain value by mathematic modelling equations as shown in Table 4.37.

In this experiment investigated the fabric performance for producing the compression garment by defining, specific pressure (P) applied on the body at 1.15 kPa (8.63 mmHg) which is suitable for medium compression garment and was conducted to make prediction for strain values. In Table 4.38, the stress values results were calculated by applying pressure value, diameter and thickness of each fabric into the modelling of polynomial equations in order to predict strain values ranging in different parts of the body.

Table 4.37 The predictive modelling of strain value of eight samples

Predictive modelling			h	Predictive modelling			h
S1	$\varepsilon = 3.45\text{E-}16\sigma^3 - 6.05\text{E-}11\sigma^2 + 9.90\text{E-}06\sigma$		0.55	S5	$\varepsilon = 2.97\text{E-}17\sigma^3 - 1.71\text{E-}11\sigma^2 + 4.66\text{E-}06\sigma$		0.61
S2	$\varepsilon = 1.14\text{E-}16\sigma^3 - 2.71\text{E-}11\sigma^2 + 8.05\text{E-}06\sigma$		0.55	S6	$\varepsilon = 3.47\text{E-}18\sigma^3 - 4.26\text{E-}12\sigma^2 + 2.31\text{E-}06\sigma$		0.57
S3	$\varepsilon = 1.29\text{E-}18\sigma^3 - 3.90\text{E-}12\sigma^2 + 2.78\text{E-}06\sigma$		0.50	S7	$\varepsilon = -8.92\text{E-}18\sigma^3 + 2.87\text{E-}12\sigma^2 + 1.58\text{E-}06\sigma$		0.79
S4	$\varepsilon = 6.27\text{E-}17\sigma^3 - 2.86\text{E-}11\sigma^2 + 6.10\text{E-}06\sigma$		0.60	S8	$\varepsilon = -1.52\text{E-}18\sigma^3 - 6.08\text{E-}13\sigma^2 + 1.89\text{E-}06\sigma$		0.64

* h is thickness unit mm, ε is strain and σ is stress unit is Pa.

Table 4.38 The results of predicted strain values with different parts of female body at 1.15 kPa pressure.

Body part	D (m)	$\sigma = \frac{DP}{2h} ; (Pa)$				Strain ε by prediction equation			
		S1	S2	S3	S4	S1	S2	S3	S4
Upper bust	0.251	262,409	262,409	288,650	240,542	4.6	2.31	0.51	0.69
Bust	0.276	288,545	288,545	317,400	264,500	6.11	2.81	0.53	0.77
Lower bust	0.232	242,545	242,545	266,800	222,333	3.76	1.98	0.49	0.63
Waist	0.228	238,364	238,364	262,200	218,500	3.59	1.92	0.48	0.62
		S5	S6	S7	S8	S5	S6	S7	S8
Upper bust	0.251	236,598	253,202	182,693	225,508	0.54	0.37	0.33	0.39
Bust	0.276	260,164	278,421	200,886	247,969	0.58	0.39	0.36	0.41
Lower bust	0.232	218,689	234,035	168,861	208,438	0.51	0.35	0.31	0.35
Waist	0.228	214,918	230,000	165,949	204,844	0.51	0.35	0.30	0.34

* D is diameter of body circumference, P is pressure unit Pa, h is thickness unit mm, ε is strain and σ is stress unit is Pa.

The predicted strain values in Table 4.38 could be evaluated to determine the performance of elastic fabric that can led to three mains garment applications such as low compression garment, medium compression garment and medical compression garment applications. For the investigation of results, compression value at 1.15 kPa based on the comfort sensation for medium compression [71, 42] were applied to analyse and discuss as follow:

In the group with low level of compression pressure (samples S1 and S2), predicted strain values, as shown in Table 4.38, were considered to be high and unsuitable for high CG production. Even though, the fabrics themselves have an immense extensibility, their predicted strain value results are too high and that could lead to the limitation of pattern construction. Thus, this group of fabric is optimal to produce fitting garments when pressure is lowered to less than 1.15 kPa and the sense of discomfort had yet to be found.

Concerning the second group with medium compression pressure (S3, S4 and S5), they appeared to have an optimal predicted strain at 1.15 kPa with strain approximately at 0.5 as shown in Table 4.38. From the mentioned, it could be assumed this particular group samples are suitable for manufacturing medium CG for sportswear, swimming suit, etc.

For samples S6, S7 and S8 known as a group with highest level of compression garment, the values of the predicted strain are lower than 0.4 at the pressure 1.15 kPa as. With this particular characteristic, these samples could effectively be used for producing various types of high compression garment including medical application, athletic application and body shaping application. And thus, S6, S7 and S8 were selected to determine higher pressure from 1.15 (8.63 mmHg) to 2.4 kPa (18 mmHg) in order to predict the strain value for high compression garment and the strain results are obtained in Table 4.39.

Table 4.39 The results of predicted strain values with different parts of the female body at pressure 2.4 kPa

Body part	D (m)	$\sigma = \frac{DP}{2h} ; (Pa)$			Strain ϵ by prediction equation		
		S6	S7	S8	S6	S7	S8
Upper bust	0.251	528,421	381,266	470,625	0.54	0.52	0.59
Bust	0.276	581,053	419,241	517,500	0.58	0.54	0.60
Lower bust	0.232	488,421	352,405	435,000	0.52	0.52	0.58
Waist	0.228	480,000	346,329	427,500	0.51	0.52	0.58

* D is diameter of body circumference.

Referring strain prediction values in Table 4.39, they were used for the circumferential strain parameters and the results were calculated to determine the initial circumference by multiplying the elastic coefficient in width dimension from the equation (3.4).

$ECW = \frac{1}{\varepsilon_{Circumferential} + 1}$ and used for an estimation of patternmaking size in width dimension as shown in Table 4.40.

Table 4.40 The size of patternmaking with different parts of the body under the pressure at 2.4 kPa

Body part	C (cm)	$C_0 = C \times ECW$; (cm)			$\overline{ab} = \overline{cd} = C \times ECW \times \frac{1}{4}$; (cm)		
		S6	S7	S8	S6	S7	S8
Upper bust	78.8	51.17	51.84	49.56	12.79	12.96	12.39
Bust	86.6	54.81	56.23	54.13	13.70	14.06	13.53
Lower bust	72.7	47.83	47.83	46.01	11.96	11.96	11.50
Waist	71.5	47.35	47.04	45.25	11.84	11.76	11.31

*C is the body circumference and C_0 is initial circumference of fabric.

In Table 4.41, procedural steps of calculating the elastic coefficient in width and length dimensions in different parts of the body circumferences are offered. Column number (1) symbolizes the predicted strain modelling of fabric tensile property in order to calculate the strain values as shown in column number (2) and finally elastic coefficients in width dimension could be found in column number (3). Likewise, the strain values from column number (2) were used in order to calculate the elastic coefficient in length dimension by predicted equations in column number (4) and the values of ECL are obtained as found in column number (5).

Table 4.41 The elastic coefficient for 2.4 kPa pressure in width and length dimensions in different body parts

No	Body part	Pattern width dimension (Course-wise direction)			Pattern length dimension (Wale-wise direction)	
		(1)	(2)	(3)	(4)	(5)
		Mathematic modelling for predictive strain	Strain	ECW	Predictive elastic coefficient	ECL
S6	Upper bust	$3.47E-18\sigma^3 - 4.26E-12\sigma^2 + 2.31E-06\sigma$	0.54	0.649	$1 + 0.2289\varepsilon$	1.124
	Bust		0.58	0.633		1.133
	Lower bust		0.52	0.658		1.119
	Waist		0.51	0.662		1.117
S7	Upper bust	$-8.92E-18\sigma^3 + 2.87E-12\sigma^2 + 1.58E-06\sigma$	0.52	0.658	$1 + 0.1916\varepsilon$	1.100
	Bust		0.54	0.649		1.103
	Lower bust		0.52	0.658		1.100
	Waist		0.52	0.658		1.100
S8	Upper bust	$-1.52E-18\sigma^3 - 6.08E-13\sigma^2 + 1.89E-06\sigma$	0.59	0.629	$1 + 0.0589\varepsilon$	1.035
	Bust		0.6	0.625		1.035
	Lower bust		0.58	0.633		1.034
	Waist		0.58	0.633		1.034

4.5.3 Patternmaking development method for stretch fabrics

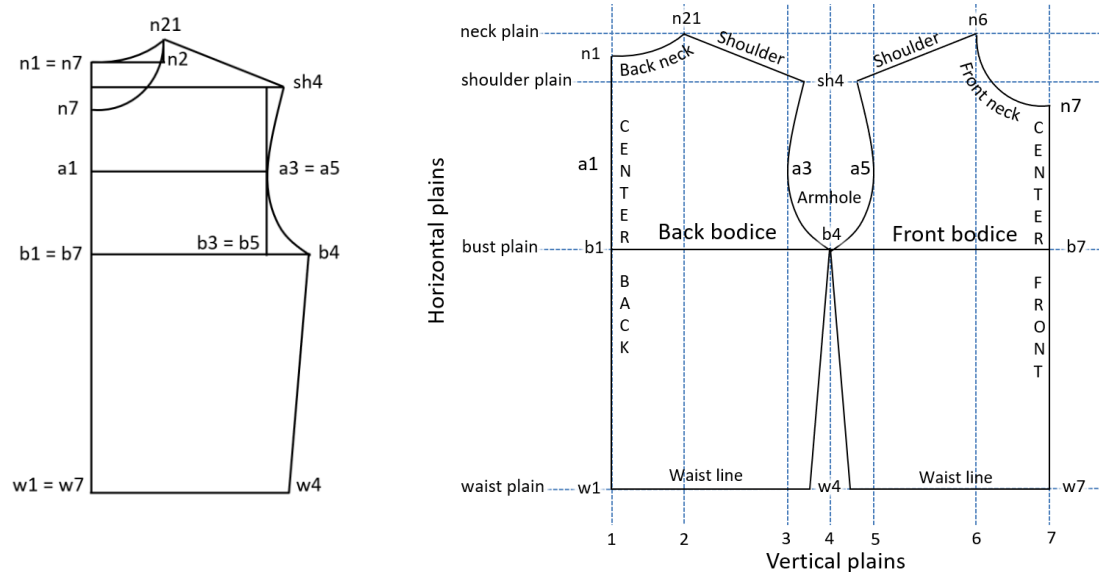
The patternmaking method introduces the formulas of block pattern construction in Table 4.42 and refers to the fundamental of pattern dimensions chart with the symbols and numbers

illustrated in Figure 4.27 (a). Besides, the final block pattern construction was linked with the vertical and horizontal plains as shown in Figure 4.29 (b). Regarding to the body measurements of mannequin, the following information are obtained including: back length or nape to waist (nw) = 38 cm, armscye depth (ard) = 15 cm, neck girth (ng) = 36 cm, back width (bw) = 33 cm, bust girth (bg) = 86.6 cm, and waist girth (wg) = 71.5 cm.

Table 4.42 Fundamental of block patternmaking formulas

No.	Details	Construction abscissa	Formula	Calculation(cm.)
1	Centre line at neck	$l \perp v$		
2	Back length	$n1w1$	Back length	38.00
3	Armscye depth	$n1b1$	Armscye depth	15.00
4	Armhole pitch	$n1a1$	$0.5K1H1$	7.50
5	Horizontal lines	$l, b, w \perp l$		
6	Shoulder line	$sh \perp l$	$0.2 K1L1$	
7	Neck width	$n1n2$	$0.17ng (-1.5cm)$	4.62
8	Neck height	$n2n21 \perp v$	1.3 cm	1.30
9	Back width	$b1b3(b5)$	$0.5bw (-6cm)$	10.50
10	Back width line	$b3sh3 \perp h$		
11	shoulder point	$sh3sh4$	1.0 cm	1.00
12	shoulder line	$n21sh4$		
13	Bust width	$b1b4$	$0.25bg$	21.65
14	Waist width	$w1w4$	$0.25wg$	17.88
15	Front neck line depth	$n7n71$	$0.17ng (-1,5cm)$	4.62

Note: $\perp v$ (k) is a vertical line and $\perp h$ is a horizontal line and $\perp l$ is a central line



(a) Fundamental of block pattern dimensions chart

(b) The patternmaking related to the vertical and horizontal plains

Figure 4.27 The block patternmaking chart

Figure 4.28 illustrates the matrix dimension points for the adjustment of patternmaking development that are related to block pattern (black line). There are nine important matrix points that present direction of the pattern which were moved by X axis and Y axis. The pattern in blue line represents the patternmaking at the pressure 1.15 kPa and the green line is the patternmaking at the pressure 2.4 kPa from the sample S7. In order to define point number 3, calculation is done by multiplying waist circumference with ECW and then plus the length dimension from armhole line to waist before multiplying with ECL. In case of point number 4, calculation can be done by multiplying the bust circumference with ECW. While in relationship of points number 5 and 6, adjustment of pattern from point number 4 will create a new armhole line and shoulder line.

Figure 4.28 describes the patternmaking by calculating the elastic coefficient of ECW and ECL of the sample S7 at the specific pressure 2.4 kPa and focuses on only particular area as the cylindrical shape at the shadow area.

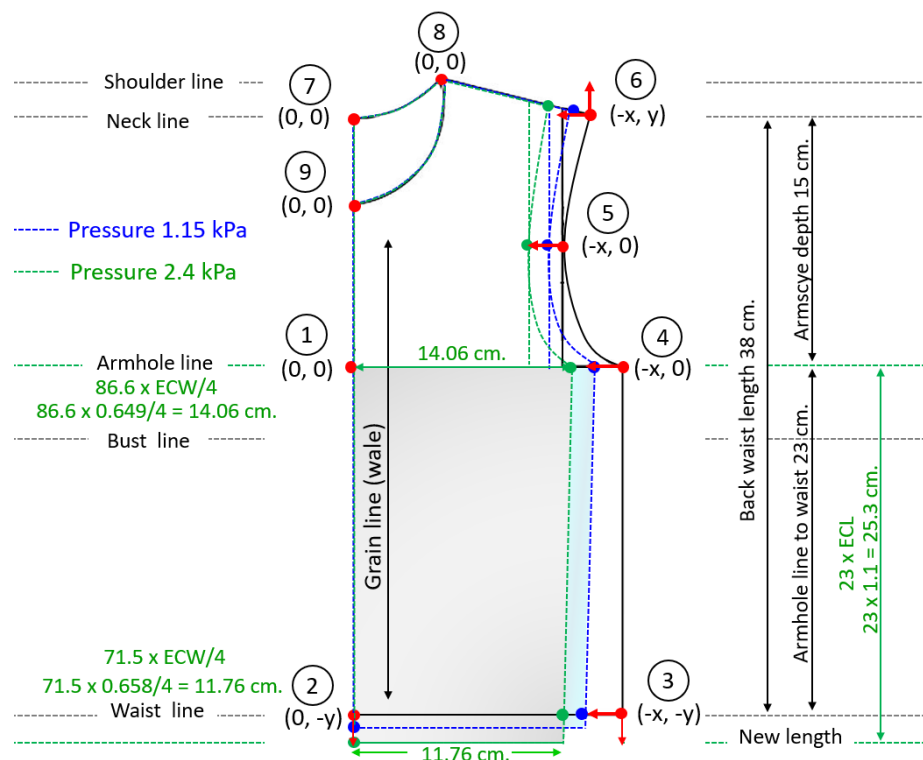


Figure 4.28 The reduction of patternmaking method based on fabric tensile property of sample S7

4.5.4 Application of patternmaking reduction with standard sizing system

The development of clothing patternmaking method for stretch fabric in this research study was complete and this brings to an achievement of creating accurate size patternmaking for

its applications. Furthermore, this research endeavours to create as a guideline for the fundamental of patternmaking for stretch fabric referring to the standard sizing system which would be helpful to understand the importance of body measurements that can be applied and integrated by the elastic coefficient to achieve accurate size of pattern dimensions. Table 4.43 represents body measurement according to standard ASTM D5585 for adult female of size 6, 7 and 8 for case study example describing the method by multiplying the elastic coefficient of ECW and ECL from the formulas were discovered.

Table 4.43 Modification standard sizing system of body measurement by applying elastic coefficient

Body measurement	Symbol	Size (cm)			Multiply elastic coefficient
		6	8	10	
Nape to waist	nw	40.6	41.3	41.9	×ECL
Armscye depth	ard	18.7	19.0	19.4	No reduction
Bust girth	bg	86.4	89.0	91.4	×ECW
Waist girth	wg	66.0	68.5	71.1	×ECW
back width	bw	36.5	37.1	37.8	×ECW
Neck girth	ng	35.6	36.2	36.8	No reduction
Shoulder length	shl	12.9	13.0	13.2	No reduction

Note: ECW is elastic coefficient in width dimension and ECL is elastic coefficient in length dimension.

Eventually, this technique of modifying standard sizing system of the body measurement could be conducted by applying the elastic coefficients which could help develop the patternmaking and thus, application of the method could be considered very helpful for the garment industries to manufacture compression garments in mass production.

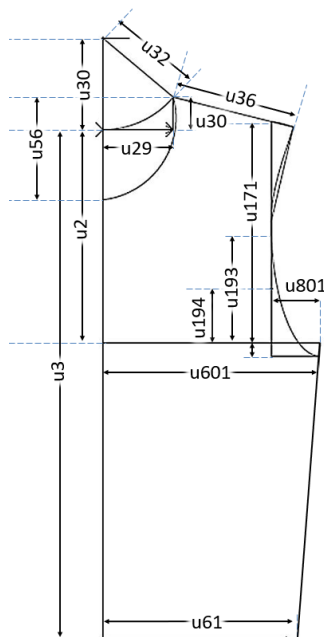
4.5.5 Application of patternmaking by using PDS tailor XQ software

In Table 4.44, parameters of body measurement are obtained by applying PDS Tailor XQ software on the mannequin. The benefit of software for predicting the pattern construction under the parameters of body measurement and elastic coefficient of elastic material. The parameters can automatically help determine the size of patternmaking with elastic coefficients under the regression formulas method. Moreover, the software will also help define patternmaking through CAD system as shown in Figure 4.29 (a and b).

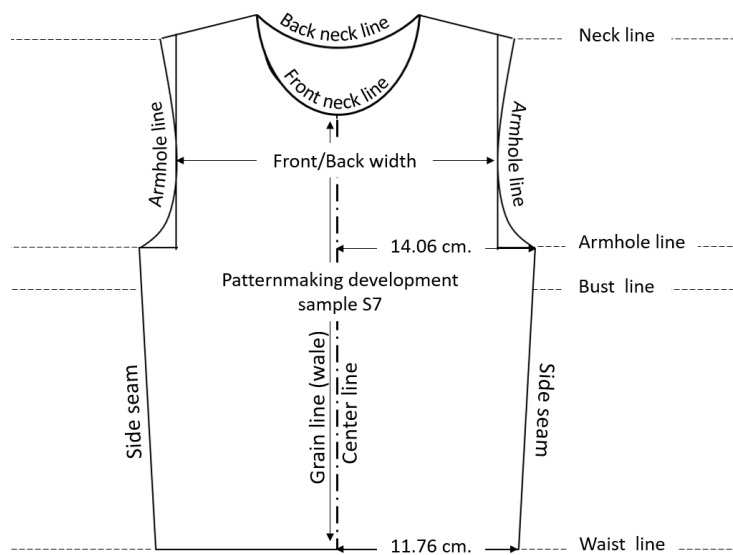
However, some parts of the pattern dimensions are not precisely as the estimating pattern reduction method, but the software can adjust the pattern in order to fix the size of patternmaking such as the construction segment of total chest-width “u6”, chest half-width “u601” and waist width measuring “u61”.

Table 4.44 Modification of the pattern construction abscissa PDS Tailor XQ software

Variable	Type	Descriptive Text	Formula	Value (cm)
MATERIAL ALLOWANCES				
Ed	C	Length elasticity coeff. of material	$1 - KE_d$	1.100
Eš	C	Width elasticity coeff. of material	$1 - KE_{\text{š}}$	0.658
Eh	C	Elasticity coeff. of material at bust	$1 - KE_{\text{š}} * KE_h$	0.649
ABSOLUTE TERMS OF CONSTRUCTION SEGMENT				
B	C	Garment length CONSTRUCTION SEGMENTS - NETWORK	L1	38.000
u1	U	Garment length	$(B + a_1) * Ed + p_1$	38.000
u2	U	Chest line placing	$(T_{39} + a_2) * Ed + p_2$	15.000
u3	U	Waist line placing	$(T_{40} + a_3) * Ed + p_3$	38.000
u6	U	Total chest width	$(0.5 * T_{16} + a_6) * Eh + p_6$	28.120
u601	C	Chest half-width	$0.5 * u_6$	14.060
u801	U	Arm scye half-width	$(K_{801} * T_{16} + a_{801} * Eh + p_{801})$	3.722
u10	V	Arm scye depression	$(K_{10} * (T_{40} - T_{39}) + a_{10}) * Ed$	0.930
u171	C	Arm scye depth	$(0.5 * T_{38} + a_{171}) * Ed + p_{171}$	17.907
u193	C	Arm scye lower part construction	$0.5 * (u_{171} + u_{10})$	9.419
u194	C	Arm scye lower part construction	$0.25 * (u_{171} + u_{10})$	4.709
CONSTRUCTION SEGMENTS - BACK PART				
u29	U	Back part neck width	$(0.185 * T_{13} + a_{29}) * Eh + p_{29}$	5.354
u30	U	Back part neck height	$(0.065 * T_{13} + a_{30}) * Ed + p_{30}$	2.286
u32	V	Back part neck radius	$(0.23 * T_{13} + a_{29}) * E_{\text{š}} + p_{29}$	6.943
u335	V	Shoulder line angle	z335	76.000
u36	V	Back part shoulder line enlargement	$K_{36} * T_{47} + a_{36}$	1.750
CONSTRUCTION SEGMENTS - FRONT PART				
u56	U	Front part neck depth	$(0.2 * T_{13} + a_{56}) * Ed + p_{56}$	5.354
u57	V	Front part neck radius	$(0.18 * T_{13} + a_{57}) * E_{\text{š}} + p_{57}$	6.273
u61	U	Waist width measuring	$(0.25 * T_{18} + a_{61}) * E_{\text{š}} + p_{61}$	11.760



(a) Pattern construction chart



(b) Patternmaking for CG at the pressure 2.4 kPa of the sample S7

Figure 4.29 The patternmaking by applying PDS Tailor XQ software

Referring the pattern construction abscissa chart of the construction segments created from the PDS Tailor XQ software shows the variables of pattern construction segment which are coordinated as shown in Figure 4.29(a). While Figure 4.29(b) presents the final patternmaking, for CG at the pressure 2.4 kPa of the sample S7 which created by PDS Tailor XQ software.

Overall, the PDS Tailor XQ software has a great efficacy to create patternmaking from stretch fabrics by inputting the parameters of elastic coefficient into the software and the database in the software could also be linked with the standard sizing system. Besides, various types of patternmaking garment designs in the software can help create patternmaking that can be transferred to CAD system. However, the pattern dimension distances are somewhat slightly different, but the final step can be adjusted for accurate size of pattern determination.

Chapter 5 Summary and Conclusions

5.1 Summary

In this thesis, a new systematic patternmaking method approach by finding out the elastic coefficient in order to modify the pattern construction for stretch fabrics and procedure to investigate the elastic fabric performance was developed. The method integrates knowledge from, multiple disciplines, including body measurement study, the fundamental block patternmaking, mechanical property of elastic fabric investigation, characterization of fabric tensile deformation, the interface pressure applied by using mathematical modelling based on the theoretical of Laplace's Law and thin-wall cylinder theory and developing the patternmaking methodology to emphasize the precise pressure value requirement of pressure garment.

This thesis can be summarised to approach the procedure of the patternmaking development method to estimate the final size of patternmaking for pressure garment. The elastic coefficients are the main parameters applied to calculate the pattern abscissa in the width and length dimensions of patternmaking. Firstly, ECW is the main key to predict the strain value from the stress-strain curve results. The pattern construction in width dimension mainly occur the pressure by reduction size of clothing patternmaking. Therefore, the specific pressure requirement in CG applied the mathematic modelling for prediction of strain value is calculated in this dimension. Secondly, ECL was used for experiment of the fabric deformation characteristic analysed by the image processing analysis. Eventually, the results of ECW and ECL were multiplied by the size of body measurement to modification the patternmaking in the main critical points from the reduction of matrix dimension.

5.2 Conclusions from the research

Efficacy of elastic fabric for pressure garment is very important to achieve the correct fabric for the garment applications end used. The mechanical fabric property could be examined and evaluated the fabric performance by classify type of compression garments applications. Due to some fabric properties, they are unsuitable to produce high compression garment applications. Therefore, the propose of this research is to define and evaluate the capacity of

fabric for compression garments and fill the knowledge gap and develop a systematic pattern construction method for high performance for pressure garment applications. By conducting a series of theoretical study and experimental investigation, the objectives of the study have been achieved and summarised as follows:

Tensile property is the initial examination of the efficacy of fabric by the percentage of elongation. It was found that a good extensibility should be over than 400 % elongation and a fabric is suitable for produce the high compression garments such a medical compression garment where it should have the fabric elongated minimum reach to 500%. As for the well-fitted garment on the body, the extensibility up to 200% is sufficient to produce the slight pressure garment less than 1.15 kPa.

The hysteresis loop test, is concerned with the stretch level of the fabric that it should be optimal stretch for investigating the stress-strain curve from the typical stretch-recovery cycle. This research defined the optimal elongation of the fabric at 50% that achieve an effective result and rescue the fabric recovery and deformation change. Further, the stress-strain cycles found the 5th cycle is applicable to apply for analysis and evaluation.

Elasticity of fabric found the elastane composition of fabric is significantly different of the influence on the elastic recovery and the results could be concluded that higher elastane composition will have higher elastic recovery. In elastane in the fabric over 10%, the elastic recovery has excellently preformed between 90 - 92% of dynamic testing.

Stress relaxation results showed that at the elastane 5.62% in the fabric the force decay rapidly decreased and reached to 18.38% of stress relaxation from the initial stress holding. In the fabrics that have elastane over than 25%, then the stress relaxation was lesser than 10%. It could be concluded that the efficacy of elastic fabric for producing the CGs that the elastane should have minimum at 25% will have a great elastic recovery and less stress relaxation.

Dynamic work recovery, of this thesis found that the percentage of elastane might be an influence on the energy loss when fabric high percentage of elastane, the less energy loss during dynamic test. It could be helpful for the sportswear application to investigate the fabric performance to improve the garment applications.

Fabric deformation of knitted structure including single jersey, interlock and locknit. The fabric deformation results agreed with the theoretical background of the appearance properties that the single jersey structure has poor dimensional stability and tendency to curl at the edge of the fabric. While the fabric structures of locknit is a bit tendency to curl at the edge and interlock is very good dimensional stability and without any curling effect when fabrics extended.

Image process by MATLAB, was well done and successful by a novel technique method to simulate the images then processing gradient deformation tensor. This new technique is accurate in calculation of the gradient deformation tensor under the different extension levels and it could be predicted the ECL.

Engineering stress (ES) VS True stress (TS), this research examined the results of ES and TS to compare the stress value. The experiment found that at the strain between 0-0.2, the TS is quite equal with ES. Then, the stress values are slightly different until the strain at the maximum 0.5 the TS is a bit higher than ES only 3%. Therefore, it could be assumed that the fabric stretches at the strain maximum 0.5 that the value of ES can be accepted for analysis of this research.

The prediction of the strain value from the mathematical modelling was successful for estimating the predicting strain in order to calculate the ECW. The designing experiment method investigated and compared with different parameters including fabric samples, strain levels, diameters and models (vitro and vivo). The results were well done to get the accurate results and agreement with the mathematical modelling based on theoretical of Laplace Law. I hope that a new modelling finding will gainful to estimate the fabric stretch depending on the pressure requirement.

Effect thickness of the compression tester, this research found that the effect of thickness sensor perturbation has occurred with the solid (vitro) cylindrical model. Therefore, the correction factor can be calculated to achieve the actual pressure results from compression tester. While the thickness sensor does not have the effect on the human skin (vivo), so the correction factor was unpractised. However, this research was used one compression tester which it is called Picopress ® and it could be assured for this device that it is accuracy and effective for measuring the pressure value and calculating the correction factor.

Patternmaking for pressure garment has defined the zone of pressure area into two zone as described in chapter 3, zone 1st is the zone of pressure area that the main focusing on determining the specific pressure and the body as assume as the cylindrical model. Zone 2nd the fabric could not stretch around body circumference because this zone of patternmaking was cut for drawing the armhole line because of this reason the patternmaking in zone 2nd was neglect.

Pattern development well done and successful to used fundamental block pattern and was applied by using the PDS Tailor XQ software. The experiment found that the PDS Tailor XQ software quickly computed the patternmaking based on function of elastic coefficient ECW and ECL. However, the construction formulas are complicated but in the final step can be adjusted the patternmaking and accuracy size of pattern requirement. Moreover, this research achieves the solution for coordinate with the standard sizing system of the body measurements then was applied the elastic coefficient to find out the reduction values before calculated with the fundamental patternmaking method.

This thesis finding in this study enhance the knowledge of patternmaking engineering technology for accomplishing a purpose a new systematic patternmaking method for stretch fabrics. However, the development of patternmaking method is applied to assume the body shape like the cylindrical shape which related to the Laplace's low theory for prediction of the strain values and could be proved that the mathematical modelling for predicting strain value is considered to be accurate for cylindrical shape from the experimental results. In fact, the body shape is not exactly cylindrical shape and thus the estimation of the size of patternmaking is suitable for some parts of the body that is similar to cylindrical shape. Hopefully, this thesis would be useful for garment industries to produce pressure clothing applications with high compression products by scientific methodology.

5.3 Recommendation from research

In this research, a lot of efforts have been made to develop the engineering patternmaking method for stretch fabrics and have applied to the scientific knowledgebase that could be fulfilled to defined to the future direction of the research activities and it would including provide the insightful reference to researchers. The recommendation for future research can hopefully expand the results obtained in this thesis are outlined as follows:

- Analysis the pressure under fabric stretch based on the complex body shape.
- Analysis the dynamic pressure testing during body movement or some activities.
- Applying the patternmaking to the seamless technology and modification the patternmaking for well fitted with the body shape.
- Simulating part would be supported the developing the strain predictive mathematic modelling that it will be compared with the finite element method (FEM) to approximate the pressure value on the simulation model.
- The develop the method of patternmaking was done for upper part of the female so the method could useful to design with another part of the body or it would help to support other compression applications areas.

References

- [1] Wang, L., Felder, M., & Cai, J. (2011). Study of properties of medical compression garment fabrics. *J. Fiber Bioeng. Inform*, 4, 15-22
- [2] Ying, X., & Tao, X. (2018). Compression garments for medical therapy and sports. *Polymers*, 10(663), 3-19.
- [3] Macintyre, L. (2007). Designing pressure garments capable of exerting specific pressures on limbs. *Burns*, 33(5), 579-586.
- [4] Makabe, H., Momota, H., Mitsuno, T., & Ueda, K. (1991). A study of clothing pressure developed by the gird. *J. Jpn. Res. Assoc. Text. End-Uses*, 32, 424-438.
- [5] Jariyapunya, N., Musilová, B., Geršák, J., & Baheti, S. (2017). The influence of stretch fabric mechanical properties on clothing pressure. *Vlakna a Textil*, 24(2), 43-48.
- [6] Jariyapunya, N., & Musilová, B. (2018). Predictive modelling of compression garments for elastic fabric and the effects of pressure sensor thickness. *The Journal of The Textile Institute*, 1-9.
- [7] Musilová, B. (2012). *Predikce konstrukčních parametrů střihů korzetových výrobků*. Liberec: Technická univerzita v Liberci, Fakulta textilní, Katedra oděvnictví.
- [8] Senthilkumar, M., Anbumani, N., & Hayavadana, J. (2011). Elastane fabrics-A tool for stretch applications in sports. *Indian J. Fibre Text. Res*, 36, 300-307.
- [9] Hu, J., Lu, J., & Zhu, Y. (2008). New developments in elastic fibers. *Polym. Rev*, 48, 275-301. ISO 13934-1: Determination of maximum force and elongation at maximum force using the strip method. (2013).
- [10] Senthilkumar, M., & Anbumani, N. (2014). *Dynamics of elastic knitted fabrics for tight fit sportswear*. Germany: LAP LAMBERT Academic Publishing.
- [11] Khaburi, J. A., Dehghani-Sanij, A. A., Nelson, A. E., & Hutchinson, J. (2012). Effect of bandage thickness on interface pressure applied by compression bandages. *Medical Engineering & Physics*, 34, 378-385.

-
- [12] Kowalski, K., Mielicka, E., & Kowalski, T. M. (2012). Modelling and designing compression garments with unit pressure assumed for body circumferences of a variable curvature radius. *Fibers & Textile in Eastern Europe*, 20(6A(95)), 98-102.
- [13] Macintyre, L., & Ferguson, R. (2013). Pressure garment design tool to monitor exerted pressure. *Burns*, 39, 1073-1082.
- [14] Kowalski, K., Mielicka, E., & Jasinska, I. (2012). Modelling a analysis of the circumferential force and susceptibility of vascular prostheses to internal pressure changes. *Fibres & Textile in Eastern Europe*, 20(3(92)), 87-91.
- [15] Macintyre, L., Baird, M., & Weedall, P. (2004). The study of pressure delivery for hypertrophic scar treatment. *Int. J. Cloth. Sci. Technol*, 16, 173–183.
- [16] Kirk, W. J., & Ibrahim, S. (1966). Fundamental relationship of fabric extensibility to anthropometric requirements and garment performance. *Text. Res*, 36, 37–47.
- [17] Macintyre, L., & M, B. (2006). Pressure garments for use in the treatment of hypertrophic scars—a review of the problems associated with their use. *Burns*, 32(1), 10-15.
- [18] Zhao, L., Li, X., Yu, J., Li, C., & Li, G. (2017). Compression sleeves design based on Laplace Laws. *J Textile Engineering & Fashion Technology*, 2(2).
- [19] Chattopadhyay, R., & Bera, M. (2017). Prediction of Pressure due to Elastic fabric Tube Following Energy Principle. *Journal of Textile Engineering & Fashion Technology*, 2(5).
- [20] Macintyre, L., Baird, M., & Weedall, P. (2006). The study of pressure delivery for hypertrophic scar treatment. In K. J. Anand SC, *Medical Textile and Biomaterials for Healthcare* (pp. 224-232). Cambridge: Woodhead Publishing Limited.
- [21] Partsch, H., Partsch, B., & Braun, W. (2004). Interface pressure and stiffness of ready made compression stockings: Comparison of in vivo and in vitro measurements. *J. Vasc. Surg*, 44, 809–814.
- [22] Vinckx, L., & Boeckx, W. (1990). Anslysis of the pressure perturbation due to the introduction of measuring probe under an elastic garment. *Medical & Biological Engineering & Computing*, 28, 133-138.

-
- [23] Khaburi, J. A., Dehghani-Sanij, A. A., Nelson, E., & Hutchinson, J. (2011). Measurement of Interface Pressure Applied By Medical Compression Bandages. *International Conference on Mechatronics and Automation*.
 - [24] Partsch, H., Clark, M., Bassez, S., Benigni, J., Becker, F., Blazek, V., . . . Neumann, M. (2006). Measurement of lower leg compression in vivo: Recommendations for the performance of measurements of interface pressure and stiffness. *Dermatologic Surgery*(32(2)), 224-233.
 - [25] Partsch, H., & Mosti, G. (2008). Thigh compression. *Phlebology*(23(6)), 252-258.
 - [26] Mosti, G., & Rossari, S. (2008). The importance of measuring sub bandage pressure and. *Acta Vulnol*, 6, 31-36.
 - [27] Musilová, B., & Nemčoková, R. (2013). Implementing Mass Customization into Clothing Production. *Vlákna a textil*, 20(4), 12-19.
 - [28] Musilová, B., & Nemčoková, R. (2014). Study of Czech male body proportions and evaluation of men's shirt pattern making methods. *Tekstil ve Konfeksiyon*, 24(4), 399-404.
 - [29] Hatch, K. (1993). *Textile Science*. Minneapolis: West Publishing.
 - [30] Baheti, S., Jariyapunya, N., & Tunák, M. (2017). Image Analysis for Characterizing Tensile Deformation of Knitted Fabric. *Vlákna a textil (Fibres and Textiles)* , 24(2), 54-58.
 - [31] Baheti, S., & Jariyapunya, N. (2017). Application of Image Analysis Method for Measurement Fabric Stretch Deformation. *IOP Conference Series*, IOP Co. United Kingdom.
 - [32] Julie, A. (2016). *Patternmaking with Stretch Knit Fabrics*. New York: Bloomsbury Publishing Plc.
 - [33] Richardson, K. (2008). *Designing and Patternmaking for Stretch Fabrics*. USA: Fairchild Books.
 - [34] Hayes, S. G., & Venkatraman, P. (2016). *Materials and Technology for Sportswear and Performance Apparel*. USA: Taylor & Francis Group.
 - [35] Zhang, X., & Ma, P. (2017). Application of Knitting Structure Textiles in Medical Areas. *AUTEX Research Journal*, -(), 1-11.

-
- [36] MacDonald, N. M. (2010). *Principles of Flat Pattern Design 4th Edition*. New York: Fairchild Books, A Division of Conde Nast Publications.
- [37] Parish, P. (2013). *Pattern cutting: The architecture of fashion*. New York: Bloomsbury Publishing Plc.
- [38] Musilová, B., Komárková, P., & Glombíková, V. (2004). *Fundamentals of clothing design*. Liberec: Technical University.
- [39] Junková, M., Musilová, B., Komárková, P., Glombíková, V., & Nemčoková, R. (2003). *Konstrukce základních druhů oděvů: text ke cvičení*. Liberec: Technická univerzita v Liberci.
- [40] Watkins, P. (2011). Garment pattern design and comfort. In *Improving Comfort in Clothing* (pp. 245-277). Philadelphia: Woodhead Publishing Limited.
- [41] Kilinc, F., & Balci in. (2011). *Improving Comfort in Clothing*. Cambridge,: Woodhead Publishing.
- [42] Liu, Y., & Dongsheng, C. (2015). An analysis on EEG power spectrum under pressure of girdle. *International Journal of Clothing Science and Technology*, 27(4), 495-505, .
- [43] Ziegert, B., & Keil, G. (1998). Stretch fabric interaction with action wearables: defining a body contour pattern system. *Clothing and Textile Research Journal*, 6, 55-64.
- [44] Watkins, P. (2011). Designing with stretch fabrics . *Indian Journal of Fibre & Textile Research*, 36, 366-379.
- [45] Macintyre, L., Baird, M., & Weedall, P. (2007). The study of pressure delivery for hypertrophic scar treatment. *International Journal of Clothing Science & Technology*, 16(1), 173-183.
- [46] NG, S. F. (1993). Medical clothing a tutorial paper on pressure garments. *International Journal of Clothing Science and Technology*, 5(1), 17-24.
- [47] Macintyre, L., & M, B. (2006). Pressure garments for use in the treatment of hypertrophic scars—a review of the problems associated with their use. *Burns*, 32(1), 10-15.

-
- [48] Doan, B. K., Kwon, Y. H., Newton, R. U., Shim, J., Popper, E. M., Rogers, R. A., . . . Kraemer, W. J. (2003). Evaluation of a lower-body compression garment. *lower-body compression garment*, 21(8), 601-610.
- [49] Chatard, J. C., Atlaoui, D., Farjanel, J., Louisy, F., Rastel, D., & GuÉzennec, C. Y. (2004). Elastic stockings, performance and leg pain recovery in 63-year-old sportsmen. *European Journal of Applied Physiology*, 93(3), 347-352.
- [50] Pratt, J., & West, G. (1995). Pressure Garments. In *Manual on their Design and Fabrication* (pp. 3-32). Oxford: Butterworth Heinemann Ltd.
- [51] Gauglitz, G. G., Korting, H. C., Pavicic, T., Ruzicka, T., & Jeschke, M. G. (2011). Hypertrophic scarring and keloids: Pathomechanisms and current and emerging treatment strategies. *Mol. Med*, 17, 113–125.
- [52] Reno, F., Sabbatini, M., Lombardi, F., Stella, M., Pezzuto, C., Magliacani, G., & Cannas, M. (2003). In vitro mechanical compression induces apoptosis and regulates cytokines release in hypertrophic scars. *Wound Repair Regen*, 11, 331–336.
- [53] Partsch, H., & Mortimer, P. (2015). Compression for leg wounds. *Br. J. Dermatol*, 173, 359–369.
- [54] Van den Kerckhove, E., Stappaerts, K., Fieuws, S., Laperre, J., Massage, P., Flour, M., & Boeckx, W. (2005). The assessment of erythema and thickness on burn related scars during pressure garment therapy as a preventive measure for hypertrophic scarring. *Burns*, 31, 696–702.
- [55] LIPOELASTIC. (2002-2018). Retrieved 11 21, 2018, from <https://www.lipoelastic.com/products/compression-garments/>
- [56] Zurada, J. M., Kriegel, D., & Davis, I. C. (2006). Topical treatments for hypertrophic scars. *J. Am. Acad. Dermatol*, 55, 1024–1031.
- [57] Sharp, P. A., Pan, B., Yakuboff, K. P., & Rothchild, D. (2016). Development of a best evidence statement for the use of pressure therapy for management of hypertrophic scarring. *J. Burn Care Res*, 37, 255–264.
- [58] Born, D. P., Sperlich, B., & Holmberg, H. C. (2013). Bringing light into the dark: Effects of compression clothing on performance and recovery. *Int. J. Sport Physiol*, 8, 4–18.

-
- [59] Duffield, R., & Portus, M. (2007). Comparison of three types of full-body compression garments on throwing and repeat-sprint performance in cricket players. *Br. J. Sport Med*, 41, 409–414.
- [60] Fu, W., Liu, Y., & Fang, Y. (2013). Research advancements in humanoid compression garments in sports. *Int. J. Adv. Robot. Sy.*, 10(66), 1-6.
- [61] Kraemer, W. J., Flanagan, S. D., Comstock, B. A., Fragala, M. S., Earp, J. E., Dunn-Lewis, C., . . . Penwell, Z. R. (2010). Effects of a whole body compression garment on markers of recovery after a heavy resistance workout in men and women. *J. Strength Cond. Res*, 24, 804–814.
- [62] Kraemer, W. J., Bush, J. A., Wickham, R. B., Denegar, C. R., Gomez, A. L., Gotshalk, L. A., . . . Putukian, M. (2001). Continuous compression as an effective therapeutic intervention in treating eccentric-exercise-induced muscle soreness. *J. Sport Rehabil*, 10, 11–23.
- [63] Sperlich, B., Haegele, M., Achtzehn, S., Linville, J., Holmberg, H. C., & Mester, J. (2010). Different types of compression clothing do not increase sub-maximal and maximal endurance performance in well-trained athletes. *J. Sport Sci*, 28, 609–614.
- [64] Morooka, H., Nakahashi, M., & Kitamura, K. (2001). Effects of clothing pressure exerted on a trunk on heart rate, blood pressure, skin blood flow and respiratory function. *J. Text. Mach. Soc. Jpn*, 54, 57–62.
- [65] Xu, D. F., Liu, D. Y., & Wu, Z. M. (2012). Analysis of physiological response by pressure developed by female swimsuit. *J. Beijing Inst. Cloth. Technol*, 32, 1-8.
- [66] Wang, C. C., & Tang, K. (2010). Pattern computation for compression garment by a physical/geometric approach. *Comput. Aided Des*, 42, 78–86.
- [67] Chan, A., & Fan, J. (2002). Effect of clothing pressure on the tightness sensation of girdles. *International Journal of Clothing Science and Technology*, 14(2), 100–110.
- [68] Little, T., & Liu, R. (2009). The 5S model to optimize compression athletic wear comfort in sports. *J Fiber Bioeng Informat*, 2, 44–55.
- [69] Fan, C. M. (2005). Venous pathophysiology. *Semin. Interven. Radiol*, 22, 157–161.
- [70] Makabe, H., Momota, H., Mitsuno, T., & Ueda, K. (1993). Effect of covered area at the waist on clothing pressure. *Sen-iGakkaishi*, 4109, 513–521.

-
- [71] Liu, H., Chen, D., Wei, Q., & Pan, R. (2013). An investigation into the bust girth range of pressure comfort garment based on elastic sports vest. *The Journal of The Textile Institute*, 104(2), 223–230.
- [72] Ito, N. (1995). Pressure Sensation (Clothing Pressure)- For the Design of Ideal Clothing. *Journal of Japan Research Association for Textile End-Uses*, 36(1), 38-43.
- [73] Denton, M. (1972). Fit, stretch and comfort. . *Textiles*, 3, 12-17.
- [74] Leung, W. Y., Yuen, D. W., Ng, S. P., & al, e. (2010). Pressure prediction model for compression garment design. *J Burn Care Res*, 31, 716-727.
- [75] Fung , Y. C. (1993). *Biomechanics: Mechanical Properties of Living Tissues* . New York: Springer-Verlag.
- [76] Lautrup, B. (2005). *Physics of Continuous Matter Exotic and Everyday Phenomena in the Macroscopic World*. London, UK: Institute of Physics Publishing.
- [77] Fung, Y. C. (1993). *Biomechanics: Mechanical Properties of Living Tissues*. 2nd ed. New York: Springer-Verlag.
- [78] Pytel, A., & Kiusalaas, J. (2012). *Mechanics of Materials Second Edition*. Stamford, USA: Global Engineering: Christopher M. Shortt.
- [79] Beer, F. P., Johnston, R. E., Dewolf, J. T., & Mazurek, D. F. (2012). *MECHANICS OF MATERIALS, SIXTH EDITION*. New York: McGraw-Hill.
- [80] Chi, Y.-W., Tseng, K.-H., Li, R., & Pan, T. (2017). Comparison of piezoresistive sensor to PicoPress in in-vitro interface pressure measurement. *Phlebology*, 1-6.
- [81] Partsch , H., & Mosti, G. (2010). Comparison of three portable instruments to measure compression pressure. *Int Angiol*, 29, 426–430.
- [82] Ferguson-Pell, M. W. (1980). Design criteria for the measurement of pressure at body/support interfaces. *Eng Med*, 9(4), 209-214.
- [83] Khaburi, J. A. (2010). *PhD Thesis Pressure Mapping Of Medical Compression Bandages Used For Venous Leg Ulcer Treatment*. Leeds: The University of Leeds School of Mechanical Engineering.
- [84] Khaburi, J. A., Dehghani-Sanij, A. A., Nelson, E., & Hutchinson, J. (2010). The effect of sensor thickness on the interface pressure measurement induced by medical

- compression bandages. *12th Mechatronics Forum Biannual International Conference, 1*, pp. 91-98. Zurich, Switzerland.
- [85] McCann, J. (2015). Environmentally conscious fabric selection in sportswear design. In *Textiles for Sportswear* (pp. 17-52). Cambridge, UK: Woodhead Publishing Series in Textiles.
- [86] Davis, R. (2014, December 17). *Linkedin*. Retrieved December 2, 2018, from <https://www.linkedin.com/pulse/understanding-elongation-knit-richard-davis/>
- [87] MacRae, B. A., Cotter, J. D., & Laing, R. M. (2011). Compression garments and exercise : Garment considerations, physiology and performance. *Sports Med*, 41, 815–843.
- [88] Geršak, J. (2013). *Design of clothing manufacturing processes*. Cambridge, UK: Woodhead publishing series in textile.
- [89] Voyce, J., Dafiniotis, P., & Towlson, S. (2005). Elastic textile. In *Textile in sport*. Cambridge, UK: Wood head publications.
- [90] Gulillaume, M., Stephane, P., Caroline, D., & Matthieu, F. (2006). The role of engineering in fatigue reduction during human locomotion - a review. *Sports engineering*, 9, 209-220.
- [91] Gokarneshan, N. (2017). Design of Compression/Pressure Garments for Diversified Medical Applications. *Biomed J Sci & Tech Res*, 1(3), 806-813.
- [92] Kim, S. A., & Suh, M. A. (2005). A Study on the knit pattern considering the characteristics of rib Stitch(2)-focused on 2×1 and 2×2 rib stitches. *The Research Journal of the Costume Culture*, 13(1), 47-59.
- [93] Anand, S. C. (2016). Technical fabric structures – 2. Knitted fabrics. In *Handbook of Technical Textiles, Volume 1: Technical Textile Processes* (pp. 107-162). Cambridge, UK: Woodhead Publishing Series in Textiles.
- [94] ASTM D 3776-96 : (2002). *Standard Test Method for Mass Per Unit Area (Weight) of Fabric*. United States: ASTM International.
- [95] WANG, X., Liu, X., & Hurren, C. (2008). Physical and mechanical testing of textiles. In *Fabric testing* (pp. 90-124). Cambridge, UK: Woodhead Publishing in Textiles.
- [96] ASTM D 1777-96: (2007). *Standard Test Method for Thickness of Textile Materials 1*. United States: ASTM International.

-
- [97] Gere , J. M. (2009). *Mechanics of materials*. London: Thomson – Engineering.
 - [98] *Wikipedia, the free encyclopedia*. (2018, December 4). Retrieved December 5, 2018, from [https://en.wikipedia.org/wiki/Deformation_\(engineering\)](https://en.wikipedia.org/wiki/Deformation_(engineering))
 - [99] Penko, T., & Geršak, J. (2016). Strip quadratic method for determining the Poisson's ratio of woven fabrics. *Textile Research Journal*, 86(1), 86-96.
 - [100] Allen , J. H. (2011). *Mechanics of materials for dummies*. Hoboken, NJ: Wiley Publishing, Inc.
 - [101] Araujo, M. D., & Fanguero, R. (2011). Weft-knitted structures for industrial applications. In *Advances in knitting technology* (pp. 136-169). Cambridge, UK: Woodhead Publishing.
 - [102] Trümper, W. (2016). Semi-finished Weft Knitted Fabrics and Weft Knitting Techniques. In *Textile Materials for Lightweight Constructions* (pp. 213-250). Springer Berlin Heidelberg.
 - [103] Ardakani, T., Asayesh, A., & Jeddi, A. A. (2016). The influence of two bar warp-knitted structure on the fabric tensile stress relaxation Part II: (locknit, satin, loop raised). *The Journal of The Textile Institute*, 107(11), 1357–1368.
 - [104] Dongsheng, C., Hong, L., Qiaoling, Z., & Hongge, W. (2013). Effects of Mechanical Properties of Fabrics on Clothing Pressure. *PRZEGLĄD ELEKTROTECHNICZNY*, 232-235.
 - [105] BS EN 14704-1: (2005).Determination of the elasticity of facrics part 1: Strip tests.
 - [106] Ilska, A., Kowalski, K., Kłonowska, M., & Kowalski, T. M. (2014). nfluence of Stress and Relaxation Characteristics of Knitted Fabrics on the Unit Pressure of Compression Garments Supporting
 - [107] Joanna, L. N., Ciara , E. C., & Melissa, L. K. (2017). Engineering mechanical gradients in next generation biomaterials - Lessons learned from medical textile design. *Acta Biomaterialia*, 56, 14-24.
 - [108] Kelly, P. (2013). *Solid Mechanics Lecture Notes* . Auckland : The University of Auckland.
 - [109] *ISO 8559-1:2017(en) Size designation of clothes(2017). Part 1: Anthropometric definitions for body measurement*. The International Organization for Standardization. Retrieved from <https://www.iso.org/standard/61686.html>

-
- [110] Jariyapunya, N., Musilová, B., & Havelka, A. (2018). Prediction of Pattern Dimensions for Pressure Garment. *22nd International Conference Structure and Structural Mechanics of Textile*. Liberec.
- [111] *EN ISO 5084*: (1996). *Textiles-Determination of Thickness of Textiles and Textile Products*. European Committee for Standardization.
- [112] ISO 13934-1: (2013). Determination of maximum force and elongation at maximum force using the strip method.
- [113] Baheti, S., Jariyapunya, N., & Tunák, M. (2017). Image Analysis for Characterizing Tensile Deformation of Knitted Fabric. *Vlákna a textil (Fibres and Textiles)*, 24(2), 54-58.
- [114] Jariyapunya, N., & Baheti, S. (2017). Application of Image Analysis Method for Measurement of Fabric Stretch Deformation. *Materials Science and Engineering*, IOP Conference Series.
- [115] Gonzalez, R. C., & Woods, E. R. (2002). *Digital image processing*. Prentice Hall Publishers.
- [116] Bansal, R. (2010). *Strength of Materials*. New Delhi: LAXMI PUBLICATION (P) LTD.

Research Outputs

List of publications in journals

- [1] **Nareerut Jariyapunya** and Blažena Musilová, Predictive modelling of compression garments for elastic fabric and the effects of pressure sensor thickness, *The Journal of The Textile Institute*, DOI:10.1080/00405000.2018. 1540285, **IMPACT FACTOR 1.174 (Q2)**.
- [2] **Nareerut Jariyapunya** and Blažena Musilová, Analysis of Stress and Strain to Determine the Pressure Changes for Tight-fitting Garment, *The Autex Research Journal*, DOI:10.2478/aut-2019-0006©AUTEX, **IMPACT FACTOR 0.957 (Q2)**.
- [3] **Nareerut Jariyapunya**, Blažena Musilová, J. Geršak and S. Baheti, The Influence of Stretch Fabric Mechanical Properties on Clothing Pressure, *Vlákna a textil (Fibres and Textiles)*, Vol.24, Issue 2, ISSN 1335-0617, p. 43 – 48, 2017. **SCOPUS**
- [4] **Nareerut Jariyapunya** and Jantana Sutdaen, Construction Simulation 3D of Tight-Fitting Sportswear to Evaluate Tension Distribution of Elastic Fabric, *Journal of Engineering*, RMUTT, Vol.15, Issue 2, ISSN 1685-5280, p. 69 – 76, 2017.
- [5] **Nareerut Jariyapunya**, Blažena Musilová and Marie Koldinská, Evaluating the Influence of Fiber Composition Structure of Knitting Fabrics on Total Hand Value (THV), *Applied Mechanics and Materials*, ISSN 1662-7482, Vol. 848, p. 211-215, 2016. doi:10.4028/www.scientific.net/AMM.848. 211 © 2016, **(Q4)**
- [6] Smita Baheti, **Nareerut Jariyapunya** and Maroš Tunák, Image Analysis for Characterizing Tensile Deformation of Knitted Fabric, *Vlákna a textil (Fibres and Textiles)*, Vol.24, Issue 2, ISSN 1335-0617, p. 54 – 58, 2017. **SCOPUS**
- [7] **Nareerut Jariyapunya and Smita Baheti**, Application of Image Analysis Method for Measurement of Fabric Stretch Deformation, *IOP Conference Series: Materials Science and Engineering*, 2017. **SCOPUS**

List of publications in conferences

- [1] **Nareerut Jariyapunya**, Blažena Musilová and Antonín Havelka, Prediction of Pattern Dimensions for Pressure Garment, *22nd International Conference Structure and Structural Mechanics of Textile*, TUL Liberec, Czech Republic, p. 287-293, 5th-7th December 2018. ISBN: 978-80-7494-430-7
- [2] Blažena Musilová, Alžbeta Hôrecká and **Nareerut Jariyapunya**, Method of Generation Zoning Areas in Pattern Construction Net of Seamless Underwear, *22nd International Conference Structure and Structural Mechanics of Textile*, TUL Liberec, Czech Republic, p. 83-89, 5th - 7th December 2018. ISBN: 978-80-7494-430-7
- [3] **Nareerut Jariyapunya**, Nadiia Kholiavko and Blažena Musilová, Designing Method for 3D Modelling for Garment Compression Values of Elastic Fabric Extension, *the 9th Central European Conference*, ISBN 978-80-7494-355-3, p. 44 – 48, 2017
- [4] **Nareerut Jariyapunya** and Smita Baheti, Application of Image Analysis Method for Measurement of Fabric Stretch Deformation, *17th World Textile Conference AUTEX*, 29th–31st May 2017.
- [5] **Nareerut Jariyapunya**, Blažena Musilová and Smita Baheti, Study on Stretch Deformation and Mechanical Properties of Knitted Fabrics for Tight-Fitting of Clothing, *44th Textile Research Symposium, IIT Delhi, India*, 14th - 16th December 2016.
- [6] **Nareerut Jariyapunya**, Jelka Geršak, Blažena Musilová and Smita Baheti, Designing and Patternmaking with Stretch Fabrics, *21st International Conference Structure and Structural Mechanics of Textile*, Liberec, Czech Republic, 1st-2nd December, ISBN 978-80-7494-269-3, p.239 - 244, 2016
- [7] Smita Baheti and **Nareerut Jariyapunya**, Characterization of Knitted Fabric Tensile Deformation by Image Analysis, *Workshop for Ph.D. Students of Faculty of Textile Engineering and Faculty of Mechanical Engineering TUL, Bílá voda*, 20th - 23rd September, ISBN 978-80-7494-293-8, p. 32 - 38, 2016.

-
- [8] **Nareerut Jariyapunya**, Blažena Musilová, Jelka Geršak and Smita Baheti, A Study of Mechanical Properties of Stretch Fabric and Pattern Construction to Evaluate Clothing Pressure, *Workshop for Ph.D. Students of Faculty of Textile Engineering and Faculty of Mechanical Engineering TUL*, 20th - 23rd September, ISBN 978-80-7494-293-8, p. 62-67, 2016.
- [9] **Nareerut Jariyapunya**, Blažena Musilová, Smita Baheti and Jantana Sutdaen, “Construction Simulation 3D of Sportswear to Evaluate Tension Distribution of Elastic Fabric for Tight-Fitting Garment,” *Rajamangala University of Technology International Conference (7th RMUTIC)*, Bangkok, Thailand, 24th – 26th August 2016.
- [10] **Nareerut Jariyapunya** and Blažena Musilová, A Study of the Elastic Flat Textile Properties Which Influence a Shape of Clothing Cut and Style, *Workshop for Ph.D. Students of Faculty of Textile Engineering and Faculty of Mechanical Engineering TUL, Světlanka, Rokytice nad Jizerou*, 22nd-25th September, ISBN978-80-7494-229-7, p. 67 – 72, 2015.
- [11] **Nareerut Jariyapunya**, Blažena Musilová and Marie Koldinská, Evaluating the Influence of Fiber Composition Structure of Knitting Fabrics on Total Hand Value (THV), *The 6th RMUTP International Conference on Science*, Bangkok, Thailand, 15th-16th July 2015.
- [12] **Nareerut Jariyapunya**, Blažena Musilová, Analysis of Female Body Measurements in Comparison with International Standard Sizing System, *20th International Conference Structure and Structural Mechanics of Textile*, Liberec, Czech Republic, 1st-2nd December, p.155-158, 2014.

Curriculum Vitae

PERSONAL INFORMATION



Nareerut JARIYAPUNYA M.Eng.,

📍 17 Listopadu 584/2, 46015 Liberec, Czech Republic

☎ +420 48 535 3241 📠 +420 77 359 1414

✉ nareerut.j@en.rmutt.ac.th

Date of birth: 16 December 1981

Nationality: Thai

EDUCATION

(January 2014 – until now)

Doctoral student

Clothing Technology Department, Faculty of Textile Engineering,
Technical University of Liberec, Czech Republic.

Topic: Clothing Patternmaking Method for Stretch Fabrics.

June 2008 – May 2010

Master's Degree of Engineering (Industrial Development),

Industrial Engineering Department, Faculty of Engineering,
Thammasat University, Thailand.

Topic: Analysis of customer Requirement with the Quality Function
Deployment Techniques in the Development of New Trekking
Products.

June 2001 – March 2005

Bachelor's Degree of Engineering (Garment Engineering),

Textile Engineering Department, Faculty of Engineering,
Rajamangala University of Technology Thanyaburi, Thailand.

WORK EXPERIENCE

(July 2006 – 2013)

Lecturer of Textile Engineering Department, Faculty of Engineering,
Rajamangala University of Technology Thanyaburi (RMUTT), Thailand.
<http://www.engineer.rmutt.ac.th/english/>

(2005 – June 2006)

Merchandiser, the Thai Silk Company Limited (Jim Thompson), Thailand.
<http://www.jimthompson.com/index.asp>

TRAINING

January - February 2017

Internship for PhD.

Faculty of Mechanical Engineering, University of Maribor, Slovenia.
Supporting by CEEPUS Mobility CIII-SI-0217-10-1617-M-97968.
Mentor: Prof. Dr. sc. Jelka Geršak.

16th - 22nd October 2016

CEEPUS Winter School DESIGN WEEK 2016.

Faculty of Mechanical Engineering, University of Maribor, Slovenia.

April 2016 – June 2016

Internship for PhD.

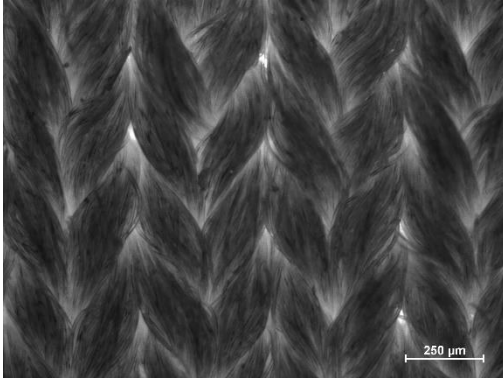
Faculty of Mechanical Engineering, University of Maribor, Slovenia.
Supporting by ERASMUS Mobility
Mentor: Prof. Dr. sc. Jelka Geršak.

Appendix

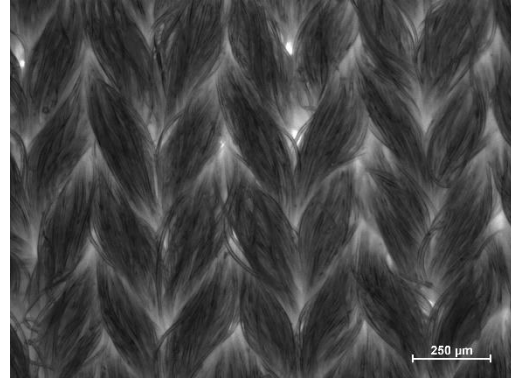
The structure of stretch fabrics samples

Single jersey structure (S1 – S6)

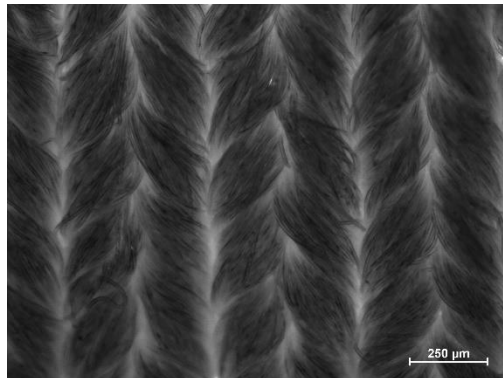
S1



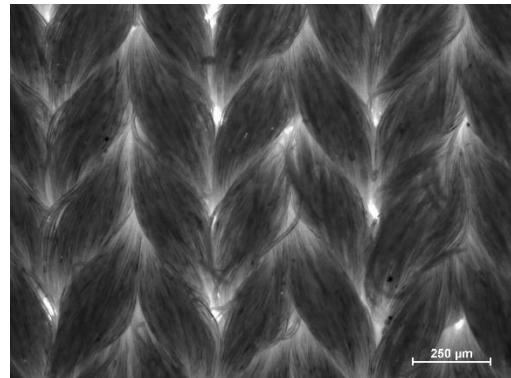
S2



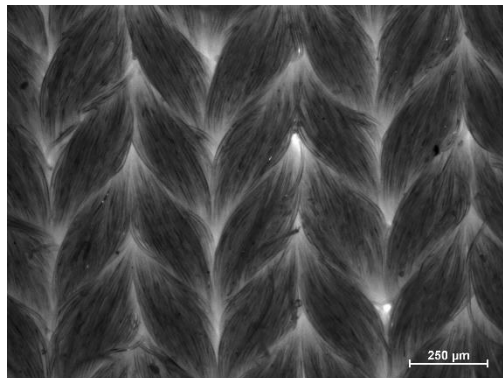
S3



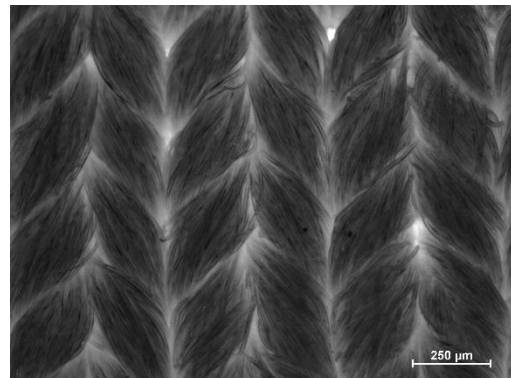
S4

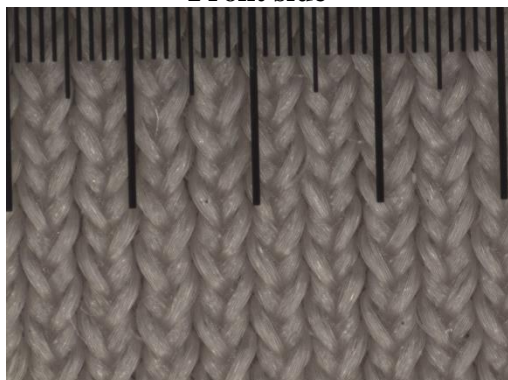
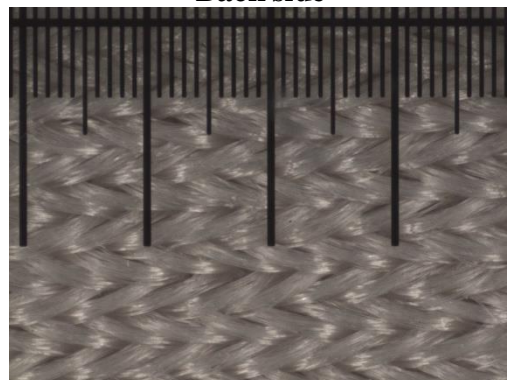


S5



S6



Locknit structure (S7)**Front side****Back side****Front side with stretched****Back side with stretched****Interlock structure (S8)****Front side****Back side**